Microalgal Photobioreactors for Carbon-Efficient Wastewater Treatment

A thesis submitted to Newcastle University in partial fulfilment of the requirements for the degree of Doctor of Philosophy in the Faculty of Science, Agriculture and Engineering

Kasim MOHAMMED
MSc, BEng

School of Civil Engineering and Geosciences
Newcastle University, United Kingdom

October, 2013

Declaration

Except where acknowledgement has been given, this thesis is the work of the author. No part of the material offered has been submitted previously for a degree or other qualifications in this, or any other University.

Kasim Mohammed.

Acknowledgement

Praise is due to Almighty God. My sincere gratitude to my former supervisor, Dr Cesar Rossas Mota, for his ideas and support towards making this research a success. My sincere gratitude and heart-felt appreciation to my supervisor, Dr Paul Sallis, for his brilliant ideas and the golden role he played in my thesis write-up and successful completion of my PhD programme. I would also like to thank my co-supervisors, Dr Ziauddin Shaikh for his brilliant ideas in my laboratory experiments, motivation and support for the entire PhD programme, and Professor David Graham, for his support and encouragement throughout my postgraduate research at Newcastle.

Further, I would like to express my gratitude to the Federal Government of Nigeria for awarding me the PhD Scholarship, through Petroleum Technology Development Fund (PTDF), Abuja, Nigeria, to undertake this research. I am also grateful to my employer, Bayero University, Kano, Nigeria, for granting me study fellowship. My special thanks to Mr Rob Hunter and Mr David Dick for fabricating my bioreactor vessels and connecting the light-emitting diodes. I am also grateful to Miss Lucy Eland for helping me with the microbiological analyses. Thanks to Mrs Donna Swan, Mr David Race and Miss Sara Smith for supporting me in the laboratory. I am grateful to my colleagues, Abdulaziz Al-Shareedah, Hamad Matar, Stephen Edwards, Olorunwa Tijani, Fatai Tijani, Mathew Brown, and Dr Khalid Bushnaf, for their supportive company.

Special thanks to my parent and family, especially my mum, Saudatu Abubakar, and my wife, Zahra'u Aliyu, for their love, and support during my academic pursuits. My sincere appreciation goes to Babah, A.J. Aliyu, Sa'adan Sa'idu, Justice A.A. Gumel, and their families, for helping me and my family during my current studies. I am ever grateful to my friend Misbahu Muhammad for accommodating me during my write-up, when my scholarship funding stopped. Finally, thanks to A.A. Ibrahim, H.A. Daura, A.B. Kadafur, M.A. Mohammed, B.S. Saulawa, S.M. Makarfi, Idris Musa, Bello Imam, Salisu Alfa, Cpt A.S. Imam, Auwal Aliyu, Y.Y. Muhammad, G.H. Yunusa, Drs S.M. Gumel, A.H. Gambo, A.M. Bayawa, Sani Yahaya, M.B. Adamu, Alhaji Mustapha, and U.M. Ba, for encouraging and helping me in one way or the other during my studies. Thanks to anyone that helped me during this research, whose name does not appear above. It was not forgotten, but because of space limitation.

Abstract

Algae-based wastewater treatment technologies are gaining popularity because of their sustainable treatment capabilities, coupled with their ability to capture carbon and consequently reduce the carbon footprint of the overall treatment process. Research was undertaken to develop a low-cost hybrid mixed microalgae-activated sludge municipal wastewater treatment system coupled with CO_2 sequestration. Red light-emitting diodes were used as light source to illuminate 1 L and 21 L microalgal photobioreactors. Three phases of laboratory experiments (I, II and III) were conducted to treat real or synthetic municipal wastewater using batch and continuous modes of operation, either with or without CO_2 addition. Phases I and II experiments were conducted in batch mode using a mixed microalgae-bacteria culture as inoculum, while Phase III was conducted in continuous mode using a mixture of microalgae and activated sludge as inoculum. The added gas in Phases I and II had O_2 supplementation whereas the gas in Phase III had no O_2 but a substantial amount of CO_2. Average 'optimal' irradiance (582.7 $\mu mol.s^{-1}.m^{-2}$) was used in Phases II and III, while Phase I investigated a range of lower light regimes (i.e. 25.3 to 234.3 $\mu mol.s^{-1}.m^{-2}$). Results showed high wastewater treatment efficiency, in terms of soluble chemical oxygen demand (SCOD) and ammonium-nitrogen (NH_4-N) removal. SCOD removal efficiency greater than 70% was achieved in all the three experimental phases. Furthermore, NH_4-N removal efficiencies greater than 90, 70 and 40%, were achieved in Phases I, II and III, respectively. However, nitrite accumulation was observed in Phases I and II, indicating that NH_4-N removal was due to partial nitrification. Furthermore, low phosphate removal efficiencies were achieved in Phase III. Results confirmed that considerable reduction of operational costs could be achieved by satisfying bacterial oxygen requirement through photosynthetic oxygenation in the hybrid microalgae-activated sludge (HMAS) photobioreactors, with considerable energy savings possible whilst maintaining high levels of SCOD removal. Typically, a dissolved oxygen concentration > 2 $mg.L^{-1}$ could be maintained in the HMAS photobioreactors without external aeration. Microbial analyses of samples collected from Phase II and III photobioreactors revealed a dominance of bacteria over microalgae. In order to prevent system failure, it was recommended that HMAS photobioreactors be set-up with an initial microalgae-bacteria ratio of at least 90:10, as determined by flow cytometry. Overall, this study demonstrated the potential for achieving high treatment efficiency by coupling wastewater treatment with carbon capture in HMAS photobioreactors. The potential for realising cost savings in wastewater treatment through use of HMAS photobioreactors at full-scale are discussed.

Table of Content

Abbreviations

A_f	Facultative pond area
ACGM	Algal culture growth medium
AISP	Acid-insoluble polyphosphate
ANOVA	Analysis of variance
AOB	Ammonia oxidising bacteria
APHA	American Public Health Association
AS	Activated sludge
ASP	Acid-soluble polyphosphate
ATL	Animal tissue lysis
ATP	Adenosine triphosphate
BOD	Biochemical oxygen demand
C_c	Carbon content
cc	Critical concentration
CDW	Cell dry weight
cfu	Coliform units
COD	Chemical oxygen demand
CUR	Carbon uptake rate
DGGE	Denaturing gradient gel electrophoresis
DO	Dissolved oxygen
DNA	Deoxyribonucleic acid
EBPR	Enhanced biological phosphorus removal
FC	Faecal coliform
FCM	Flow cytometry
HMAS	Hybrid microalgae –activated sludge
HRAP	High-rate algal ponds
HRT	Hydraulic retention time
IC	Inorganic carbon
LED	Light-emitting diodes
MBBM	Modified Bold's Basal medium
MLVSS	Mixed liquor volatile suspended solids
MSWM	Modified synthetic municipal wastewater
M:B	Microalgae-bacteria ratio
$NADPH_2$	Reduced nicotinamide adenine dinucleotide phosphate
NOB	Nitrite oxidising bacteria
OC	Organic carbon
OD	Optical density
PAO	Phosphate accumulating organisms
PBR	Photobioreactors
PBS	Phosphate buffer saline
PC	Personal computer
PCR	Polymerase chain reaction
PFA	Paraformaldehyde

PGA	Phosphoglyceric acid
qPCR	Quantitative real-time PCR
R1 to R12	Bench-scale photobioreactors
RC	Reaction centre
RNA	Ribonucleic acid
rRNA	ribosomal RNA
RuBisCO	Ribulose bisphosphate carboxylase/oxygenase
SCOD	Soluble COD
SRT	Solid retention times
STPBR	Stirred-tank photobioreactors
SR	Same as STPBR (batch-operated)
TC	Total carbon
TCMP	2-chloro-6-trichloromethyl pyridine,
TKN	Total Kjeldahl nitrogen
TP	Total phosphorus
TSS	Total suspended solids
WSP	Waste stabilisation ponds

List of Tables

List of Figures

Related Publications

Mohammed, K., Ahammad, S. Z., Sallis, P. J. and Mota, C. R. (2013) 'Energy-efficient stirred-tank photobioreactors for simultaneous carbon capture and municipal wastewater treatment' full paper submitted to *Journal of Water Science and Technology* on 06-10-2013 (currently under review).

Mohammed, K., Ahammad, S. Z., Sallis, P. J. and Mota, C. R. (2013) 'Energy-efficient photobioreactors for simultaneous carbon capture and municipal wastewater treatment' *10th IWA International Conference on Ponds Technology: Advances and Innovations in Wastewater Pond Technology.* Cartagena, Colombia, 19th - 23rd August, 2013.

Mohammed, K., Ahammad, S. Z., Sallis, P. J. and Mota, C. R. (2013) 'Optimisation of red light-emitting diodes irradiance for illuminating mixed microalgal culture to treat municipal wastewater' *7th International Conference on Sustainable Water Resources Management.* New Forest, UK, 21-23 May 2013.

Mohammed, K., Ahammad, S. Z., Sallis, P. J. and Mota, C. R. (2013) 'Effects of CO_2 addition on bench-scale microalgal bioreactors treating municipal wastewater', a poster presented at *Glasgow-Newcastle-Durham Networking Conference.* Lindisfarn Centre, Durham University, Durham, United Kingdom, 14th March, 2013.

Chapter 1

Introduction

1.1 Background and Research Justification

Wastewaters from homes and industries require certain level of treatment prior to discharge into natural water courses. Municipal wastewater has traditionally been treated using waste stabilisation ponds (WSP), activated sludge (AS), trickling filters, etc. Wastewater treatment involves the use of energy with consequent emission of carbon dioxide (CO_2) into the atmosphere. For example, AS process requires considerable amount of energy usually generated through the combustion of fossil fuels. However, stringent regulations on reducing carbon emissions (Department of Energy and Climate Change, 2009; Environment Agency, 2009), coupled with escalating energy prices, now call for the need to develop energy-efficient carbon-neutral wastewater treatment technologies.

Treatment processes that couple carbon capture and wastewater treatment with low or no carbon emission can be considered as the most sustainable option. Microalgae use light, CO_2, nutrients and water to produce biomass through photosynthesis (Hsueh *et al.*, 2009). Commercial cultivation of microalgae usually involves the use of freshwater resources and considerable amount of nutrients. Synthetic fertilisers are also used as source of nutrients in such systems and this adds to the overall cost of the process. Interestingly, such nutrients are naturally available in municipal wastewater (Yun *et al.*, 1997), and potentially can be obtained at low-cost from this source. This can considerably reduce the cost of microalgal cultivation process with consequent benefit of water pollution control and conservation of freshwater resources. In view of these benefits, this study investigated the potential for using microalgae to treat municipal wastewater.

Unlike sludge from AS which has traditionally been considered as a waste, microalgal biomass has a number of possible commercial applications. This includes use of the biomass, or its extracts, where appropriate, in biodiesel and biogas production (Meng *et al.*, 2009; Chisty, 2007), human and animal nutrition (Spolaore *et al.*, 2006), healthcare products

(Yamaguchi, 1997), cosmetics and personal care products (Stolz and Obermayer, 2005), etc. As such, microalgal biomass is more of a resource than a waste. Hence, the end use of microalgal biomass eliminates or reduces the need for sludge disposal, and maximises the benefits of using microalgae to treat municipal wastewater.

The idea of using microalgae to treat municipal wastewater is not novel as early publications identified this over 50 years ago (Oswald *et al.*, 1957). Studies have also been undertaken on the cultivation of microalgae with CO_2 supplementation, both within and outside the realms of wastewater treatment (e.g. Park and Craggs, 2011; 2010; Cheng *et al.*, 2006; Takeuchi *et al.*, 1992). However, research has rarely been undertaken to evaluate the effects of coupling carbon capture with municipal wastewater treatment with a view to develop a 'low-cost' technology that can potentially minimise the use of fossil fuel as a source of energy in wastewater treatment, and reduce atmospheric CO_2 levels at the same time.

Treatment of wastewater in microalgal systems is achieved through algal-bacterial (cyclic) symbiosis (Van Den Hende *et al.*, 2010; Humenik and Hanna-Jr, 1971; Oswald *et al.*, 1953; Ludwig *et al.*, 1951). This is a relationship dependent on the exchange of metabolic by-products between the two organisms. Algae produce oxygen through photosynthesis which is used by bacteria to degrade organic matter with concomitant production of CO_2 (Humenik and Hanna-Jr, 1971). The CO_2 produced is in turn used by algae in photosynthesis (Van Den Hende *et al.*, 2010; Oswald *et al.*, 1957). Therefore, this study explored such a symbiotic relationship to develop a hybrid microalgae-activated sludge system that would potentially offset the limitations of the individual systems. In this system, sufficient carbon, as organic matter and CO_2, and optimum illumination are required to sustain the above symbiotic relationship and allow the wastewater to be treated effectively.

In view of the above, this research has focussed on the two key limiting parameters in microalgal cultivation, i.e. carbon and illumination. In addition, the key limiting parameter of the AS system, i.e. oxygen, was also investigated. Such considerations were done with a view to avoid carbon limitation through CO_2 addition (concomitant with illumination), light limitation through the use of red light-emitting diodes (LED) as light source, and consequently exploring the potential of microalgae to satisfy bacterial oxygen requirement for biodegrading organic matter, through oxygenic photosynthesis. The other main nutrients,

nitrogen and phosphorus, are not considered to be limiting parameters as they are readily available in domestic wastewater (Yan *et al.*, 2013; Yun *et al.*, 1997; Humenik and Hanna-Jr, 1971).

Amount and quality of illumination play a key role in the photoautotrophic cultivation and growth of aquatic photosynthetic organisms such as microalgae. These illumination requirements can influence the ability of microalgae to remove nutrients from wastewater. Conventional light sources such as fluorescent and incandescent lamps are widely used to externally illuminate microalgal photobioreactors (PBR). However, light attenuation resulting from long path lengths in PBR, coupled with a high algal concentration, can be one of the shortcomings of using external illumination.

Internally illuminating microalgal PBR with LED can overcome the above shortcomings. However, little attention has been paid to determining the optimum amount of irradiance required to illuminate microalgae during wastewater treatment. Hence, there is need to optimise the quantity and quality of LED irradiance required to illuminate microalgal PBR. Although light requirement may differ from one system to another, light optimisation will always be a prerequisite to the development of any energy-efficient, carbon-neutral microalgal wastewater treatment technology. LED emitting monochromatic light have recently gained popularity in microalgal cultivation (e.g. Yan *et al.*, 2013; Wang *et al.*, 2007), but little attention has been paid to their application in wastewater treatment.

In view of the above, LED emitting red light at 660 nm characteristic wavelengths, rather than fluorescent or incandescent lamps, were chosen as source of illumination for this study based on the premise that red photons are most efficient in deriving photosynthesis and that they are weakly absorbed by water molecules leading to minimal loss of light due to scattering and absorption (Blankenship, 2002). Moreover, use of red LED as light source has the potential to enhance performance of photoautotrophic microalgal systems (Wang *et al.*, 2007). Additionally, the above wavelength was chosen for the current research in order to maximise photon energy utilisation based on the fact that it falls within the maximum photon absorption peaks of *chlorophyll a* and *b* molecules (i.e. 663 and 645 nm, respectively; Blankenship, 2002).

Potentially, LED can replace conventional artificial light sources for algal cultivation due to the advantages of the former over the latter (Mehta *et al.*, 2008). These advantages include low power consumption, luminous efficacy (Matthews *et al.*, 2009), low start-up time, easy control, monochromatic emission, and a long life-span (Mehta *et al.*, 2008) of up to 10 years. Consequently, LED have lower carbon footprint than fluorescent or incandescent lamps, have an associated opportunity for generating carbon credits and promoting environmental sustainability (Mehta *et al.*, 2008), and are more economical and more efficient in deriving photosynthesis than conventional light sources due to their narrow bands (Yan *et al.*, 2013). Interestingly, used LED can be recycled easily as they contain fairly benign substances, compared to fluorescent lamps which contain mercury, and incandescent lamps which contain tungsten, posing higher pollution risk to the environment (Mehta *et al.*, 2008).

Consequently, research was undertaken to develop a hybrid microalgae-activated sludge (HMAS) system through the formulation of research questions, presented in Section 1.2, which defined the aims and objectives, presented in Section 1.3. Subsequently, laboratory experiments, briefly outlined and presented in Section 1.5, were designed and conducted in order to achieve these goals.

1.2 Research Questions

The following questions were formulated and addressed in this research.

(i) what effects will CO_2 addition have on the wastewater treatment efficiency; microalgal growth rate and biomass productivity of a red LED-illuminated microalgal wastewater treatment system?

(ii) what level of monochromatic light is needed to operate a laboratory-scale CO_2-enriched HMAS?

(iii) will the amount of irradiance found in (ii) be enough to prevent light limitation, affect biomass concentration, solid retention times, and wastewater treatment efficiency (i.e. chemical oxygen demand and nutrient removal) of the HMAS system?

(iv) is a specific algae-bacteria ratio required to develop the HMAS system?

(v) will the microbial community in the HMAS be stable or differ temporally?

(vi) is there any fundamental difference between the HMAS, conventional algal ponds and AS systems in terms of treatment performance?

1.3 Aims and Objectives

1.4 Aim

The aim of this research was to develop a hybrid microalgae-activated sludge system coupling wastewater treatment with carbon capture.

1.5 Objectives

The objectives of the research were to:

(a) assess the effect of CO_2 addition and variation in red LED irradiance on wastewater treatment efficiency in a red LED-illuminated mixed bacteria-microalgal system

(b) determine the maximum microbial growth rate, biomass productivity and nutrient removal efficiencies in a CO_2-enriched microalgae-bacteria system

(c) determine the optimum red light irradiance from LED for illuminating a HMAS system

(d) assess the effect of different mixed liquor volatile suspended solids (MLVSS) and solid retention times (SRT) on wastewater treatment efficiency, and net carbon uptake rate in the HMAS system

(e) compare the performance of the HMAS with that of conventional algal ponds and activated sludge system

(f) evaluate the microalgal and bacterial dynamics in the mixed culture of the HMAS system

(g) propose optimum conditions for designing and operating HMAS wastewater treatment system

1.6 Research Scope and Limitations

This research was laboratory-based and employed mixed cultures of photosynthetic (i.e. freshwater microalgae) and non-photosynthetic (i.e. aerobic bacteria) organisms to biologically treat municipal wastewater in bench- and up-scaled photobioreactors, under external and internal illumination, respectively. The illumination was provided by a monochromatic light source – 660 nm red LED. Wastewater quality parameters were monitored using biological, chemical and physical techniques to evaluate treatment performance and efficiency. However, neither heavy metals nor pathogenic microorganisms were monitored in this research. Lack of total nitrogen and organic phosphorus analyses, where appropriate, might have limited the interpretation of nitrite and phosphate accumulation encountered unexpectedly in this research.

1.7 Outline of Experiments

Three phases of experiments were conducted in the laboratory as briefly outlined below.

Phase I

This phase of experiments involved the operation and monitoring of twelve 1 L bench-scale Pyrex microalgal PBR operated in batch mode, 6 with (designated R1 through R6) and 6 without (designated R7 through R12) CO_2 addition (sometimes referred to as CO_2 enrichment). The bioreactors were used to treat real municipal wastewater for 19 d. Illumination was provided externally at the top of the bioreactors. The experiments were designed to achieve objectives 'a' and 'b' (Section 1.3.2). Chapter 3 gives detailed information about these experiments.

Phase II

In this phase, experiments were conducted in 3 internally illuminated 21 L microalgal stirred-tank photobioreactors (STPBR) designated as SR with a control bioreactor operated in the dark, with and without CO_2 enrichment. The bioreactors had an initial effective volume of 16 L and were also operated in batch mode, but with pH control, under the laboratory ambient conditions. These bioreactors were used to treat synthetic municipal wastewater for 30 d. This phase of experiments was designed to investigate objective 'c' (Section 1.3.2). Chapter 4 gives detailed information on these experiments but they shared some methods with Phase I experiments which were detailed in Chapter 3.

Phase III

This phase of experiments involved the operation of the same 21 L STPBR, with CO_2 enrichment, treating synthetic municipal wastewater, for 64 d. These bioreactors were the same with the SR in Phase II except that they were operated in continuous mode and designated as STPBR. The STPBR were started with different MLVSS but same initial microalgae-bacteria ratio (M:B) of about 90:10, and operated at optimum irradiance determined in Phase II. MLVSS was used as the control parameter in operating the STPBR. Settled biomass collected from the bottom of clarifiers downstream was returned into the STPBR at every cycle of the operating hydraulic retention time (HRT) of 4 d.

This phase of experiments was designed to investigate objective 'd' (Section 1.3.2). Chapter 5 gives detailed information on these experiments but they also shared some methods with

Phase I and II experiments (Chapter 3). Objectives ‘e’; ‘f’ and ‘g’ were addressed in the discussion sections throughout the thesis and, in Chapters 6 and/or 7.

Microbial analyses

Samples were collected from Phases II and III, and analysed using flow cytometry (FCM) and quantitative real-time polymerase chain reaction (qPCR), with a view to evaluating temporal microbial dynamics in the STPBR.

1.8 Thesis Structure

Eight chapters make up this thesis, with the current Chapter serving as Introduction. Chapter 2 presents a literature review, from the use of microalgae in municipal wastewater treatment to the potential sustainable use of LED as light source in microalgal wastewater treatment systems. A study on the effects of coupling CO_2 addition with municipal wastewater treatment at bench-scale is presented in Chapter 3. Chapter 4 presents an optimisation study on the amount of monochromatic LED irradiance needed to treat municipal wastewater in up-scaled microalgal STPBR.

Furthermore, an experimental study on the effects of variation in MLVSS with operating SRT in a HMAS system is presented in Chapter 5. Chapter 6 presents the results of microbial analyses on selected samples to estimate the number of bacteria and microalgae present in Phase II and III experiments. Chapter 7 presents a general discussion of the results of this research in comparison to the three experimental phases as well as the significance of the study in relation to current and future trends of wastewater treatment principles and practices. Lastly, Chapter 8 presents the conclusions of the research findings and recommendations for future work, with a view to furthering our understanding in this area of research.

Chapter 2

Literature Review

2.1 Introduction

This chapter presents a literature review on the application of microalgae in municipal wastewater treatment (Section 2.2). It also presents a review on microalgal carbon capture (Section 2.3). The main systems used to cultivate microalgae are presented in Section 2.4, with some review on hybrid microalgal cultivation systems and suggestions for improvement through coupling of such systems with carbon capture and use of monochromatic light sources. Considering the problems and cost of sludge disposal in other wastewater treatment processes, Section 2.5 presents a review on commercial ways of valorising microalgal biomass. Review on photosynthesis as a fundamental process for microalgal metabolism is also presented in Sections 2.6 and 2.7. The Chapter ends with a review on light-emitting diodes as prospective and promising light sources for illuminating microalgae during wastewater treatment (Section 2.9).

2.2 Use of Microalgae in Wastewater Treatment

Microalgae play important roles in wastewater treatment in WSP through, among other things, provision of oxygen needed for bacterial biochemical oxygen demand (BOD) and ammonia removal (Weatherell *et al.*, 2003). WSP have been used worldwide in both temperate and tropical climates for domestic wastewater treatment, especially for small communities (Mara and Johnson, 2007; Oliveira *et al.*, 1996). The major pollutants usually removed from wastewater using WSP include BOD, nitrogen (N), phosphorus (P), suspended solids and pathogens. Many studies have been undertaken to remove these pollutants from wastewater using WSP systems (e.g. Del Nery *et al.*, 2013; Park *et al.*, 2011; Park and Craggs, 2010; Camargo-Valero *et al.*, 2009a; Abis and Mara, 2003; Oswald, 1995; Oswald, 1990; Pearson *et al.*, 1987; Oswald *et al.*, 1957; etc.).

Although WSP have been used to treat domestic wastewater worldwide, their performance depends on climatic conditions, which are variable between geographical locations; and

process parameters such as dissolved oxygen (DO) and pH which affect chemical equilibrium of wastewater pollutants (e.g. ammonium ions and free ammonia; Paterson and Curtis, 2005). Temperature plays important role in wastewater treatment in WSP. This is due to its thermodynamic effect on solubility of pollutants and microbial activities in wastewater consequently affecting the rate of biochemical reactions (Paterson and Curtis, 2005). Due to the dynamic and passive nature of WSP, temperature is practically uncontrollable in these systems.

Removal of pollutants in algal-based WSP is aided by algae-bacterial symbiotic relationship (Van Den Hende *et al.*, 2010; Medina and Neis, 2007; Humenik and Hanna-Jr, 1971; Oswald *et al.*, 1953; Ludwig *et al.*, 1951). Algae produce oxygen through photosynthesis which is used by bacteria to biodegrade organic matter and produce carbon dioxide (CO_2); the CO_2 produced by the latter is then utilised by the former for photosynthesis (Humenik and Hanna-Jr, 1971). However, algae also consume oxygen during respiration, especially at night, with concomitant production of CO_2 (Ludwig *et al.*, 1951). Therefore, a thriving algal-bacterial symbiosis is essential for efficient performance of algal-based WSP and other algal wastewater treatment systems. The evaluation of performance and process design of WSP are usually based on effluent quality requirements set locally and/or internationally by regulatory agencies (Mara, 1996).

Several studies have been undertaken on wastewater treatment using WSP in, for example, the UK (Abis and Mara, 2003), France (Racault *et al.*, 1995), Spain (Soler *et al.*, 1995), Brazil (de-Oliveira *et al.*, 1996; Ceballos *et al.*, 1995), Australia (Hodgson and Paspaliaris, 1996), Tanzania (Mayo, 1996), and other parts of the world. Most of these studies were aimed at removing pollutants from different types of wastewater ranging from domestic to industrial; with a view of reusing the treated effluent or disposing of it into natural watercourses. Seasonal variations as well as physico-chemical parameters apparently affect the performance and treatment efficiency of the WSP systems situated in these locations and elsewhere.

Abis and Mara (2003) studied the effect of surface BOD loading on treatment efficiency of pilot-scale facultative ponds in the UK, with reference to seasonal variations. They reported soluble BOD and TSS removal efficiencies of more than 90%, respectively. These removal

efficiencies were reported to be independent of seasonal variation, with the former dependent on surface BOD loading (Abis and Mara, 2003). In addition, they reported nitrogen removal of about 50 and 80% in winter and summer, respectively, which were also dependent on surface BOD loading in the facultative ponds. However, algae disappeared from the facultative ponds during winter period which was apparently due to low temperature leading to unfavourable thermal gradient (Abis and Mara, 2003). These authors concluded that low surface BOD loading has hindered the maintenance of aerobic condition and achievement of optimum BOD and total suspended solids (TSS) removal in the facultative ponds, under UK climatic conditions.

A survey on the performance of WSP system, mainly treating domestic wastewater, with average organic loading rate (OLR) of about 25 kg.BOD.ha^{-1}.d^{-1}, was conducted in France (Racault *et al.*, 1995). Statistical analyses on the survey data in the study revealed filtered chemical oxygen demand (COD) and BOD removal efficiencies of more than 85 and 95%, respectively, in the majority of the ponds. In addition, TSS, total N and total P removal efficiencies of more than 70, 60 and 50%, respectively, were also reported. Racault *et al.* (1995) pointed out that only the nutrient removal efficiencies were considerably influenced by seasonal variation. They concluded that, besides other factors, long detention times and strong seasonal variations, influencing the treatment process in WSP, could lead to dispersed data that may be difficult to interpret, and hence may limit the application of statistical modelling and accurate prediction of effluent quality in these systems.

Soler *et al.* (1995) evaluated the performance of two WSP, treating a mixture of municipal sewage and fruit processing and cannery wastewater situated in south-eastern Spain in relation to seasonal variation. They reported average winter BOD and COD removal efficiencies of more than 70 and 75% respectively. They also reported pathogens removal efficiencies ranging from 72 to 98% for four different indicator organisms, mostly coliforms. However, BOD and COD removal efficiencies decreased to about 20 and 30% respectively in summer due to increase in population caused by tourism. This consequently increased the strength of the organic load into the WSP but with fairly the same pathogen removal efficiencies except for total coliform that improved by about 20% (Soler *et al.*, 1995).

A study by de-Oliveira *et al.* (1996) evaluated the performance of a series of WSP treating municipal sewage in northeast Brazil operated at mean temperature of 23 °C and hydraulic retention times (HRT) of about 20 and 30 d, respectively, for two different experimental periods. They reported BOD, COD and TSS removal efficiencies of up to 96, 85 and 91%, respectively, in some of the studied maturation ponds. However, use of relatively long HRT could serve as practical limitation of the treatment efficiencies achieved in the above study. Ceballos *et al.* (1995) also evaluated the treatment performance of a full-scale facultative pond treating domestic sewage in northeast Brazil and reported BOD removal efficiency similar to that reported by de-Oliveira *et al.* (1996).

The facultative pond was operated at HRT of about 60 d and maximum temperature of 30 °C, with a view of using the treated effluent for unrestricted irrigation. These authors reported a BOD, helminth eggs and coliform removal efficiencies of 95, 100 and 99.6%, respectively, but with faecal coliform (FC) concentration of more than 4.0×10^5 coliform units (cfu) per 100 mL in the treated effluent which is far above the permissible limit set by the WHO guideline for reuse of treated wastewater in unrestricted irrigation. However, Ceballos *et al.* (1995) have partly attributed this non-compliance to system design limitation due to closeness of the pond inlet to its outlet which might have reduced the HRT and consequently affected the FC removal efficiency.

Another study by Pearson *et al.* (2005) in northeast Brazil evaluated the effect of variation of depth (from 1.0 to 2.3 m) on the treatment performance of a series of WSP. They reported constant rate of BOD removal irrespective of the HRT used in the study. Nevertheless, they reported higher values of first-order reaction rate constants (i.e. k values) for FC removal in shallower ponds than in the deeper ones. In addition, nutrients were reported to be more efficiently removed in the shallower ponds with almost 50 and 90% removal for N and P, respectively. Under treated effluent reuse situation and at a temperature of at least 25 °C, they suggested that deep facultative ponds can be used in series by allowing a factor of safety of 40% to design HRT values to compensate for FC removal. They concluded that deep facultative ponds have no advantage over shallow ones with respect to BOD and nutrient removal efficiency.

Hodgson and Paspaliaris (1996) evaluated the performance of full-scale lagoons treating a mixture of domestic sewage and industrial wastewater at 3 different facilities each comprising of 11 ponds (including 1 anaerobic) operating at HRT of 120 d, in Australia. The study was conducted year round with a temperature difference of at least 10 °C between summer and winter. These authors reported reduction in effluent BOD and inorganic N concentrations down to 2 and 20 $mg.L^{-1}$, respectively, and almost complete pathogens removal. They also reported higher treatment efficiencies in summer compared to winter period.

Mayo (1996) evaluated the BOD removal efficiency of pilot and full-scale facultative ponds treating a mixture of domestic and industrial wastewater in Tanzania. The ponds received average BOD loading of 450 $kg.ha^{-1}.d^{-1}$ at different HRT ranging from about 4 to 11 d with mean monthly temperature at the vicinity of the ponds ranging from 23 °C to 28 °C. The maximum BOD removal efficiencies of the pilot and full-scale ponds were, approximately, 72 and 88% respectively. He reported that BOD removal rate was dependent on HRT, besides organic loading rate (OLR) and other process parameters. He recommended the use of real BOD concentration rather than the usual practice of using an assumed value in the design of facultative ponds in Tanzania.

Apparently, wide variations exist in the performance of WSP worldwide as evident from the pollutant removal efficiencies of the above studies. Overall, it is understood that the performance of these systems is higher in tropical climates than in temperate ones, under 'optimum' conditions. Nevertheless, the influence of process parameters, pond geometry, and hydraulics are also important in evaluating the performance and treatment efficiencies of WSP systems (Abis and Mara, 2005; Pearson *et al.*, 1995).

2.2.1 Nitrogen removal

Nitrogen can be removed in algal wastewater treatment systems through various ways. The main mechanisms for N removal explored by many researchers include biological uptake of ammonium and nitrate by algae (Camargo-Valero *et al.*, 2009a; Martinez *et al.*, 2000), sedimentation of algal biomass containing organic N (Camargo-Valero *et al.*, 2009a; Zimmo *et al.*, 2004), ammonia stripping to the atmosphere (Camargo-Valero and Mara, 2007b; Zimmo *et al.*, 2004; Pano and Middlebrooks, 1982b), denitrification of oxidised forms of

nitrogen to N_2 gas (Zimmo *et al.*, 2004), and various combinations thereof (Camargo-Valero *et al.*, 2009b; Camargo-Valero and Mara, 2007b).

However, conflicting arguments exist in the literature on which mechanisms are mainly responsible for N removal in WSP systems (Camargo-Valero and Mara, 2010; Lai and Lam, 1997; Reed, 1985; Pano and Middlebrooks, 1982b). Nevertheless, there are instances where researchers tend to agree on one or more pathways as the dominant mechanisms for N removal in WSP, depending on the prevailing conditions in such systems. Interestingly, most of the published works on algal wastewater treatment systems agree that N removal is influenced by pH, temperature and retention time, but this has neither resolved the conflicts nor established the dominant mechanism for N removal in algal wastewater treatment systems (Reed, 1985).

Owing to the fact that the wastewater in WSP is exposed to complex ecosystem, environmental conditions and biochemical activities greatly influence the transformation mechanisms for N removal in these systems (Reed, 1985). Reed (1985) pointed out that N can go through several transformation pathways involving oxidation-reduction cycles as a result of long HRT in facultative ponds. He argued that nitrification could only occur as an intermediate step of nitrogen transformation in facultative ponds and that denitrification cannot be practically demonstrated as a permanent mechanism for N removal in WSP.

To strengthen the above argument, Reed (1985) posited that anaerobic condition is necessary for denitrification to ensue in WSP and that this can only happen in settled sludge at the pond bottom at times of high N removal. He pointed out that nitrate production under such conditions in the benthic sludge is unlikely and that its available concentration should only be compared to that in the water column. He then concluded that coupled nitrification-denitrification is unlikely to be the main mechanism for N removal in WSP systems.

Nevertheless, this argument does not seem to completely dismiss the possibility of having nitrification-denitrification as a mechanism for N removal in WSP. Lai and Lam (1997) also concurred with Reed (1985). However, they differed on his position that denitrification can only prevail under anaerobic condition by pointing out that it is an anoxic process. They

further pointed out that although it is unlikely for denitrification to prevail under anaerobic condition, diurnal and nocturnal variations of DO concentration leading to low DO levels at night (possibly due to algal respiration) may favour denitrification.

Contrary to Reed (1985)'s view on nitrification-denitrification, Camargo-Valero *et al.* (2009b) considered simultaneous occurrence of these pathways as a promising route for N transformation and removal in pilot-scale maturation ponds. They demonstrated, through tracer study with stable isotopes of N (i.e. ^{15}N-labelled ammonium and nitrite), with their findings supported by results from molecular microbial analyses, that nitrification can be considered as an intermediate step in N removal in WSP under conditions leading to low algal activity. Based on the results from the tracer experiments with ^{15}N-labelled ammonium, they reported that complete nitrification of ammonium to nitrate seemed to be the preferred N transformation pathway followed by algal uptake of oxidised forms of nitrogen in maturation ponds. This finding apparently supports the argument by Reed (1985) that nitrification is an intermediate step for N removal in WSP.

In the same study, Camargo-Valero *et al.* (2009b) pointed out that denitrification can be considered as another mechanism that can feasibly remove N from maturation ponds. They supported their argument through comparison of results from molecular microbial analyses with corresponding tracer study on samples collected from both the benthic sludge and water column of one of the studied maturation ponds. They used polymerase chain reaction (PCR) to confirm the presence or absence of the microbial groups responsible for N transformation in these samples, and denaturing gradient gel electrophoresis (DGGE) to confirm the identity of the microorganisms belonging to these groups. They reported the presence of ammonia-oxidisers, nitrite-oxidisers, denitrifiers and methanotrophs-like organisms in both the water column and the sludge samples collected from the maturation ponds.

The above findings reported by Camargo-Valero *et al.* (2009b) demonstrate the possibility of having both nitrification and denitrification occurring simultaneously in maturation ponds and opposes Reed (1985)'s argument that coupling of these mechanisms for permanent N removal is only feasible in principle rather than in practice. They pointed out that in winter, when unfavourable environmental conditions prevail in WSP leading to low algal activity;

ammonium oxidation ensues with subsequent permanent N removal via denitrification as gaseous N. Camargo-Valero *et al.* (2009b) then concluded that algal uptake and coupled nitrification-denitrification were the dominant mechanisms for N removal in maturation ponds. However, Lai and Lam (1997) concurred with Reed (1985) and reported that long retention times can favour N removal via complete nitrification with subsequent considerable algal growth resulting from biological uptake of ammonium or nitrate. They further pointed out that permanent N removal can subsequently be achieved via denitrification under low DO concentration. This also partly agrees with the findings of Camargo-Valero *et al.* (2009b).

Furthermore, attention was paid to ammonia volatilisation as a mechanism for N removal in WSP (Rockne and Brezonik, 2006; Lai and Lam, 1997; Reed, 1985; Pano and Middlebrooks, 1982b). The presence of ammonia and/or ammonium in wastewater depends on pH; with ammonium dominating at or below pH 8 (Pano and Middlebrooks, 1982a). However, pH values higher than 8 shift the equilibrium of the reaction between ammonia and water towards free ammonia which volatilises to the atmosphere (von-Sperling and Chernicharo, 2005; Pano and Middlebrooks, 1982a) while ammonium remains in solution and serves as source of N to algae (von-Sperling and Chernicharo, 2005). Around pH 7, only ammonium exists in solution whereas equal amount of free and ionised ammonia exist around pH 9.5 with complete free ammonia dominance at pH 11 or higher (von-Sperling and Chernicharo, 2005).

Pano and Middlebrooks (1982b) developed some mathematical models for predicting N removal in facultative WSP. The models were premised on ammonia volatilisation as the dominant mechanism for nitrogen removal in WSP under the influence of pH and temperature. The simplifying assumptions employed in their models included completely mixed reactor situation, neglect of the influence of other N removal mechanisms such as algal uptake and ignorance of the possible involvement of ammonia in complex biochemical transformation pathways such as partial nitrification which may lead to accumulation of nitrite in pond water column. Considering the design principles of maturation ponds, however, Camargo-Valero *et al.* (2009a) demonstrated that the contribution of ammonia volatilisation as a mechanism for N removal in WSP is negligible and that algal activity plays

an important role in N transformation and removal in these systems. Nevertheless, WSP systems may passively perform contrary to design principles thereby unexpectedly favouring other N removal mechanisms over algal uptake due to variation in environmental conditions and process parameters, system failure or malfunction.

Moreover, due to over simplification in the mathematical models for predicting N removal via ammonia stripping, Camargo-Valero and Mara (2010) demonstrated the weakness of such models due to their failure to accurately predict N removal in WSP systems. They used the model equations developed by Pano and Middlebrooks (1982b) to predict ammonium concentration for their experimental ponds, in an attempt to validate these models. The predicted results did not compare favourably with real effluent ammonium concentration of the ponds (Camargo-Valero and Mara, 2010). In addition, comparison of linear regression results of the maturation ponds with Pano and Middlebrooks (1982b)'s model resulted in poor correlation as evident from the values of the regression coefficient, gradient of the plot and the coefficient of determination of 75%, 0.73 and 0.3, respectively.

In another study, Camargo-Valero *et al.* (2009a) investigated the influence of organic nitrogen sedimentation on ammonium and total N removal in pilot-scale maturation ponds. They monitored nitrogen sedimentation rates, among other parameters. They reported N content in the ponds sediments ranging from 4 to 7% with corresponding N sedimentation rates ranging from about 270 to 2900 $g.ha^{-1}.d^{-1}$ and concluded that algal uptake of inorganic N, and subsequent sedimentation of dead algal biomass could be responsible for N removal in maturation ponds under favourable environmental and operational conditions.

van-der-Linde *et al.* (2009) investigated the removal of N in pilot-scale facultative pond operated at HRT of 30 d, in summer and winter, using stable isotope tracking technique with ^{15}N-labelled NH_4Cl as the tracer. They found out that considerable amount of ammonium was assimilated by algae and subsequent release of soluble organic N into the pond water; with higher algal uptake of N in the summer than in the winter. They attributed the release of soluble organic N to the degradation of dead algal biomass. Nevertheless, some of the dead algal biomass might have settled to pond sediments and led to underestimation of the actual amount of organic N present in the system. Nevertheless, their study demonstrated

the role played by algal assimilation as a mechanism for N removal in facultative ponds. The findings therefrom agree with that of Camargo-Valero *et al.* (2009a).

When investigating the influence of environmental and operational conditions on nitrogen removal mechanisms, Zimmo *et al.* (2004) studied the effects of temperature and OLR on nitrogen removal in WSP via three different transformation mechanisms: sedimentation, denitrification and ammonia volatilisation, in pilot-scale WSP systems treating low and medium strength domestic wastewater at 7-d HRT with temperature ranging from 7 to 25 °C. They reported that sedimentation was responsible for the highest N removal whereas ammonia volatilisation was negligible. Nevertheless, they reported N removal rates higher than 1500 and 1300 $mg.m^{-2}.d^{-1}$ under warm temperatures in the WSP systems. In addition, they developed a model for predicting N removal rates in these systems. These findings agree with Camargo-Valero *et al.* (2009a) and differ with Pano and Middlebrooks (1982b).

Martinez *et al.* (2000) studied the effect of stirring and temperature on the use of pure culture of the microalga *Scenedesmus obliquus* to remove ammonium from a pretreated municipal wastewater in the laboratory focussing on algal uptake and ammonia stripping as mechanisms for N removal. They reported N removal efficiency of up to 100%. However, it was not clear which of these mechanisms was mainly responsible for achieving this excellent N removal efficiency. Nevertheless, the studies by Martinez *et al.* (2000) and Zimmo *et al.* (2004) demonstrated the influence of operating conditions on some of the mechanisms responsible for nitrogen removal in microalgal wastewater treatment systems.

Furthermore, von-Sperling and Chernicharo (2005) concurred with Pano and Middlebrooks (1982b) and argued that ammonia stripping appears to be the dominant mechanism in shallow maturation ponds due to higher photosynthetic activity with consequent pH values higher than 11 and high DO production. They pointed out that maturation ponds arranged in series favour more ammonia stripping than single-celled ponds with removal efficiency as high as 80% or even higher than 90% in a series of shallow maturation ponds. They further argued that N removal via algal uptake is of less importance especially when high efficiencies are required. They also argued that nitrification-denitrification and sedimentation of algal biomass can occur simultaneously, concurring with Camargo-Valero

et al. (2009b), but are considerably less important than other nitrogen removal mechanisms; and that nitrification is usually negligible in facultative ponds.

In the contrary, Camargo-Valero and Mara (2010) demonstrated that ammonia volatilisation has little or even no influence on N removal in WSP irrespective of the season. They argued that temperature increase in WSP increases algal activity with consequent high uptake of ammonium leading to higher N removal than via ammonia volatilisation as posited by Pano and Middlebrooks (1982b). They further argued that high pH and temperature may not necessarily favour ammonia stripping over other N removal mechanisms such as biological uptake since these parameters could simultaneously favour other removal mechanisms.

Apparently, no consensus has, hitherto, been reached concerning the dissension on the mechanisms and transformation pathways mainly responsible for N removal in WSP systems. Most of the previous as well as current studies on such mechanisms did not attempt to resolve the aforementioned conflicts. Rather, they focussed on the influence of certain environmental and operational conditions on some of these mechanisms, and tried to demonstrate their relevance to N removal in algal wastewater treatment systems. Hence, it is apparent that nitrogen can be removed from WSP via any or combination of algal uptake, sedimentation into benthic sludge, denitrification and ammonia volatilisation through various intermediate biochemical reactions, and one or more mechanism(s) may dominate over the other(s) depending on the prevailing environmental and operational conditions in the algal wastewater treatment systems.

Nevertheless, different values of N removal efficiency in algal ponds as well as photobioreactors have been reported in the literature. On the one hand, for example, Camargo-Valero and Mara (2007a) reported ammonium (NH_4-N) removal efficiency due to algal assimilation of up to 90% in pilot-scale maturation ponds operated under natural conditions and Park and Craggs (2011) reported NH_4-N removal efficiency greater than 80% in a pilot-scale high-rate algal ponds (HRAP) operated at 4-d HRT with CO_2 addition.

On the other hand, Aslan and Kapdan (2006) achieved different values of NH_4-N removal efficiency in bench-scale bioreactors with pure culture of *C. vulgaris* treating synthetic wastewater for corresponding initial substrate concentrations. They reported variation in

NH_4-N removal efficiency ranging from 100% at initial NH_4-N concentration of about 13 to 21 mg.L^{-1} to less than 24% at NH_4-N concentration of at least 129 mg.L^{-1}. Their removal efficiency generally decreased with increasing initial substrate concentration.

2.2.2 Phosphorus removal

Besides N, P is the other nutrient element responsible for eutrophication of natural watercourses. Although WSP have been used for wastewater treatment, they are characterised by low P removal efficiency (Powell *et al.*, 2009; Mbwele, 2006); which may not be unconnected with low P uptake and its content in microalgal biomass (Powell, 2009), and less attention paid to the process design of WSP (Camargo-Valero, 2008). In addition, low concentration of algal biomass usually found in WSP may also be responsible for low P removal in these systems (Powell *et al.*, 2011; Powell *et al.*, 2009).

Although the P content of microalgal biomass is low, about 1% on cell dry weight basis, P has been recognised as an important growth-limiting nutrient in algal metabolism which may be due to its property in easily binding to some ions (e.g. carbonates) to form precipitates and consequently reducing its bioavailability to algae (Grobbelaar, 2004). However, over supply of P has been reported to provide no solution to P limitation as it may even lead to stress with consequent low algal growth (Grobbelaar, 2004). Microalgae use P in the synthesis of intracellular compounds such as deoxyribonucleic acid (DNA), ribonucleic acid (RNA), protein (Grobbelaar, 2004; Miyachi *et al.*, 1964) as well as energy-rich compounds such as adenosine diphosphate (ADP) and adenosine triphosphate (ATP) which are essential in intracellular energy transfer processes (Borchardt and Azad, 1968).

Phosphorus is mainly present in wastewater as soluble inorganic orthophosphates, complex inorganic phosphate compounds such as sodium pyrophosphates, polyphosphates such as polymers of phosphoric acid or as organic P compounds found in organic matter and cellular materials such as phosphoproteins, complex sugars or nucleic acids (Nurdogan and Oswald, 1995; Nesbitt, 1969). Polyphosphates and organic P compounds are biodegraded to inorganic phosphates by bacteria forming, for example, more than 70% of the total P in facultative and high rate algal ponds (HRAP; Nurdogan and Oswald, 1995). Procedure for measuring P in wastewater is available in Standard Methods. However, Nesbitt (1969) argued that such procedure does not discriminate between these forms of P and that the

basic test for phosphate only measures orthophosphates. He pointed out that the separation of soluble and insoluble forms of phosphorus can be achieved through filtration and that the latter can be converted to the former for the purpose of analysis through boiling with inorganic acids, especially sulphuric and nitric acids or their mixture thereof. Nevertheless, methods for measuring different forms of phosphorus using chemical extraction techniques are now available although they are cumbersome (Powell, 2009) and need further improvement.

Microalgae take up P in the form of soluble inorganic orthophosphate (Grobbelaar, 2004) for cell growth. P has been reported to be removed from wastewater in WSP mainly through biological assimilation by algae and bacteria and absorption onto sediments (Powell *et al.*, 2011; Mbwele, 2006). It is interesting to note that algal uptake and sedimentation are common mechanisms for removing both N and P in WSP, but algal uptake of P is usually much lower than N uptake as the content of the latter in algal biomass is about ten times higher than content of the former (Nurdogan and Oswald, 1995). Chemical addition leading to phosphate precipitation is another mechanism for removing P in WSP which may be 'natural', due to the presence of carbonates, iron or aluminium ions, in solution etc.; or artificial, through addition of these ions into the wastewater (Surampalli *et al.*, 1995). Nevertheless, precipitation of P with these ions occurs at high pH values (Nurdogan and Oswald, 1995).

Phosphate uptake in microalgae has been demonstrated to be of three types: metabolic uptake for cell growth, starvation uptake by P-starved cells and luxury (i.e. storage) uptake (Azad and Borchardt, 1970). Algal phosphate assimilation has been reported to depend on the chemical energy provided by photosynthesis in the presence of light or by energy-rich P-containing compounds during respiration in the dark (Becker, 1994). In addition, it also depends on other factors such as phosphate concentration in the substrate and algal biomass, pH, temperature and the concentration of trace metals such as sodium, magnesium, potassium as well as concentration of heavy metals in the cultivation medium (Powell *et al.*, 2011; Martinez *et al.*, 1999; Becker, 1994; Borchardt and Azad, 1968). Moreover, P removal usually occurs simultaneously with N removal in WSP.

Bogan (1961) used mixed microalgal culture, dominated by *Chlorella* and *Scenedesmus*, to remove P from a mixture of lake water, treated and untreated domestic sewage both in the laboratory and at pilot-scale. He focussed on algal uptake as a mechanism for P removal from the wastewater with a view to develop a high-rate P removal procedure. He reported that up to 90% of the added phosphate was removed from the cultivation medium within the first 2 h. Due to the detection of pH values of up to 10 in the culture medium and the tendency of phosphate to bind with calcium ions at high pH, Bogan (1961) suspected that coagulation of algae with calcium sulphate also played a considerable role in P removal. He found out that calcium ion concentration and pH were the main factors influencing the solubility of orthophosphate in the wastewater.

Borchardt and Azad (1968) studied biological assimilation of P using pure microalgal cultures under controlled excess ammonia and phosphate concentrations, pH, temperature, illumination and mixing, at steady-state. They evaluated the effects of cell density, temperature and light on P uptake by microalgal culture dominated by *Chlorella* and *Scenedesmus*. They achieved phosphate removal efficiency of 30 % in the effluent at steady-state microalgal cell mass of 0.05 $g.L^{-1}$ (i.e. from phosphate concentration of 13 to 4 $mg.L^{-1}$) with subsequent complete phosphate removal in the culture medium. They reported that the depletion of phosphate in the medium had no immediate effect on the microalgal growth rate. In another set of experiments with varying lower phosphate concentration than the previous, however, Borchardt and Azad (1968) observed decrease in growth rate below 1.5 $mg.L^{-1}$ phosphate concentration, which they termed as critical concentration (cc).

Below the cc, Borchardt and Azad (1968) reported direct variation of growth rate with phosphate concentration whereas the growth rate remained constant above the cc. They further reported that no phosphate was detected in the effluent above the cc until the added substrate phosphate concentration reached 4.5 $mg.L^{-1}$. This finding demonstrated the ability of microalgae to store phosphate under excess supply and availability. They proposed three phosphate zones under steady-state and controlled conditions of cultivation at algal density of 0.05 $g.L^{-1}$: growth-dependent regime, from 0 to 3% phosphate uptake corresponding to phosphate-free situation up to the cc; storage regime, from 3 to 9% phosphate uptake; and saturation regime above 9% uptake.

Chen *et al.* (2003) used pilot-scale HRAP to remove nutrients and other pollutants from domestic wastewater in summer and winter, in China, and reported average phosphate (PO_4-P) and total phosphorus (TP) removal efficiencies of 40 and 46%, respectively. Through linear regression, they demonstrated that the P removal efficiency positively correlated with the P concentration, HRT, temperature and illumination. They suggested that the two main mechanisms for P removal in the HRAP were algal uptake and chemical precipitation with calcium and iron at high pH values; with higher TP removal efficiency in the summer than in the winter. They pointed out that adequate mixing in the HRAP prevented the settling of algal biomass to the pond bottom and precluded sedimentation as a mechanism for P removal.

Rockne and Brezonik (2006) reported TP removal efficiency similar to that reported by Chen *et al.* (2003). The former authors also indicated that TP removal efficiency varies considerably with season. They reported that about 40 and 50% of the influent P were removed from water column in winter and summer treatment periods, respectively, in full-scale WSP in Minnesota. In contrast, Rockne and Brezonik (2006) detected concentration of P in the pond sediments which suggested that sedimentation was also responsible for P removal in the WSP system. They concluded that TP removal was less efficient than N removal as over half of the influent TP left the WSP in the effluent.

In view of low P removal of WSP systems, Powell *et al.* (2009) identified two options for improving P removal efficiency in WSP: upgrading WSP effluent through chemical precipitation or replacement of ponds with another wastewater treatment technology. Addition of chemicals such as iron and aluminium salts to precipitate phosphate is believed to be an effective means for removing P from WSP but its associated material cost and that of handling precipitated sludge and disposal make this option unattractive (Powell *et al.*, 2009). Replacing WSP with another technology is not a viable option either, due to possible loss of investment and considering the worldwide acceptance of this treatment system because of their simplicity, ease of operation, and low-cost (Powell *et al.*, 2009).

In view of the above bottlenecks, Powell *et al.* (2009) studied an alternative way of improving P removal efficiency of WSP. They studied luxury uptake of P by microalgae analogous to enhanced biological P removal (EBPR) in AS systems. They conducted the study

with a view of developing a method for P removal in WSP as effective as EBPR in AS based on the ability of microalgae to accumulate and store orthophosphates under excess availability for subsequent use under condition of phosphate limitation.

In the study, Powell *et al.* (2009) used chemical extraction techniques to determine two forms of internal inorganic polyphosphate in microalgal biomass: acid-soluble polyphosphate (ASP) and acid-insoluble polyphosphate (AISP). ASP is used in the synthesis of intracellular phosphorus compounds while AISP is temporarily stored in microalgal cells under excess supply of inorganic polyphosphate to be used under limited availability (Powell *et al.*, 2009; Miyachi *et al.*, 1964). Powell *et al.* (2009) further investigated the effect of external phosphorus concentration, temperature and irradiance on the cellular inorganic polyphosphate concentration in mixed culture of microalgae. They focussed on luxury uptake of inorganic polyphosphate as a mechanism for P removal by microalgae in bench-scale batch photobioreactors (PBR) using chemical extraction methods focussing on ASP and AISP concentration in the algal biomass.

Powell *et al.* (2009) reported the accumulation of both ASP and AISP in the microalgal biomass at high external phosphate concentration. In addition, they observed decrease in concentration of these polyphosphates after exhaustion of the external phosphate in the culture medium. They attributed this observation to partial utilisation of the ASP for cell growth and storage of the AISP by the microalgae for subsequent utilisation under limited availability of external phosphate. They confirmed this observation by noticing subsequent slight decrease in AISP concentration after reaching a threshold value in the microalgal biomass and corresponding constant concentration of this polyphosphate in the culture medium.

They concluded that although ASP is utilised by microalgae for intracellular metabolism, it can also be stored shortly in microalgal biomass whereas AISP can serve as a long term polyphosphate reservoir. They further concluded that polyphosphate dynamics in algal system is influenced by environmental conditions and that the luxury uptake of polyphosphates by microalgae depends on the phosphate concentration in the cultivation medium. This demonstrated the use of microalgae in phosphorus removal and the potential of using luxury uptake to improve phosphorus removal efficiency in algal wastewater

treatment systems. However, chemical extraction techniques are cumbersome with respect to both procedure and time (Powell *et al.*, 2009). In addition, luxury uptake of phosphorus by algae has been rarely studied and is apparently poorly understood.

2.2.3 COD removal

COD and/or BOD are used to determine the relative strength of wastewater with respect to biodegradability of its organic matter content. BOD measurement is an empirical test used to determine the amount of oxygen required by bacteria to biodegrade the organic matter contained in polluted waters whereas COD is a standard method which determines the amount of chemical oxidant required to react with the organic waste in a given amount of wastewater through combustion with the oxidant, which is subsequently expressed as equivalent oxygen demand of the polluted water (APHA, 2005). In simple terms, BOD is the measure of biodegradable organic carbon whereas COD is the measure of total organic carbon contained in a given sample of polluted water (Kiely, 1997).

Although BOD has been used for this purpose by many researchers for many years, its test procedure is cumbersome and may be prone to errors. For example, extra care has to be taken to prevent exposure of the test sample to light to avoid photosynthetic activity which may increase the amount of DO during the test, and the test procedure entails the use of nitrification inhibitor (i.e. 2-chloro-6-trichloromethyl pyridine, TCMP; APHA, 2005) to prevent nitrification in order not to affect the amount of oxygen measured during the test.

BOD test has conventionally been conducted on wastewater samples under controlled conditions at a temperature of 20 ± 1 °C for 5 d (APHA, 2005). In view of the relatively long duration of conventional BOD test and its associated cost, Chaudhuri *et al.* (1992) attempted to shorten the duration of the test to 3 d at 27 °C which is the typical ambient water temperature in the tropical region of India. In collaboration with their colleagues, they assessed the BOD of various wastewater samples ranging from surface to industrial, and reported similarities in the results obtained. They concluded that the conventional 5-d BOD can alternatively be determined in 3.5, 2.6 and 2 d at temperatures of 25, 27 and 35 °C, respectively. However, there are considerable discrepancies in the average BOD values reported in this study with much closer similarities in the values obtained from surfactant-polluted wastewater and surface water samples.

In the contrary, Mara and Horan (1993) argued on the validity of the conclusion drawn by Chaudhuri *et al.* (1992) on the basis of BOD kinetics and the appropriateness of the test method to developing countries. They pointed out that the oxygen uptake in BOD test follows first-order reaction kinetics with the rate constant following Arrhenius-type equation as opposed to the assumption of second-order reaction kinetics in the computation of the above BOD values by Chaudhuri *et al.* (1992). Mara and Horan (1993) discerned on the appropriateness of BOD test method in determining the strength of wastewater especially in tropical developing countries. They argued that the test method is only still surviving due to its familiarity rather than its accuracy. They pointed out the inherent disadvantages of the BOD test method including the cost of the test apparatus, poor reproducibility of results and long incubation time.

As such, Mara and Horan (1993) recommended the replacement of BOD with COD test method which is more appropriate, rapid (as it can be conducted in 2.5 h as opposed to 5 d), simple, reproducible and can be repeated immediately if need be. They pointed out some development regarding the preference of COD test method by regulatory agencies that set effluent standards through the incorporation of maximum permissible COD values for discharge into receiving waters. They recognised that although COD test does not indicate the biodegradability of the wastes contained in a water sample, simple techniques that discriminate the COD of polluted water sample as non-biodegradable, slowly biodegradable and rapidly biodegradable are currently available. Methods for measuring COD as either inorganic or organic are also available (APHA, 2005).

However, the major limitations of the COD test method are the interference by non-metallic ions that can inactivate silver ions with consequent formation of precipitates; partial or lack of oxidation of some chemical compounds such as pyridine and ammonia that are commonly found in wastewater; and exertion of COD by nitrites at concentration higher than 2 $mg.L^{-1}$ (APHA, 2005). For example, more reactive halides can react with dichromate to form chromate ions and elemental halogens thereby restricting the oxidising power of dichromate (APHA, 2005). These interferences affect the accuracy of the test results, especially at high interferent concentrations, although appropriate measures could be taken to minimise them prior to sample digestion (APHA, 2005).

The consortia of microalgae and aerobic bacteria have been used to remove COD from domestic wastewater. However, the use of COD as a wastewater quality parameter has received lesser attention than BOD despite the advantages of the former over the latter. Table 2.1 summarises the COD removal efficiencies from some studies on WSP and other algal wastewater treatment systems.

Table 2.1 COD removal efficiencies of some algal wastewater treatment systems

Treatment system	COD removal efficiency (%)	Reference
Facultative pond	55-70	Mara *et al.* (1998)
Facultative pond	64-73	de-Oliveira *et al.* (1996)
Maturation ponds	71-85	de-Oliveira *et al.* (1996)
Photobioreactor	90	Humenik and Hanna-Jr (1971)
Maturation ponds	7-25	von-Sperling and Mascarenhas (2005)
Facultative ponds*	7-17	Soler *et al.* (1995)
Facultative ponds*	19-37	Soler *et al.* (1995)
Facultative ponds	55	Mendes *et al.* (1995)
HRAP	92	Shelef (1982)
Facultative ponds	61-67	Schetrite and Racault (1995)
Facultative pond	93	Kumar and Goyal (2010)

* Ponds located at two different sites

2.2.4 Heavy metals removal

Water pollution by heavy metals is a problem that requires attention in wastewater treatment. Microalgae require heavy metals as trace nutrients since the metals form part of active sites of essential enzymes (Wilde and Benemann, 1993). As such, microalgae can be used to remove heavy metals from wastewater although this bioremediation technique has its associated benefits as well as problems. Some of the advantages of heavy metals removal with microalgae include low-cost, rapid kinetics of metal uptake, selectivity in removing specific metals, applicability on wastewater mixed with different heavy metals, minimal need for addition of other chemicals, possibility for recovering adsorbed metals from the spent algal biomass, etc., (Wilde and Benemann, 1993).

However, some of the problems of this bioremediation technique may include toxicity of the metal ions to microalgae which may inhibit growth with consequent adverse effect on the overall wastewater treatment process, handling of the metal-rich biomass, cost of chemical used for metal recovery or biomass disposal, and possible adverse effect of some heavy metals (such as lead) to automobile engines when the biomass is used to produce biodiesel as well as conflicting interest between this technique and biofuel production. In

addition, the cost of pH control (Wilde and Benemann, 1993) in large full-scale systems such as WSP may make this technique unattractive.

Microalgae have been used to remove variety of heavy metals from wastewater. Nevertheless, the amount of removal varies between algal species and physicochemical conditions, especially pH and temperature of the growth medium, and the concentration and relative toxicity of the metal ions to microalgae (Wilde and Benemann, 1993). The main mechanisms for the removal of heavy metals from wastewater using algae include active uptake into the cells and adsorption onto living and dead cells surfaces (Golab and Smith, 1992).

Several studies have been undertaken to remove heavy metals from wastewater using pure and mixed culture of microalgae. For example, removal of lead and zinc from domestic wastewater by mixed microalgal culture (Kumar and Goyal, 2010), removal of cadmium, chromium and copper ions from synthetic wastewater by *Scenedesmus incrassatulus* (Pena-Castro *et al.*, 2004), removal of cadmium and copper from heavy metal polluted synthetic wastewater by *C. vulgaris* (Miskelly and Scragg, 1996), removal of lead ions from industrial wastewater by *C. vulgaris* and *Chlamydomonas* sp. (Golab and Smith, 1992), and selective removal of cadmium from industrial wastewater by *C. pyrenoidosa*, (Hart and Scaife, 1977), etc.

Kumar and Goyal (2010) reported removal efficiencies of up to 66 and 70% for lead and zinc, respectively, by *Chlorella*-dominated mixed culture of microalgae in WSP treating domestic wastewater during winter, in India. However, they also reported perceived zinc toxicity on the microalgae as a result of decline in its cell density. Correspondingly, these authors also observed increase in pH and DO resulting from the heavy metal removal. These microalgae were reported to tolerate lead concentration of up to 20 $mg.L^{-1}$, with maximum zinc and lead uptake of about 34 and 42 mg per g of microalgal biomass, respectively. The absence of lead toxicity was apparently evident from the increase in the algal productivity at this high lead concentration.

Golab and Smith (1992) investigated the lead uptake by the freshwater microalgae *C. vulgaris* and *Chlamydomonas* sp. after long and short exposure, respectively, with the

former alga exhibiting higher lead accumulation than the latter. They reported that the accumulation depended on the type of nutrient medium used in cultivating the algae and the lead concentration in the water column. They further reported that growing the algae in a lead-containing medium prior to the study resulted in more lead accumulation than when the algae were grown in lead-free medium. They found out that the algae exhibited both intracellular and extracellular (i.e. on cell surfaces) lead accumulation under relatively long-term exposure of up to 7 d. In contrast, the algae, pre-cultured in lead-free medium, were reported to only exhibit extracellular lead accumulation under short term exposure of less than half an hour as evident from the results of electron microscopy conducted on the algal cells.

Similarly, Hart and Scaife (1977) much earlier reported the ability of *C. pyrenoidosa* to accumulate cadmium ions from wastewater. Such accumulation was reported to be light-dependent, directly proportional to the cadmium concentration in the cultivation medium, and was unaffected by the presence of other metal ions (i.e. calcium, cobalt, copper, magnesium, molybdenum and zinc). This finding demonstrates the ability of microalgae to selectively remove heavy metals in solution. However, the above metal accumulation was reported to be completely inhibited at molybdenum concentration of 0.2 $mg.L^{-1}$. This shows the toxic effect of molybdenum to these microalgal species, especially at, at least, this reported concentration.

2.3 Photosynthetic Carbon Capture

The use of microalgal photosynthesis to capture CO_2 as a biological mitigation of carbon emissions has received much attention in recent years. CO_2 concentration is commonly reported in the literature as percentage volume per volume (v/v). Traditionally, CO_2 has been photosynthetically captured by microalgae in ponds at concentration well below 1% in ambient air. Ambient CO_2 concentration seems too low to fully exploit the carbon capture potential of microalgae in order to slow down or stabilise the current atmospheric CO_2 levels resulting from increasing greenhouse gas emissions.

In addition, such concentration could lead to low microalgal biomass productivity due to possible carbon limitation (Wang *et al.*, 2008) and consequently decrease the amount of biomass that could be used as a raw material for carbon-neutral renewable fuel production.

However, industrial-grade compressed gas mixtures and industrial flue gas contain considerable amount of CO_2, can provide a richer carbon source than ambient air, and may potentially lead to dramatic carbon capture (Wang *et al.*, 2008) when used in microalgal wastewater treatment systems. In order to achieve considerable carbon capture, therefore, it is extremely important to use concentrated forms of CO_2 in microalgal wastewater treatment systems either from these sources or from coal-fired wastewater treatment plants, from breweries, etc.

Microalgae have been shown to grow in wastewater (Yun *et al.*, 1997) supplied with concentrated forms of CO_2 (Hanagata *et al.*, 1992) and flue gas (Brown, 1996; Negoro *et al.*, 1993) as inorganic carbon sources. This has been possible because of the photosynthetic activity of microalgae to produce biomass utilising light energy, inorganic carbon, and wastewater nutrients. Flue gas typically contains CO_2 ranging from 10 to 20% (v/v) which can be obtained at little or no cost (Wang *et al.*, 2008; Yamada *et al.*, 1997). Several studies have demonstrated the tolerance of microalgae to elevated CO_2 concentration. For instance, a unicellular microalga, *Oocystis* sp., was reported to be tolerant to 20% CO_2 although it exhibited optimum biomass productivity at only half of this concentration (Takeuchi *et al.*, 1992). Similarly, the blue-green alga (i.e. cyanobacterium) *Thermosynechococcus* sp. has exhibited an optimum growth rate of 2.7 d^{-1} at 10% CO_2 concentration (Hsueh *et al.*, 2009).

Furthermore, the freshwater green alga *C. vulgaris* has tolerated up to 15% CO_2 concentration contained in industrial flue gas (Yun *et al.*, 1997). In another study, this alga was reported to grow favourably in air containing up to 30% CO_2 but exhibited optimum growth rate at 5 to 10% CO_2 and 20% CO_2, respectively (Sung *et al.*, 1999). Separate studies by Brown (1996) and Zeiler *et al.* (1995) demonstrated the tolerance of the green alga *Monoraphidium minitum* to about 14% CO_2 contained in flue gas. Yamada *et al.* (1997) also reported the tolerance of the cyanobacterium *Anacystis nidulans* to 30% CO_2 contained in flue gas. However, this tolerance is contrary to the failure of the same organism to tolerate 20% CO_2 contained air in an earlier study (i.e. Yun *et al.*, 1996) by the same authors in which no explanation was given regarding such discrepancy. Nevertheless, the intolerance might be due to initial decrease in pH in the microalgal culture in the earlier study which might have resulted in conditions unfavourable for algal growth. Therefore, the tolerance to relatively high CO_2 concentration, shown in the above studies, demonstrates the potentials

of using microalgae to capture concentrated forms of CO_2, especially those emitted by the water industries.

However, there is a limit to the tolerance of microalgae to CO_2 levels as some concentrations have been reported to inhibit algal growth although the inhibition could be reversed by resorting to lower concentration (Hanagata *et al.*, 1992). Nevertheless, early inhibition could lead to lasting adverse effect throughout the cultivation period thereby affecting overall biomass productivity. Growth of *Chlorella* was completely inhibited at 80% CO_2 whereas *Scenedesmus* grew favourably at this concentration but was inhibited at 100% CO_2 (Hanagata *et al.*, 1992). However, the inhibition in *Chlorella* was reported to be reversible when the concentration was reduced to 20% CO_2. The growth of these two green algae was reported to be independent of gas flow rate ranging from 0.1 to 1 litre per litre of algal culture per minute. In a study by Sung *et al.* (1999), the growth of *Chlorella* sp. was inhibited by air containing 70% CO_2. From the foregoing, it is noteworthy that elevated CO_2 concentration higher than 30% has the tendency to inhibit microalgal growth and that microalgae can grow optimally at 10 to 20% CO_2, provided all other growth conditions remain favourable.

Microalgae have been reported to be the most productive photosynthetic organisms that can assimilate higher amounts of carbon than terrestrial plants (Brown, 1996). Microalgal CO_2 fixation rate can be determined from experimental results using expressions developed in the literature such as Equation 2.1 (Yun *et al.*, 1997).

$$R_{CO_2} = C_c \times \mu_L \times \left(\frac{M_{CO_2}}{M_C}\right) \qquad (2.1)$$

The parameters in Equation 2.1 were defined as follows: R_{CO_2} denotes CO_2 fixation rate in $mg.L^{-1}.h^{-1}$; C_c denotes average carbon content in g carbon g^{-1} algal dry weight; μ_L denotes algal volumetric growth rate in $g.L^{-1}.h^{-1}$ dry weight; and M_{CO_2} and M_C are, respectively, the molar masses of CO_2 and elemental carbon. Table 2.2 gives the maximum rate of CO_2 fixation of some microalgae reported in the literature. Equivalent annual CO_2 fixation has been calculated next to the hourly values in Table 2.2. It is clear that the fixation rates vary with microalgal species and cultivation conditions and that variation may be eminent even

among same species. The highest fixation rate exhibited by *C. vulgaris* (Table 2.2) was achieved by cultivating the microalga in membrane photobioreactor.

Table 2.2 Maximum CO_2 fixation rates of some microalgae

Microalga	CO_2 fixation rate		Concentration (%, v/v)	Reference
	($mg.L^{-1}.h^{-1}$)	($mt.L^{-1}.y^{-1}$)		
C. vulgaris	52	0.454	20	Yun *et al.* (1996)
Ditto	26	0.227	15	Yun *et al.* (1997)
Ditto	260	2.271	1	Cheng *et al.* (2006)
	64	0.559	0.033	Keffer and Kleinheinz (2002)
Ditto	36	0.314	5	Ogbonna *et al.* (1999)
Ditto	10	0.087	Ditto	Sydney *et al.* (2010)
Dunaliella Tertiolecta	11	0.096	Ditto	Ditto
Spirulina platensis	13	0.114	Ditto	Ditto
Botryococcus braunii	21	0.183	Ditto	Ditto

Note: $mt.L^{-1}.y^{-1} = mg.L^{-1}.h^{-1} \times 8.736 \times 10^{-3}$

Moreover, CO_2 fixation has also been reported in terms of mass of carbon in microalgal biomass per mass of carbon supplied into a given cultivation medium, in $g.g^{-1}$ (de-Morais and Costa, 2007b) or as efficiency in % (de-Morais and Costa, 2007a). A study by de-Morais and Costa (2007a) investigated the CO_2 fixation of *Scenedesmus obliquus* and *Spirulina* sp. in tubular photobioreactors. They reported the maximum CO_2 fixations for *S. obliquus* of about 28 and 14% at 6 and 12% CO_2, respectively. The CO_2 fixations for *Spirulina* sp. were reported to be about 53 and 46% corresponding to these CO_2 concentrations. This shows decrease in fixation with increasing CO_2 concentration for both algae; demonstrating that they grew more favourably at 6% CO_2.

Another study by de-Morais and Costa (2007b) investigated the daily CO_2 fixation of four microalgal species in tubular photobioreactors under various CO_2 concentration. The algal strains included those in the above study and two species of *Chlorella*, *C. vulgaris* and *C. kessleri*. They reported that all the microalgal strains tolerated up to 18% CO_2 but *Spirulina* sp., grown in modified Zarrouk medium, achieved the best overall results in the study. However, the highest daily CO_2 fixation of up to 99.9% was achieved by this cyanobacterium at 0.04% CO_2. This suggests that operating conditions or substrate limitation might have adversely affected the CO_2 fixation ability of this alga under higher CO_2 concentration.

2.4 Microalgal Cultivation Systems

Microalgae are cultivated in different systems including open ponds, closed photobioreactors and hybrid systems. Open ponds and photobioreactors are the most commonly used methods of algal cultivation (Packer, 2009). These cultivation systems, their advantages and disadvantages, and design and operation principles are discussed in the following sections.

2.4.1 Open ponds

Open ponds (i.e. WSP and open raceways or HRAPs) are the most commonly used open algal systems for domestic wastewater treatment in small communities (Mara, 2003a). The importance of well-designed ponds had been postulated to increase in this century due to their several advantages (Oswald, 1995). Ponds have been considered as bioreactors that are formed through excavation and compaction of earth surface, designed to hold and treat wastewater for a certain period of time (Oswald, 1995). According to Oswald (1995), if ponds are properly designed and well-maintained, they can produce consortia of algae and bacteria that can biodegrade organic wastes contained in wastewater and consequently produce energy-rich algal biomass. They can produce effluents of high quality that can be reused in both restricted and unrestricted crop irrigation (Mara, 2008). WSP are designed for hydraulic and process performance using empirical and rational equations available in the literature (Finney and Middlebrooks, 1980).

Open ponds have advantages over other microalgal wastewater treatment systems due to their low construction, operation and maintenance costs, negligible or absence of electrical energy requirement, high performance and ease of operation (Mara, 2008; 2003a). However, the major disadvantages of these systems are huge land requirement, especially where land is scarce and expensive; difficulty in controlling environmental conditions, such as temperature, due to their passive nature; and susceptibility to contamination by unwanted algal species, grazers, and other organisms, and water loss due to evaporation, especially in tropical and semi-arid regions (Mara, 2008; 2003a).

WSP typically comprise of series of anaerobic, facultative and one or more maturation ponds (Mara, 2008; 2003a). Anaerobic ponds are sometimes omitted, especially in small treatment system, if the strength of the wastewater is low (Mara, 1987). Since microalgae

usually grow in facultative and maturation ponds but not in anaerobic ponds (Mara, 2003a), this review only focuses on facultative and maturation ponds. Detailed discussion on anaerobic ponds is available in the literature (e.g. Mara (2008); 2003a).

Facultative ponds are usually 1 to 2 m deep (Mara, 2006; 2003a). They are considered as primary when they receive their influent organic load directly from raw wastewater source or secondary when they receive a pretreated wastewater; for example, the effluent of anaerobic pond or wastewater from primary settling tank (Mara, 2006). Wastewater treatment is achieved in these ponds through algal-bacterial symbiosis as described previously (see Section 2.1). Based on the biochemical processes that take place in facultative ponds, three zones have been identified: anaerobic, facultative and aerobic (von-Sperling and Chernicharo, 2005).

Anaerobic zone, which lacks oxygen, could be formed as a result of biodegradation of settled organic matter to methane, CO_2, hydrogen sulphide, etc., at the pond bottom; oxygen-rich aerobic zone is formed at the upper water column dominated by fine particulate and dissolved organic matter; and facultative zone, characterised by intermittent availability and absence of oxygen, is formed in the water column between the aerobic and anaerobic zones (von-Sperling and Chernicharo, 2005). Due to the slow rate of waste stabilisation in facultative ponds, HRT longer than 20 days is usually required in order to achieve considerable level of BOD removal (von-Sperling and Chernicharo, 2005).

Facultative ponds are designed for BOD/COD removal based on permissible areal (surface) organic loading with typical OL from 100 to 400 kg BOD $ha^{-1}.d^{-1}$ (Mara, 2003a; Finney and Middlebrooks, 1980). Treatment efficiencies of facultative ponds in terms of filtered and unfiltered BOD/COD and TSS removals could be greater than 95, 70 and 90%, respectively, which are comparable to those obtained by other wastewater treatment systems (Mara, 2006). Besides oxygen production from algal photosynthesis, these ponds receive additional oxygen from the atmosphere through the surface due to wind action (Mara, 2003a). However, it is also reported that the oxygen produced by algal photosynthesis is more useful in waste stabilisation than that supplied by wind aeration (Shilton and Harrison, 2003).

According to Mara (1987), the process design of facultative ponds can be accomplished using Equations 2.2 and 2.3.

$$\lambda_s = \frac{10 L_i Q}{A_f} \quad (2.2)$$

$$\lambda_s = 350(1.107 - 0.002T)^{T-25} \quad (2.3)$$

In the above equations, λ_s is the surface BOD loading (kg.ha^{-1}.d^{-1}); L_i, the influent BOD (mg.L^{-1}); Q, the pond inflow (m^3.d^{-1}); A_f, the pond area (m^2); and T (°C), the mean temperature of the coldest month (Mara, 2006). Noteworthy, the areal OL varies with the strength and quantity of influent wastewater at any particular time and the operating temperature. Equation 2.3 is based on best design λ_s and T values of 350 kg.ha^{-1}.d^{-1} and 25 °C, respectively, obtained from a study on facultative ponds under abundant algal population with surface OL ranging from 100 to 600 kg BOD ha^{-1}.d^{-1} with corresponding temperature ranging from 10 to 35 °C (Mara, 1987).

Maturation ponds usually receive their effluent from facultative ponds. They could be shallower than or as deep as facultative ponds with their depth ranging from 1 to 1.5 m (Mara, 2006; 2003a). They are designed for pathogens and ammonia nitrogen removals although some level of BOD removal can be achieved simultaneously (Mara, 2006). Predictive models for estimating ammonia nitrogen removal are available in the literature. However, controversies exist regarding the predictive ability of some of the equations used in designing these ponds for ammonia nitrogen removal and the accuracy of the results therefrom (Camargo-Valero and Mara, 2010). Maturation ponds effluents can be upgraded, for example, by further treatment with rock filters if enhanced ammonia nitrogen removal is required (Mara and Johnson, 2007). The main disadvantage of maturation ponds is large land area requirement though this is often overlooked where land is readily available at low-cost (Mara, 2006).

Similarly, maturation ponds are also suitable for algal growth but are mainly used for pathogen removal (Mara, 2006). The pathogen removal in maturation ponds results from increase in temperature due to high solar radiation, elevated pH due to accumulation of hydroxide ions from aqueous dissociation of carbonate-bicarbonate ions (Mara, 2006), and photo-oxidation resulting from the combined effect of high irradiance and high DO concentration (Curtis *et al.*, 1992). The design of maturation ponds is based on first-order bacterial removal rate constant which is greatly dependent on temperature (Mara, 2006).

Equations 2.4 and 2.5, developed by Marais (1974), can be used for process design of maturation ponds.

$$N_e = \frac{N_i}{(1+k_{B(T)}\,\theta_F)(1+k_{B(T)}\,\theta_{M_1})(1+k_{B(T)}\,\theta_M)^n} \quad (2.4)$$

$$k_{B(T)} = 2.6(1.19)^{T-20} \quad (2.5)$$

Where N_i and N_e are the coliform concentrations in the influent and effluent wastewater (peR100 mL), respectively; $k_{B(T)}$, the first-order faecal bacteria removal rate constant (d^{-1}); $\theta_{F;M_1;M}$, the HRTs for the preceding facultative and succeeding maturation ponds in series, respectively; and T is the same as in Equations 2.2 and 2.3.

Raceway ponds (also synonymously called open raceways) are another type of open systems in which microalgae are commonly cultivated. They are used to produce biomass of *S. platensis* and *Dunaliella salina* commercially in the USA and Israel, for example (Tredici, 2004). Raceway ponds consist of shallow ditch dug into the ground with a paddle wheel attached to aid mixing of microalgae with the cultivation medium (Tredici, 2004). They may have one or multiple units or cells.

Open raceways share some characteristics and advantages with facultative ponds but some of their disadvantages include long light path due to large volume per pond area leading to low algal biomass concentration which consequently increases harvesting cost; light shading; lack of control of environmental conditions; difficulty in achieving low flow velocity as turbulence is required for stirring the paddle wheel, loss of water through evaporation and difficulty in screening algal species for specific application (Tredici, 2004; Sheehan *et al.*, 1998). According to Sheehan *et al.* (1998), the major problem in screening algal species grown in open ponds is the inability of the isolated strains to dominate in such systems as they are easily out-competed by contaminant native algal species in the vicinity. To offset this bottleneck, these authors recommended the integration of laboratory and outdoor systems in microalgal research and development.

Furthermore, open raceways are designed for maximum algal biomass productivity considering pond depth, water circulation velocity, retention time, frequency of culture dilution, temperature, and pH as key design parameters (Sheehan *et al.*, 1998). As a result of

improvement in pond design, biomass productivity of up to 37 $g.m^{-2}.d^{-1}$, at culture dilution frequency of 3 d, was reported in a pilot-scale raceway, amounting to photon-to-biomass conversion efficiency of about 10% (Sheehan *et al.*, 1998). Microalgal biomass productivity ranging from 15-25 $g.m^{-2}.d^{-1}$ dry algal biomass for cultivation period as long as 90 d, and 30-40 $g.m^{-2}.d^{-1}$ for shorter cultivation period are commonly obtainable in outdoor algal systems (Goldman, 1979).

A recent study by Park and Craggs (2010) investigated the influence of CO_2 addition on the algal productivity and wastewater treatment performance of two pilot-scale HRAP operated at 4 and 8 d HRT, respectively. They reported maximum areal algal productivity of about 24.7 and 9 $g.m^{-2}.d^{-1}$ for the 4 and 8 d HRT, respectively. They also reported BOD removal efficiency of up to 95% in both ponds. They observed considerable stability of the algal population in both ponds and ascribed it to the condition obtained as a result of CO_2 addition which favoured algal growth. The CO_2 addition was reported to have controlled the pH in the ponds within optimum range for algal growth (i.e. 6.25-8.06 and 6.45-7.95 for 4- and 8-d HRT, respectively). These authors pointed out that CO_2 addition into the HRAP served as pH control, enhanced BOD removal, increased biomass productivity, facilitated biomass settling leading to easy harvesting, and resulted in reduced HRT required to achieve considerable wastewater treatment performance.

A more recent study by Park and Craggs (2011) investigated the influence of CO_2 addition on N removal in the same HRAP systems under similar operating conditions. They reported higher N removal in the pond operated at 4-d HRT than in the one operated at 8-d HRT under CO_2 addition. They attributed the lower N removal in the pond operated at the longer HRT to low biomass productivity and probable substrate limitation caused by loss of N via coupled nitrification-denitrification. These authors reported overall N removal efficiency of about 60 % in the ponds enriched with CO_2. They suggested that CO_2 addition can reduce loss of N through ammonia stripping due to consequent pH control below the level favourable for ammonia volatilisation thereby favouring algal N uptake. They concluded that pH control through CO_2 addition decreased nitrogen loss due to reduced ammonia stripping, increased bioavailability of nitrogen to algae and enhanced biomass productivity. However, these authors employed the use of tap water in order to achieve the 4-d HRT through

dilution, in both studies which can adversely impact on freshwater resources, especially when applied to full-scale systems.

2.4.2 Closed systems

These microalgal cultivation systems are mainly closed PBRs with their different types. PBRs are illuminated reactor devices in which microalgae and other photosynthetic organisms can be grown in aqueous medium (Tredici, 2004). They may be wholly closed or slightly open at the top. Although some PBR may have some openings, they can nevertheless be considered as closed systems as they are covered unlike WSP whose surface is traditionally wide open and exposed to the atmosphere. PBRs are usually made of transparent materials such as Pyrex or Plexiglas to allow passage of light. The advantages of PBRs over open ponds include control of contamination and cultivation conditions such as temperature and pH (though easier at bench-scale), high biomass productivity, flexibility in choice of growing either axenic or mixed cultures, and possibility of manipulation for optimum light utilisation (Ugwu *et al.*, 2008; Tredici, 2004).

Design classification of PBRs, on one hand, is based on length of light path (e.g. flat or tubular), orientation (e.g. horizontal or vertical) shape and complexity (e.g. manifold or serpentine; Tredici, 2004), and position of illumination (e.g. internally- or externally-illuminated; Ogbonna *et al.*, 1999). On the other hand, operational classification of PBR could be based on mixing (e.g. stirred-tank type), mode of gas supply and mass transfer (e.g. airlift, bubble column, single-phase, two-phase), etc. (Ugwu *et al.*, 2008; Tredici, 2004). PBRs are designed to achieve high productivity of microalgal biomass and high efficiency of conversion of light energy to biomass based on surface-to-volume ratio, material transparency and orientation for optimum light supply and utilisation; gas supply, mixing and degassing for optimum gas-liquid mass transfer; ease of maintenance; temperature control and possibility for scale-up and ease of operation; bearing in mind their capital and operating costs (Tredici, 2004).

Although research and development of PBRs and their application in microalgal cultivation have received much attention in recent years, their commercial application cannot be compared to that of open ponds (Tredici, 2004). This could, perhaps, be due to their capital and operating cost and problem of light limitation with respect to scale-up. Therefore, more

research attention needs to be paid on the optimisation of light supply and utilisation in order to overcome this limitation. In addition, PBRs have been rarely used for wastewater treatment; hence there is need to integrate microalgal production with wastewater treatment in these systems.

2.4.3 Hybrid systems

The integration of open ponds with photobioreactors and modification in design and mode of operation can produce hybrid systems that can have the advantages of both with consequent improvement on the limitations of the individual systems. Such systems may include integrated pond-photobioreactor; photobioreactors incorporating solar and artificial light using optical fibres to supply light from solar collectors sited outdoor; closed photobioreactors that are placed outdoor (Ogbonna *et al.*, 1999), and microalgae-activated sludge bioreactors illuminated with monochromatic light sources of specific quantum energy, for wastewater treatment. These latter systems could, among other things, possess dual benefit of satisfying aerobic bacterial oxygen requirement through microalgal photosynthesis leading to energy saving resulting from minimal or zero artificial aeration and considerable level of COD removal through bacterial oxidation of organic matter in the wastewater.

Ogbonna *et al.* (1999) developed a simple and sterilisable internally-illuminated PBR with integrated artificial-solar light collection and distribution system. The system supplies the collected light into the reactor via optical fibres. Mixing is achieved in the reactor by mechanical stirrer similar to that of conventional stirred tank reactors. The integrated light system in the reactor automatically supplies artificial light when the intensity of solar radiation falls below a pre-set minimum required value. Using this reactor with 5% CO_2 (v/v), these authors reported average biomass productivity of *C. sorokiniana* of 0.3 $g.L^{-1}.d^{-1}$ with corresponding CO_2 fixation rate of 0.846 $g.L^{-1}.d^{-1}$. These findings demonstrate the feasibility of achieving considerable biomass productivity through the use of hybrid PBR systems.

In another study, Ogbonna *et al.* (2001) investigated mixotrophic cultivation of *Euglena gracilis*, using the reactor in the earlier study under similar environmental conditions, but with addition of ethanol as organic carbon source during the heterotrophic phase. They reported biomass concentrations of 6 and 12 $g.L^{-1}$ for the photoautotrophic and

heterotrophic cycles, respectively. These findings indicate that the microalga grew more favourably in the dark with ethanol as carbon source than in the light with CO_2 as carbon source. However, use of ethanol as carbon source has both economic and practical limitations especially in pilot- and full-scale systems.

In an attempt to evaluate the performance of the above PBR, however, it appears difficult to compare the findings of this study with the earlier one since each study involved the use of different microalga. In addition, the major limitation of the illumination system of this bioreactor is the high loss of more than 60% of the collected light. This might have limited the growth and productivity of the microalgae thereby masking the potentials of the hybrid PBR system. Moreover, although the authors claimed simplicity and low-cost of this bioreactor, critical look at the components used in the system may dismiss such a claim, especially considering the possibility for commercial scale-up and sustainability issues. Hence, further studies may be required in order to optimise both the integrated system and its associated cost.

2.5 Valorisation of Microalgal Biomass

Unlike waste activated sludge and other nuisance particulate suspended materials in some wastewater treatment processes, microalgal biomass is an important resource that has various commercial applications including, but not limited to, the production of biodiesel and biogas (Chisti and Yan, 2011; Chisti, 2007), as animal feed (Stanley and Jones, 1976), in healthcare (Harun *et al.*, 2010), and in personal care products (Carlsson *et al.*, 2007; Prance, 2006). These applications are mainly based on the chemical composition and nutritional values of microalgal biomass (Spolaore *et al.*, 2006). Some of these applications are reviewed in the following sections.

2.5.1 Biodiesel

Microalgae have been considered by many researchers as source of biodiesel due to their lipid content (Chisti, 2007) which may range from 1 to 90% of their cell dry weight, depending on species and cultivation conditions (Spolaore *et al.*, 2006). The consideration of microalgal biomass as a potential source of biodiesel is continuously attracting attention due to escalating prices of petroleum products, the need for sustainable climate change mitigations, and as an alternative renewable energy source as opposed to the use of food

crops (Chisty, 2007; Sheehan *et al.*, 1998). The most commonly used methods of biodiesel production, such as trans-esterification of triglyceride, had been developed and tested more than half a century ago (Chisty, 2007). However, such methods are not devoid of limitations.

In trans-esterification of triglyceride, for example, three molecules each of glyceride and methanol react at about 65 °C, in the presence of acid, alkali or lipase enzyme as catalyst, to produce three molecules each of glycerol and methyl esters (Chisty, 2007). As pointed out by Chisty (2007), the choice of catalyst is driven by cost and the amount of biodiesel to be produced; thus alkali as the least expensive catalyst is commonly used. However, the cost of chemical catalyst and energy requirement makes this method unattractive. Despite the current cost of microalgal biodiesel, it has been considered as the most sustainable form of biofuel that has the potential to minimise the use of fossil fuels (Chisti, 2008).

However, there is need to develop cheaper methods of biofuel production although progress can be made in the near future considering the continuing trend in technology and market development (Harun *et al.*, 2010). For example, Chisti (2008) proposed a strategy for optimal utilisation of spent biomass from a biodiesel production process by integrating anaerobic digestion (AD) with biodiesel production (BP) and microalgal cultivation unit (MCU). In the integrated system, biomass could be harvested from the MCU to be used for BP.

The spent biomass from BP can be used in AD, and the effluent from AD can be recycled to MCU to supply nutrients to the algae or it could be used as fertiliser on farmlands. Alternatively, part of the spent biomass from BP can be used as animal feed and/or production of other value-added products. Interestingly, the energy generated from the AD process can be used to power the integrated system. If it is in excess, the surplus can be used to power other facilities such as small fossil-fuel based wastewater treatment plant with subsequent utilisation of the plant flue gas in the MCU.

2.5.2 Biogas

Another way of valorising microalgal biomass, as hinted above, is digesting the biomass anaerobically to produce methane which is a biogas of commercial importance. Energy generated from the methane produced can be used to power a small microalgal production system, and the surplus, if any, can be supplied to small wastewater treatment plant to

minimise the use of fossil fuel and tap the flue gas from the plant to further cultivate microalgae thereby making the process self-maintained and carbon-neutral (Chisti, 2008).

However, some recent studies on anaerobic digestion of microalgal biomass reported low methane yield and low biomass-to-biogas conversion efficiency (Zamalloa *et al.*, 2012; Gonzalez-Fernandez *et al.*, 2011). Zamalloa *et al.* (2012) attributed such low yields to the cellulosic nature of algal cell wall and its resistance to bacterial attack even at thermophilic temperatures. Surprisingly, even co-digestion with other wastes such as swine manure exhibited low methane yield (Gonzalez-Fernandez *et al.*, 2011). Nevertheless, it may be imperative to either pre-treat the biomass prior to anaerobic digestion or restrict the application of this process to microalgal species with easily biodegradable cell walls (Gonzalez-Fernandez *et al.*, 2011).

Although anaerobic digestion of microalgal biomass has received much attention recently, studies in this field are still on-going. Exploitation of substances that can enhance biodegradability of algal cell wall may be a potential research area. In addition, co-digestion of microalgal biomass with other organisms such as fungi and well biodegradable organic wastes may yield impressive results.

2.5.3 Food and nutrition

Microalgal biomass and its extracts have also been applied in food and nutrition. This includes food colouring materials in human nutrition, food supplements, or as feeds to different types of animal ranging from birds to fish (Spolaore *et al.*, 2006). For example, fresh or spent microalgal biomass from biodiesel production can serve as animal feed in aquaculture and poultry (Chisti, 2008; Stanley and Jones, 1976). This will produce protein that is useful in human nutrition when these animals feed and grow on microalgal biomass (Oswald, 1995). Interestingly, Chlorella and Spirulina powder are commercially available as food supplement for humans. For instance, those produced and packaged under the Naturya brand, marketed by Holland & Barrett. Such algae are said to be produced in outdoor raceways.

However, feeding animals with fresh algal biomass may conflict with biofuel production. Therefore, it may be preferable to use the spent biomass from biodiesel production as animal feed in order to avoid this conflicting interest. Nevertheless, feeding aquatic animals

with microalgal biomass eliminates the need and the difficulty involved in harvesting the biomass from the cultivation medium (Stanley and Jones, 1976) or sludge disposal as is the case with activated sludge systems, thereby minimising cost.

2.5.4 Pharmaceuticals

Another commercial application of microalgal biomass is in the manufacture of healthcare products (Carlsson *et al.*, 2007). For example, extracts from the green alga *Chlorella* and the cyanobacterium *Spirulina* are used to cure infectious diseases and as immune boosters in humans (Raja and Hemaiswarya, 2010). The potential of using *Chlorella* extracts to treat ailments such as anaemia, diabetes, constipation, infant malnutrition, etc., has been successfully tested (Yamaguchi, 1997).

Similarly, a complex sugar extract of *Spirulina*, *Calcium-Spirulan*, was reported to inhibit the replication of human immunodeficiency virus (HIV) and other rotaviruses (Raja and Hemaiswarya, 2010). Other healthcare uses of Spirulina extract include suppression of hyperlipidaemia, hypertension, and elevated blood glucose; and prevention of renal failure (Yamaguchi, 1997). However, this and other similar applications require the cultivation of pure microalgal cultures devoid of contamination.

2.5.5 Skin and personal care products

Microalgal extracts are also used in the manufacture of cosmetics, skin and personal care products (Stolz and Obermayer, 2005). This application exploits the chemical compounds present in photosynthetic pigments contained in microalgal biomass (Spolaore *et al.*, 2006). For example, β-carotene, a type of carotenoid usually available in the microalga *Dunaliella* was reported to be anti-carcinogenic (Yamaguchi, 1997) and thus has the potential to treat cancer when administered orally or applied onto skin. In addition, *γ*-linolenic acid, a fatty acid available in *Spirulina* biomass, with growth-promoting effect on skin cells is used to treat chapped skin (Yamaguchi, 1997).

2.6 Photosynthesis and Microalgal Metabolism

2.6.1 Photosynthesis

The principles and applications of photosynthesis are important in the research and development of carbon-neutral wastewater treatment technologies using microalgae. Photosynthesis is the process through which microalgal biomass, as a potential source of

renewable energy, is produced (Hall and Rao, 1999). It literally means building up by light - the process through which plants use light energy to synthesise organic materials from inorganic substances (Hall and Rao, 1999; 1994; 1981). Blankenship (2002) defined photosynthesis as a biological process in which organism captures and stores solar energy and uses the stored energy to carry out cellular metabolic processes; light is used in photosynthesis to drive a series of chemical reactions. The primary and natural source of light energy is the sun (Hall and Rao, 1999). Photosynthesis consists of two phases: the *light* and *dark* reactions (Collings and Critchley, 2005a).

In light reaction, light energy is absorbed by antenna chlorophyll molecules in thylakoids and transferred to reaction centre chlorophylls that generate ATP and reduced nicotinamide adenine dinucleotide phosphate ($NADPH_2$, also known as reduced pyridine nucleotide; Collings and Critchley, 2005a). The ATP and $NADPH_2$ produced serve as precursors to dark reaction (Collings and Critchley, 2005a). In dark reactions, ATP, $NADPH_2$ and CO_2 are used, with the aid of the chloroplast enzyme, ribulose bisphosphate carboxylase/oxygenase (i.e. RuBisCO), to form carbohydrate and oxygen (Collings and Critchley, 2005a). RuBisCO was reported to be responsible for catalysing the addition of CO_2 to ribulose bisphosphate in the chloroplasts of photosynthetic organisms (Collings and Critchley, 2005a).

Since algae, cyanobacteria and terrestrial plants can capture solar energy and use it to synthesise carbohydrates and other energy-rich cellular compounds (Hall and Rao, 1981), they are usually termed photosynthetic organisms. An organism is photosynthetic if it is capable of obtaining part or all of its energy for cellular processes from light (Blankenship, 2002). Two major classes of photosynthetic organisms have been reported in the literature: O_2-evolving and the non O_2-evolving (Barber, 1987). The generally known organisms that drive their cellular energy from light are higher plants and green algae (Blankenship, 2002). However, there are organisms that solely or partly, under certain conditions, drive their energy for cellular processes from light but do not carry out photosynthesis (Blankenship, 2002). Interestingly, photosynthetic organisms use energy-poor compounds (Hall and Rao, 1999): H_2O, CO_2; nutrients: N and P and light energy to synthesise carbohydrate with evolution of oxygen, O_2 (Blankenship, 2002) with simultaneous liberation of energy (Hall and

Rao, 1999). The process of photosynthesis is governed by organic pigments (Hall and Rao, 1999) at sub-cellular level (Blankenship, 2002).

2.6.2 Oxygenic and anoxygenic photosynthesis

In oxygenic photosynthesis, molecular oxygen is a by-product whereas in anoxygenic photosynthesis, molecular oxygen is not produced (Blankenship, 2002). Green algae and cyanobacteria are the typical examples of microorganisms that exhibit oxygenic photosynthesis (Blankenship, 2002). In contrast, organisms that exhibit anoxygenic photosynthesis include purple bacteria, green sulphur bacteria, and green non-sulphur bacteria (Blankenship, 2002). Irrespective of the type of photosynthesis, certain pigments are essential for this process to proceed.

2.6.3 Photosynthetic pigments

In eukaryotic photosynthetic organisms, photosynthesis is carried out by membrane-based pigment-containing proteins and mediated by proteins that are freely diffusible in aqueous solution (Blankenship, 2002). It takes place in cellular structures called chloroplasts (Blankenship, 2002). Photosynthetic pigments are chemical substances in the chloroplast that absorb visible light to possess a colourful appearance and play important roles in photochemical reactions (Gregory, 1989b).

Photochemical reactions proceed with the aid of four protein complexes: photosystem I and ATP synthase (also known as F-ATPase), both located in stroma lamellae; photosystem II, located in grana; and cytochrome b_6/f located in grana and its margins that are present in thylakoids which are contained in chloroplasts (Nelson and Yocum, 2006). The thylakoids enclose the lumen (an aqueous space) with two distinct interconnected physical structural units, the grana and the stroma lamella (Nelson and Yocum, 2006). Depending on the type of organism, the chloroplasts contain chlorophyll (Blankenship, 2002) and/or other photosynthetic organic pigments such as carotenoids and phycobilins that can absorb light energy to initiate photochemical reactions (Hall and Rao, 1999).

Chlorophylls (i.e. type *a*-*d*), carotenoids (i.e. α and β-carotenes, luteol, violaxanthol, etc.) and phycobilins (i.e. phycoerythrins, phycocyanins, allophycocyanins) are the major photosynthetic pigments that are appropriately found in higher plants; green, red and brown algae; diatoms and cyanobacteria (Hall and Rao, 1999). Carotenoids and phycobilins

are usually considered as accessory pigments serving as antennas that collect light and transfer it to photosynthetic reaction centres (Blankenship, 2002; Hall and Rao, 1999). These pigments give photosynthetic organisms their characteristic distinct colour with chlorophyll, for example, constituting about 4% of chloroplast dry mass (Hall and Rao, 1999).

The characteristics of major photosynthetic pigments in terms of colour, optical absorbance, solubility in water and organic solvents as well as occurrence in organisms are summarised in Table 2.3. Noteworthy, chlorophyll *a* is bluish-green and is commonly found in O_2-evolving photosynthetic organisms while chlorophyll *b* is yellowish-green and is usually found in leaves of higher plants and green algae (Hall and Rao, 1999). The chemical formulae for chlorophylls *a* and *b* molecules are, respectively, $C_{55}H_{72}N_4O_5Mg$ (Blankenship, 2002; Hall and Rao, 1999) and $C_{55}H_{70}N_4O_6Mg$ (Hall and Rao, 1999).

Table 2.3 Optical characteristics of major photosynthetic pigments

Pigment	Colour	Solubility	Occurrence	Absorption band (nm)
Chlorophylls	Bluish- to yellowish-green	Insoluble in H_2O, soluble in organic solvents	Higher plants, diatoms and algae	420 – 690
Carotenoids	Yellow or orange	Insoluble in H_2O, soluble in organic solvents	Higher plants, red, brown algae and diatoms	400 – 550
Phycobilins	Blue or red	Soluble in H_2O	Cyanobacteria and red algae	490– 650

Adapted from Hall and Rao (1999).

Chlorophyll molecules contain a porphyrin head and a phytol tail with a water-soluble porphyrin nucleus made up of a tetrapyrrole ring and a magnesium atom (Hall and Rao, 1999). Basically, chlorophyll molecules are cyclic tetrapyrroles (Gregory, 1989b). Low pH values (i.e. acidic conditions) usually promote the displacement of the central magnesium atom in chlorophyll (by hydrogen ions) rendering it into a metal-free molecule known as pheophytin (Blankenship, 2002). Pheophytins are important constituents of some photosynthetic reaction centre complexes and could also be formed through degradation of chlorophyll molecules or through transformation pathways of photochemical reactions (Blankenship, 2002). In microalgae, chlorophyll concentration is usually determined through optical density (OD) measurements and application of some empirical equations available in the literature (Hall and Rao, 1999; Becker, 1994).

Carotenoids are usually found in the chloroplast of some photosynthetic cells with carotenes occurring as hydrocarbons and carotenols as oxygenated hydrocarbons (Hall and Rao, 1999). The cellular location of carotenoids was reported to be the chloroplast lamella; they are bound to proteins in close contact with chlorophylls (Hall and Rao, 1999). Carotenoids absorb light energy and pass it on to chlorophyll for photosynthesis; the former also protects the latter from photo-oxidation resulting from prolonged photoinhibition caused by excessive radiation (Hall and Rao, 1999).

Phycobilins are linear tetrapyrroles (Hall and Rao, 1999; Gregory, 1989b). They are structurally related to chlorophylls except that they lack phytyl chain and magnesium atom (Hall and Rao, 1999). Cyanobacteria and red algae contain phycobilins (Blankenship, 2002; Hall and Rao, 1999) whose chromophores are linked to polypeptides to form phycobiliproteins which absorb visible light during photosynthesis (Hall and Rao, 1999).

Furthermore, two types of chlorophyll *a* exist in chloroplast with one considered as that generating an oxidant and the other generating a reductant (Hall and Rao, 1999). The two parts of photosynthesis associated with the type of chlorophyll *a* that generates a reductant and the other that generates an oxidant are known as photosystem I and photosystem II, respectively (Hall and Rao, 1999). These photosystems form two out of the four types of photosynthetic reaction centres (Rutherford and Faller, 2001; Gregory, 1989a).

Photosystem I

Photosystem I (PSI) is the protein complex that catalyses the photo-reduction of ferredoxin (Hall and Rao, 1999) by reduced plastocyanin in higher plants (or cytochrome 552 in some algae) in the thylakoids (Gregory, 1989a). The plastocyanin (located in the lumen) and ferredoxin (located in the stroma) serve as electron donor and acceptor, respectively, in photochemical reactions (Hall and Rao, 1999; Gregory, 1989a). About 50% of the light absorbed by PSI is converted to chemical energy of reduced ferredoxin with the latter reducing NADP to $NADPH_2$ catalysed by the enzyme ferredoxin-NADP reductase (Hall and Rao, 1999). Similarities exist between the path of electron transfer in PSI of cyanobacteria and higher plants with cyt-553 as the electron donor to P700, i.e. a special type of chlorophyll *a* with absorption peak around 700 to 705 nm (Clayton, 1963), in some species of the latter rather than plastoquinone (Hall and Rao, 1999).

Photosystem II

Photosystem II (PSII) is the protein complex that catalyses the photo-oxidation of water and the reduction of plastoquinone (Hall and Rao, 1999) to plastoquinol (Renger and Renger, 2008). PSII is responsible for oxidative splitting of water into one dioxygen molecule and four protons with stepwise removal of 4 electrons (Renger and Renger, 2008; Hall and Rao, 1999). The water splitting mechanism in PSII comprises 3 sequential reactions: photo-induced charge separation leading to generation of ion radical pair of oxidised reaction centre (RC) pigment ($P680^{+}$) and reduced RC plastoquinone (Q^{-}_{A}), oxidative water splitting, and reduction of plastoquinone to plastoquinol (Renger and Renger, 2008).

2.6.4 Chlorophyll absorption bands

It has been reported that all types of chlorophyll possess two absorption bands: one at high-energy wavelengths (in the blue or near ultraviolet region) and the other at low-energy wavelengths (in the red or near the infrared region) of the visible light spectrum (Blankenship, 2002). Interestingly, possession of negligible absorption in the green region of the spectrum gives chlorophyll molecules their characteristic blue-green or green colour (Blankenship, 2002). The maximum photon absorption of chlorophylls *a* and *b* are at about 663 and 645 nm wavelengths, respectively (Hall and Rao, 1999). This literally falls within the red region of the visible light spectrum and hence there lies the potential for using red light to illuminate microalgal systems for optimum photon energy utilisation.

2.6.5 Roles of enzymes in photosynthesis

Many enzymes, whose activities are modulated by light, catalyse the chemical reactions in photosynthesis (Hall and Rao, 1981). Such enzymes include phosphoribulokinase (PRK), fructose-1,6-bisphosphatase (FBPase), sedoheptulose-1,7-bisphosphatase (SBPase), pyruvate phosphate dikinase, malate dehydrogenase, ribulose bisphosphate carboxylase/oxygenase (rubisco), phosphoglycerate kinase, NADP-glyceraldehyde-3-phosphate dehydrogenase, triose phosphate isomerase, etc. (Yokota and Shigeoka, 2008; Blankenship, 2002; Hall and Rao, 1981).

Of all these photosynthetic enzymes, rubisco has been reported as the key and one of the two most important in photosynthetic carbon fixation (Blankenship, 2002; Ellis, 1979). It catalyses the CO_2-fixation step in photosynthesis with formation of two molecules of 3-

phosphoglycerate (i.e. phosphoglyceric acid, PGA) for each ribulose bisphosphate molecule reacting with CO_2. It also plays a key role in photorespiration (Roy and Cannon, 1988), a process that occurs at high irradiance, leading to inorganic carbon depletion resulting from high algal activity and concomitant high oxygen production; this condition leads to algal oxygen consumption higher than that of dark respiration (Pearson, 2005). The dual role in carbon consumption (through carbon fixation process, i.e. carboxylase activity) and oxygen consumption at the expense of carbon fixation, facilitated by the above condition (i.e. oxygenase activity), owes rubisco the 'co' in its name (Pearson, 2005).

The other key enzyme in photosynthetic carbon fixation is phosphoribulokinase that catalyses the final step of the regeneration phase of Calvin cycle – the phosphorylation of ribulose 5-phosphate to produce ribulose bisphosphate (Blankenship, 2002). Furthermore, rubisco has been reported to be responsible for catalysing the reaction of ribulose bisphosphate with O_2 molecules leading to the production of PGA and 2-phosphoglycolate (Roy and Cannon, 1988). It has been considered as the most likely abundant protein on earth (Blankenship, 2002) and a gateway through which atmospheric CO_2 is captured and converted into biomass via Calvin cycle which is comprised of 13 enzymatic reactions (Atomi, 2002; Ellis, 1979).

Of the 13 enzymatic reactions contained in Calvin cycle, only the one catalysed by rubisco fixes CO_2 (Atomi, 2002). Hence, the importance of this enzyme in photosynthetic carbon capture cannot be overemphasised. Nevertheless, the other 12 enzymatic reactions are also important as they generate ribulose-1,5-bisphosphate (RuBP) which is a reactant of the rubisco-catalysed reaction (Atomi, 2002). According to Atomi (2002), the process of CO_2 fixation by the rubisco-catalysed reaction can be summarised as follows: a molecule each of CO_2, H_2O and RuBP react to form two molecules of 3-PGA. In the process, a total of 3 molecules of CO_2 are fixed which react with 3 molecules of RuBP to produce 6 molecules of 3-PGA. Five of the six 3-PGA molecules produced are used to regenerate 3 molecules of RuBP with the remaining molecule used in cellular biomass synthesis.

Another enzyme that plays an important role in photosynthetic carbon fixation is carbonic anhydrase (Badger and Price, 1994). It is a zinc-containing enzyme that catalyses the

reversible conversion of CO_2 to HCO_3^-, simply represented by Equation 2.6 (Badger and Price, 1994).

$$CO_2 + H_2O \leftrightarrow HCO_3^- + H^+ \quad (2.6)$$

CO_2 reacts with an intermediate of Zn-OH in the forward reaction whereas HCO_3^- reacts with Zn-H_2O in the reverse reaction, at the active site of the enzyme (Badger and Price, 1994). Due to the slow nature of the reversible conversion of the inorganic carbon species shown in Eq. 2.6, carbonic anhydrase is essential in photosynthetic cells as it accelerates the interconversion reaction of these inorganic carbon species (Badger and Price, 1994). Carbonic anhydrase plays a role in the supply of CO_2 to the active site of rubisco in the chloroplast stroma at a higher rate than the uncatalysed interconversion reaction (Badger and Price, 1994). Nevertheless, Badger and Price (1994) illustrated that the photosynthetic requirement of carbonic anhydrase differs from one type of photosynthetic organism to another.

2.6.6 Photosynthetic efficiency

The photosynthetic efficiency of microalgae directly influences their growth and productivity (Grobbelaar, 2009). Microalgae have been reported to be 10 to 50 times photosynthetically more efficient than higher plants (Wang *et al.*, 2008). Photosynthetic efficiency is usually expressed as the energy of the biomass produced through the process divided by the energy of the incident light photons (Grobbelaar, 2009). Although up to 2000 $\mu mol.s^{-1}.m^{-2}$ of solar irradiance reaches the earth surface, only a fraction of this irradiance is used to photosynthetically capture CO_2 with efficiency ranging from 0.1 to 8% or even higher (Grobbelaar, 2009). However, controversies exist on photosynthetic efficiencies reported in the literature as some of the values reported are based on theoretical calculations (Grobbelaar, 2009).

It has theoretically been estimated that maximum quantum efficiency of 0.125 mol carbon per mol of light quanta; which is equivalent to 12 $g.m^{-2}.d^{-1}$ or about 30 g(dry weight of fixed carbon).$m^{-2}.d^{-1}$ (Grobbelaar, 2009). This theoretical efficiency has been estimated to reach 200 $g.m^{-2}.d^{-1}$ of carbon in systems operated with light pulsing, which is about 8-fold the maximum observed in practice (Grobbelaar, 2009). Grobbelaar (2009) reported light pulsing at high frequencies equivalent to turnover of electrons in photosynthetic electron transport

chain, and limiting antennae sizes as some of the strategies used for achieving high photosynthetic efficiencies. However, he pointed out that scaling from bench to full scale still remains a major problem affecting microalgal cultivation due to low photosynthetic efficiency.

2.6.7 Photoautotrophy in microalgae

Microalgae are said to be autotrophic if they require inorganic carbon (e.g. CO_2, carbonates and bicarbonates) as carbon source (Lee, 1999; Tuchman, 1996). They are photoautotrophic if they require inorganic carbon as carbon source and light as source of energy to carry out photosynthesis; or chemoautotrophic if they require inorganic carbon as carbon source and obtain their required energy for metabolism through oxidation of inorganic compounds rather than from light (Lee, 1999; Tuchman, 1996). Algae that strictly require light in their metabolic processes could be termed obligate autotrophs (Tuchman, 1996).

2.6.8 Heterotrophy in microalgae

Conversely, microalgae could be heterotrophic if they require organic carbon as carbon source; they may either be photoheterotrophic if they use organic carbon as carbon source and light as source of energy, or chemoheterotrophic if they use organic carbon as carbon source and obtain their metabolic energy through oxidation of organic compounds (Lee, 1999; Tuchman, 1996). Similarly, those algae that strictly require organic carbon as carbon source and get their energy from oxidation of chemical compounds in the absence of light could be termed obligate heterotrophs (Tuchman, 1996).

Although certain microalgal species may exhibit autotrophic (Terry and Raymond, 1985) or heterotrophic growth (Perez-Garcia *et al.*, 2011b), some algae may intermittently exhibit both forms of metabolism depending on presence or absence of light and the type of carbon source available in the cultivation medium and could be considered as mixotrophic or facultative mode of metabolism (Lee, 1999; Tuchman, 1996). Mixotrophy in microalgae could be beneficial in that it could eliminate or minimise the profound effect of light and carbon limitations and consequently result in no adverse effect on algal growth and productivity which could in turn greatly influence wastewater treatment efficiency.

2.7 Factors Affecting Microalgal Photosynthesis

The factors that commonly limit microalgal photosynthesis include the amount and quality of irradiance used to illuminate the algal culture, concentration and bioavailability of carbon and nutrients for metabolism, photo-inhibition due to excessive irradiance (Kirk, 1994), presence of inhibitory substances or conditions, such as high dissolved oxygen concentration, etc (Shelp and Canvin, 1980). Algal growth may be inhibited by certain substances at high concentration or under unfavourable conditions. The most common forms of inhibition in algae include those caused by high free ammonia concentration; high nitrite concentration; and inhibition due to strong photon flux density (i.e. photoinhibition; Powles, 1984).

2.7.1 Inorganic carbon concentration

Inorganic carbon concentration plays a critical role in microalgal photosynthesis as reflected by the carbon content of microalgal biomass. Microalgal biomass is about 50% carbon (Vonshak, 1986). Algae require inorganic carbon to carry out photosynthesis (Becker, 1994). Since ambient CO_2 concentration is not sufficient to sustain optimal algal growth, provision of inorganic carbon at higher concentration is essential to enhance algal growth and biomass productivity (Becker, 1994). Availability of CO_2 in aqueous medium is based on the equilibrium of inorganic carbon species, which is pH dependent (Becker, 1994). See section 2.7.4 for a brief review on pH-dependent inorganic carbon species equilibrium in aqueous medium.

Hall and Rao (1981) reported that lowering CO_2 concentration in light-limiting stage did not affect the rate of photosynthesis in *Chlorella* cultures. They pointed out that CO_2 does not directly participate in photochemical reactions. However, they stated that increasing CO_2 concentration at light intensities above the rate limiting stage considerably enhances photosynthesis. They suggested that increasing CO_2 concentration up to 1000 ppm can result in fairly high rate of photosynthesis.

2.7.2 Nutrients

Next to carbon, the most important chemical substances in algal photosynthesis are the nutrients N and P. N is an essential constituent of algal growth media and algae are generally able to use ammonium, nitrate, or other organic substances such as urea as

sources of nitrogen, whilst nitrite is rarely used due to its toxicity at high concentration (Becker, 1994). High nitrite concentration and its toxicity on algae are briefly reviewed in Section 2.7.8. P plays key roles in photochemical reactions such as photophosphorylation that generate the key energy-rich compound, ATP; P is often considered as growth-limiting in natural algal systems (Becker, 1994). Photophosphorylation is the light-driven synthesis of ATP from ADP and inorganic phosphate (Hall and Rao, 1999).

Algae usually assimilate inorganic P in the form of orthophosphate in an energy-dependent process with the energy provided by photosynthesis or respiration, and that optimum phosphate uptake and tolerance vary with algal species (Becker, 1994). Algal P uptake has been reported to be dependent on pH and concentrations of metal ions such as those of magnesium, potassium and sodium (Becker, 1994). In commercial algal production systems, nutrients are provided in the form of inorganic fertilizers which may be expensive.

2.7.3 Illumination

At low light intensity, the rate of photosynthesis, measured as O_2 evolution, of pure cultures of *Chlorella* cultivated under atmospheric CO_2 concentration increased linearly with light intensity up to the end of light-limiting stage (Hall and Rao, 1999). After this stage, any increase in light intensity resulted in no further increase in the rate of photosynthesis (Hall and Rao, 1999). However, photosynthetic efficiency can be enhanced by the use of supplementary light of lower wavelength than the main light source (Hall and Rao, 1999).

The above light enhancement, discovered by Emerson and his colleagues in 1940 in the USA, has been reported to be based on studies of action spectra of photosynthesis and chlorophyll fluorescence for various algal species including *Chlorella* (Hall and Rao, 1999). In this context, an action spectrum of photosynthesis has been described (Hall and Rao, 1999) as a plot of rate of photosynthesis by visible light measured as CO_2 fixation or O_2 evolution versus light absorbance or wavelength. Emerson and co-workers measured yield of photosynthesis as a function of monochromatic light used to illuminate *Chlorella* (Hall and Rao, 1999). They found that red and blue lights were the most absorbed by chlorophyll in the algal cells with the former and the latter monochromatic lights having absorbance ranging from 650 to 680 nm and 400 to 460 nm, respectively (Hall and Rao, 1999).

They further discovered that the photosynthetic efficiency of the red light was almost 40% higher than that of the blue light. They obtained increase in photosynthetic yield in far-red light with wavelength of about 700 nm by supplementing the illumination with red light of lower wavelength of about 650 nm. They further found out that the photosynthetic yield obtained for the light mixture was higher than the sum of the yields for the individual lights used in separate experiments. Such increase in photosynthetic efficiency due to the supplementary light was termed *Emerson enhancement effect* (Hall and Rao, 1999). The enhancement of photosynthesis by the use of supplementary light has been related to energy absorption and its transfer to chlorophyll *a* by accessory pigments (Hall and Rao, 1999).

2.7.4 pH

One of the important factors influencing microalgal photosynthesis is pH as it plays a considerable role on the availability of inorganic carbon in aqueous solution. The concentration of inorganic carbon species in water is greatly influenced by pH (Emerson and Green, 1938) and the availability of carbonate (CO_3^{2-}), bicarbonate (HCO_3^-) and free carbonic acid ($CO_2 + H_2CO_3$) vary with variation in pH (Hsueh *et al.*, 2009; Emerson and Green, 1938). Photoautotrophic carbon assimilation in microalgae depends on the availability of inorganic carbon species in aqueous medium.

Emerson and Green (1938) studied the effect of hydrogen ion concentration on *Chlorella* photosynthesis, using various carbonate-bicarbonate mixtures. The variation of available inorganic carbon species (from 0 to 100%) with respect to pH (from below 4 to 12) can be described according to Emerson and Green (1938) as follows. Free CO_2 is maximally available in solution at pH 4 or lower and decreases with increasing pH up to almost its negligible concentration at pH 8.

Conversely, CO_3^{2-} is not available in solution on the acid side of pH 8. However, it is minimally available at pH 8 and increases with increase in pH up to its maximum concentration around pH 12. On the contrary, HCO_3^- is available in solution within the range of the acidic and alkaline pH mentioned above. Its concentration is minimally available around pH 4 but increases with increase in pH and predominates at pH 8. It subsequently decreases with increase in pH up to its second minimum value around pH 12. Predominance

of free CO_2 in solution results in acidic pH which is not unconnected to the formation of H_2CO_3. However, CO_2 assimilation with concomitant accumulation of hydroxyl ions (OH^-) due to algal photosynthesis raises the pH towards alkaline side (Mara, 2003b).

2.7.5 Dissolved oxygen

Dissolved oxygen is an important by-product of microalgal photosynthesis which plays a key role in bacterial COD removal in a consortium involving these two organisms. As an alternative to algal assimilation of CO_2, DO production has been employed by many researchers as a means of measuring algal photosynthesis. High DO evolution in an algal system can signify high rate of photosynthesis or algal activity.

DO profile and algal activity vary with depth, and DO can reach supersaturation level during maximum photosynthetic activity at the upper layers of algal ponds (Pearson, 2005). Aerobic conditions resulting from algal photosynthesis can be obtained up to the depth of 0.6 m in maturation ponds but can hardly go beyond 0.3 m in facultative ponds, under maximum light intensity (Pearson, 2005).

In every mg of DO available in algal ponds, about 0.8 mg or more comes from algal photosynthesis and that ponds are mainly aerated through algal activity rather than surface aeration. Based on the chemical constituents of microalgal biomass, an average of 1.55 g of oxygen was estimated to be produced from every g of biomass (Pearson, 2005).

2.7.6 Temperature

Temperature is the key environmental factor that influences microalgal growth. Such influence can be due to the role played by temperature in biochemical reactions and microbial metabolism (Paterson and Curtis, 2005). Maximum microalgal productivity can only be achieved when the temperature in the cultivation system is optimum for growth (Tredici, 2004). Microalgae can grow at both low and high temperatures with some algal species tolerating higher temperatures than others.

However, the optimum temperature for microalgal growth may differ between species. For example, the blue-green algae, *Thermosynechococcus* sp. has exhibited increase in cell density at temperatures ranging from 40 to 55 °C (Hsueh *et al.*, 2009) while the green algae

Scenedesmus and *Chlorella* showed increase in growth rate when temperature was increased from 25 to 35 °C (Hanagata *et al.*, 1992).

2.7.7 Free ammonia

Unionised ammonia (NH_3) has been reported to be toxic to algae (Mara, 2003b). Its toxicity increases with increasing pH (Mara, 2003b). Microalgal tolerance to toxic effect of NH_3 may vary from one algal species to another. The toxicity of NH_3 to algae has been linked to its neutral state, its lipid-soluble property and its ability to permeate through biological membranes (Kleiner, 1985). For example, NH_3 concentration of 2 mM (i.e. about 34 $mg.L^{-1}$) at pH 8 was reported to inhibit photosynthesis and growth of *Scenedesmus obliquu*s in HRAP treating domestic sewage (Abeliovich and Azov, 1976). Conversely, a study by Konig *et al.* (1987) reported the tolerance of Chlorella to NH_3 concentration up to 170 $mg.L^{-1}$ at pH 9.

Besides the total concentration of both free and ionised ammonia, pH and temperature were reported as the most important factors influencing the availability of NH_3 in a given solution (Konig *et al.*, 1987) and that its concentration varies exponentially with increase in pH (Ruffier *et al.*, 1981). Temperature was also reported as an important parameter influencing the concentration of free ammonia in aqueous media. Ruffier *et al.* (1981) estimated that temperature rise by one order of magnitude can double the NH_3 concentration of a given solution. As such the concentration of NH_3 in a given solution can be controlled in the laboratory through pH and temperature control. Although pH control can be achieved in out-door systems through CO_2 addition as reported by Park and Craggs (2010), temperature is practically uncontrollable.

2.7.8 High nitrite concentration

High nitrite concentration is an important water quality indicator due to the toxicity of this chemical substance to macro- and microorganisms (Philips *et al.*, 2002). Nitrite accumulation in both laboratory and full-scale microalgal wastewater treatment systems is rarely reported in the literature. Nevertheless, this phenomenon has been reported in higher plants, bacterial and general aquatic systems (Philips *et al.*, 2002). In a review, Philips *et al.* (2002) discussed the possible causes, effects and origins of nitrite accumulation in aquatic environment. They listed DO, pH, inorganic phosphate, volatile fatty acids (VFAs) and reactor operation, as some of the factors influencing nitrite accumulation in aquatic

systems. Owing to the fact that nitrite is an intermediate in both nitrification and denitrification process, they reported that it can accumulate in aquatic environment under both aerobic and anoxic conditions.

Philips *et al.* (2002) pointed out that ammonium oxidation via incomplete nitrification and nitrate reduction via incomplete denitrification under aerobic and anoxic conditions, respectively, can result in elevated nitrite concentration. It can be said that neither complete nitrification of ammonium to nitrate nor complete denitrification of nitrate to nitrogen gas results in nitrite accumulation. Nevertheless, elevated equilibrium concentration of nitrite may be mistaken as nitrite build-up or accumulation (Philips *et al.*, 2002). Therefore, consistency may be a yardstick for deciding whether nitrite accumulates in a given system or not despite recorded high nitrite concentration. Nitrite usually accumulates in aquatic systems if the processes of nitrification and/or denitrification proceed at non-steady state conditions (Philips *et al.*, 2002).

Due to the coupling of ammonium and nitrite oxidation in the nitrification process, imbalance in the activity of ammonia oxidising bacteria (AOB) or nitrite oxidising bacteria (NOB) may result in nitrite accumulation, especially when the rate of ammonium oxidation exceeds that of nitrite due to possible inhibition of NOB (Philips *et al.*, 2002). This may be due to repression of nitrite reductase, the enzyme catalysing the reduction of nitrite, or the inhibitory effect of high nitrate concentration on this enzyme (Philips *et al.*, 2002).

Therefore, it may be argued that nitrite accumulation is quite unusual during normal algal activity under conditions favourable for growth. Although this mysterious phenomenon may be desirable in bacterial systems due to the possibility in cost saving resulting from the minimisation of oxygen needed for COD removal, algal ammonium assimilation is preferred here over partial nitrification which may lead to nitrite build-up with apparent inhibition of algal growth which can consequently affect wastewater treatment efficiency.

2.7.9 Photoinhibition

Although light is essential for microalgal photosynthesis, certain amount of irradiance can inhibit microalgal growth and hinder productivity. Such irradiance values are those higher than full sunlight, i.e. above 2000 $\mu mol.s^{-1}.m^{-2}$ (Powles, 1984). However, photoinhibition of algal cells in light-limited zone due to sudden exposure to irradiance values as low as 50

$\mu mol.s^{-1}.m^{-2}$ has also been reported (Powles, 1984). Although the short-term inhibition by strong light photons is reversible, prolonged exposure may result in photo-oxidative bleaching of photosynthetic pigments (Powles, 1984) leading to inactivation or damage of photosystem II (Long *et al.*, 1994).

Nevertheless, the problem of photoinhibition in microalgal systems can be avoided through proper reactor design, determination of the amount of irradiance optimum for algal growth and use of high density algal cultures. In addition, photoinhibition can also be minimised or avoided through pulsing of the light source, especially under conditions of high irradiance (Jeong *et al.*, 2013). However, caution must be taken to avoid excessive light attenuation due to high algal concentration which may consequently affect algal productivity especially in reactors with long light path length.

2.8 Light-Emitting Diodes

Light-emitting diodes (LED) are semiconductor devices (Gillessen and Schairer, 1987) which convert electrical energy into electromagnetic radiation with the wavelength of part or all the radiation falling within the visible light spectrum (Bergh and Dean, 1976; Bergh and Dean, 1972). Klingenstein (2004) has defined semiconductors as solid materials which due to their lattice structure, depending on temperature, have a larger or smaller number of free-moving or hole (i.e. missing) electrons. The process of converting electrical energy into light is known as electroluminescence (Ng, 1995). Electroluminescence can occur at ambient temperatures as compared to incandescence, which is also visible electromagnetic radiation emitted from solid material but only when heated at high temperature usually above 750 ^{o}C (Fred, 2006). Apparently, incandescence requires more energy input than electroluminescence.

LED is considered as cold light source. That is, its temperature is far from been in equilibrium with that of the emitted radiation (Gillessen and Schairer, 1987). Non-equilibrium has to be achieved through charge carrier injection within a semiconductor crystal (Gillessen and Schairer, 1987). The injection is usually done across a p-n junction (i.e. positive-negative referring to the boundary of two different semiconductor materials) within the crystal into a region where the injected carrier electron can convert its excess energy into light (Gillessen and Schairer, 1987). LED essentially consists of one p-n junction

where excess injected charge carriers recombine in the n or p layer to emit light photon (Klingenstein, 2004).

Semiconductor crystals are condensed materials having regularly organised structure (Gillessen and Schairer, 1987). Many semiconductor compounds have a structure closely related to diamond lattice with atoms belonging to one sub-lattice of one type and the atoms belonging to the other sub-lattice of another (Gillessen and Schairer, 1987). In theory, semiconductor crystal lattices are considered under ideal situation whereas, however, in practice they are not (Gillessen and Schairer, 1987). They have been reported to contain defects that are usually classified based on their dimensions as point, line, two- or three-dimensional, which may be due to presence of impurities (Gillessen and Schairer, 1987).

Interestingly, impurities are intentionally introduced into semiconductor crystals, usually referred to as 'doping', to create a p-n junction thereby modifying their electrical properties (Gillessen and Schairer, 1987). However, unwanted impurities in semiconductor materials may adversely influence the property of the crystal which may eventually affect the performance of the LED produced (Gillessen and Schairer, 1987). Semiconducting materials are usually made of layers of same or different compounds with the active layers grown by liquid- or vapour-phase epitaxy on crystal substrates having close lattice match to the active layers (Ng, 1995). Typical semiconductor material substrates include aluminium gallium arsenide (AlGaAs), gallium arsenide (GaAs), gallium phosphide (GaP), indium phosphide (InP), silicon carbide (SiC), etc. (Klingenstein, 2004; Ng, 1995; Bergh and Dean, 1972).

Compounds of group III-V elements have been reported to be more suitable as semiconducting materials (with gallium as the main element,) although group II-VI compound semiconductors have direct energy gap and are expected to produce more efficient LED (Matthews *et al.*, 2009; Gillessen and Schairer, 1987). However, the latter semiconductor compounds have inherent disadvantage over the former due to impurity doping in forming p-n junctions making them practically unsuitable in LED production (Gillessen and Schairer, 1987).

2.8.1 Prospects of LED over other artificial light sources

LED are gaining increasing popularity in microalgal research. They have the tendency to replace other light sources such as incandescent and fluorescent lamps due to advantages of the former over the latter (Mehta *et al.*, 2008). Such advantages include low power consumption, low input voltage, low heat output, luminous efficacy (a measure of the amount of light provided by a light source in lumens for an input amount of power in watts; Matthews *et al.* (2009)), lower start-up time, easy control, different colour bands and longer life span (Mehta *et al.*, 2008). Light-emitting diodes have lifespan of up to 100,000 h or more.

Interestingly, used LED can be recycled easily as they are composed of fairly benign substances compared to incandescent lamps that contain mercury which poses higher pollution risk to the environment (Mehta *et al.*, 2008). In addition, Mehta *et al.* (2008) reported LED electroluminescence efficiency of about 90% with luminous flux as high as 120 lumen.W^{-1}.

More importantly, LED have very low carbon footprint with associated opportunity for carbon credits as well as high potential towards enhancing environmental sustainability (Mehta *et al.*, 2008). They have lower carbon footprint than fluorescent and incandescent lamps. Moreover, the problems of light limitation associated with the scale-up of PBR can be overcome through focussed research on the use of LED to replace conventional fluorescent and incandescent lamps. Due to their small size, many LED can be mounted on a narrow strip of Vero board and inserted into PBR in a water-tight material (to prevent short-circuiting when in contact with water) in order to fully utilise their light output.

Interestingly, LED can also be used in hybrid microalgal cultivation systems. For example, LED can be used to illuminate a pilot-scale pond located outdoor, housed in an enclosure (analogous to greenhouse) made of water-proof transparent material. The transparent material can serve dual purpose: preventing the pond from rain and facilitating intermittent utilisation of solar radiation during the day. The LED light can be solely used at night or as supplement to solar radiation on cloudy days. Alternatively, LED can be used to illuminate hybrid algae-activated sludge reactor. Panels of matrix board with mounted LED can be incorporated into such a hybrid reactor to treat municipal wastewater with a view to

minimising operational cost in terms of elimination of artificial aeration required by aerobic bacteria through algal photosynthetic oxygenation.

2.8.2 Classification of LED

Various classifications of LED are available in the literature. Such classifications are mostly based on structural configuration (Ng, 1995); light intensity, luminous flux, colour or wavelength (Vishay Intertechnology Inc, 2004); chemical nature of the substrate, e.g. organic substrate layer insertion between semiconductor layers (Yamada *et al.*, 2003); etc. Ng (1995) classified LED based on structural configuration as edge-emitting and surface-emitting. In edge-emitting LED structure, for instance, light is confined to a plane and radiates parallel to p-n junction whereas light is radiated orthogonal to the junction in surface-emitting LED structure (Gillessen and Schairer, 1987).

2.8.3 Prospect of red over other coloured LED in photosynthesis

The prospect of red over other coloured LED can easily be demonstrated with reference to the characteristics of red light photons in visible light spectrum of the solar radiation. This can be done with respect to the energy and wavelength of different colour of monochromatic light photons of the spectrum. The visible light spectrum, with its wavelength ranging from 400 to 700 nm, is usually referred to as photosynthetic active radiation (PAR) with respect to chlorophyll *a*-bearing organisms (Blankenship, 2002).

Scattering and absorption of sunlight by greenhouse gases and other particles in the atmosphere reduce the amount of solar radiation reaching the earth surface (Blankenship, 2002). In the lower region of the spectrum, ultraviolet light is mainly absorbed by ozone molecules before reaching the earth surface whereas infrared light is greatly absorbed by CO_2 and water vapour, in the upper part of the spectrum (Blankenship, 2002).

Chapter 3

Effects of CO_2 addition and variation in red LED irradiance on bench-scale microalgal bioreactors treating real municipal wastewater

3.1 Introduction

This chapter presents the data of experiments conducted in twelve 1-litre bench-scale bioreactors, 6 with and 6 without CO_2 addition. The experiments were conducted to evaluate the effects of CO_2 addition and variation of irradiance on microbial growth rate, biomass productivity and the efficiency of the bioreactors in treating real municipal wastewater. The results of the experiments served as a basis for subsequent experiments using pilot-scale photobioreactors whose data are presented in Chapter 4. Red LED with wavelength of 660 nm were used as an external light source to illuminate the microalgae in the 1-L bioreactors during the treatment of settled municipal wastewater.

3.2 Materials and Methods

3.2.1 Light source and light measurement

Red LED with electrical power of about 0.04 W (i.e. typical current of 20 mA and voltage of 2.2 V) and characteristic wavelengths of 660 nm (N45AT, Maplin Electronics) were used as light source in these experiments. The LED were 8.6 mm long and 5 mm in diameter. They were soldered unto Vero boards (JP51, Maplin Electronics) with flying leads of insulated 1 mm diameter copper wires were connected to variable AC-DC power supply (VN10L, Maplin Electronics) set at 9 V. The power supply was plugged to a mains timer and operated at 12:12 light-dark cycle (Jacob-Lopes *et al.*, 2009; Lee and Lee, 2001b).

Four LED were connected in series, with a 300 Ω resistor (M300R, Maplin Electronics) also connected in series on the Vero boards. The values of the irradiance, number of LED and clamping heights for all the bioreactors are shown in Table 3.1; R1 and R7 were operated in the dark and served as the control bioreactors. All light measurements were performed with LI-192 underwater quantum sensor connected to LI-250 light meter (LI-COR Biosciences, USA).

Table 3.1 Average values of irradiance measured at the culture surface of the bioreactors

Reactor	Clamping height (cm)	Number of LED	Irradiance (µmol.s^{-1}.m^{-2})
R1; R7	n/a	0	0
R2; R8	30.6	16	25.29
R3;R9	28.0	16	64.47
R4; R10	23.0	16	113.87
R5; R11	15.5	16	181.19
R6; R12	16.0	24	234.30

n/a = not applicable

The LED banks were clamped horizontally with retort stands (facing downwards) to illuminate the microalgal culture. Different clamping heights (Table 3.1) were used for the experimental bioreactors in order to achieve five different values of irradiance.

3.2.2 Microalgal inoculum

A mixed culture of microalgae (and bacteria) was used to inoculate the bioreactors. The original microalgal culture was a mixture of strains isolated from natural wasters collected from Cramlington Sewage Treatment Works, UK (predominantly *Scenedesmus* and *Chlorella* sp; data not shown). The algal culture was virtually free from grazers. It was grown in batch mode on Bold's Basal medium (Culture Collection of Algae and Protozoa, 2010) in externally-illuminated 20-L transparent polythene jars prior to its use in this study. The culture was illuminated with cool white fluorescent lamps at average light intensity of about 71 µmol.s^{-1}.m^{-2} and aerated with compressed air at flow rate of 2 L.min^{-1}, to serve as carbon source. After 7 days, the resulting microalgal culture was centrifuged at 1000 g for 20 min at 22 °C using a centrifuge (Cryofuge 5500i; Thermo Fisher, Germany) to concentrate the algal biomass and separate it from the medium according to Standard Methods (10200 C.; APHA, 2005).

3.2.3 Wastewater

Settled domestic wastewater was collected from the effluent of the primary settling tanks at Sedgeletch Sewage Treatment Works, Houghton-le-Spring, UK, and used without addition of any nutrient media, as substrate in the experiments. Prior to the experiments, the wastewater was centrifuged at 5346 g at 22 °C, for 30 min, using the above centrifuge and the supernatant was filtered through 0.45 µm glass fibre filters (GF/A 513-5207; VWR, UK) to remove all suspended solids. The filtered wastewater was then stored at 4 °C (for 48 h)

prior to the experiments to minimise possible changes due to biochemical activity and maintain its characteristics.

A portion of the filtered wastewater was analysed to determine initial quality parameters and the result obtained is shown in Table 3.2. The filtered wastewater was used as growth medium with its natural ammonium content as sole source of nitrogen for the microalgae as only a small amount of nitrate was detected during the analytical tests. It is notable that no nitrite was detected in the wastewater. Sixty-five mL of the concentrated centrifuged microalgal culture was added to 12.35 L of the filtered wastewater resulting in 1-in-200 dilution to obtain an initial average biomass concentration of 0.092 $g.L^{-1}$ in the inoculated wastewater.

Table 3.2 Filtered wastewater and microbial culture characteristics

	Parameter ($mg.L^{-1}$)*							
	NH_4-N	COD	IC	OC	NO_3^-	PO_4^{3-}	DO	pH
a	45 (0.0)	83 (1.0)	60.0 (1.9)	52.4 (1.0)	0.27 (0.01)	11.8 (0.3)	4.22 (0.01)	7.76
b	49 (2.1)	83 (3.0)	59.6 (0.3)	54.0 (0.5)	0.32 (0.01)	12.6 (0.2)	4.22 (0.01)	7.50

* Except for pH; a: settled domestic wastewater; b: inoculated wastewater

A total volume of 13 L of low density mixed algal culture was achieved for the experiments after inoculation. One litre of this culture was applied to each of the 12 bioreactors. The inoculated wastewater characteristics are shown in Table 3.2. About 60 mL of mixed liquor was withdrawn from each of the bioreactors for routine measurements every 48 hours. The wastewater was filtered through a 0.2 µm filter (17597Q, Sartorius, UK) prior to chemical analyses and the nutrient content was not supplemented with any medium or stock solution as practiced in previous studies (e.g. Wang *et al.*, 2007; Yun *et al.*, 1997) in order to test the treatability of the wastewater devoid of any nutrient supplementation. In addition, the culture was not adapted to high CO_2 concentration prior to these experiments as practiced in previous studies reported in the literature (e.g. Yun *et al.*, 1997).

3.2.4 Bioreactor set-up and operation

Experiments were conducted to evaluate the effects of CO_2 addition on the microalgal growth rate and biomass productivity as well as municipal wastewater treatment efficiency. Two sets of microalgal bioreactors were used in the experiments: one set with and the other without CO_2 addition. The experiments were conducted in bioreactors consisting of 1-L

Pyrex beakers illuminated with red LED. A total of 12 bioreactors were set up and monitored for 19 d.

Six bioreactors were supplied with premixed industrial-grade gas composing of CO_2, O_2 and N_2. The remaining 6 bioreactors were operated without artificial CO_2 addition but only natural supply of CO_2 from ambient air through surface aeration. Ten of the bioreactors were illuminated with the LED with every pair having the same amount of irradiance except a pair that served as control (i.e. 1 each with and without CO_2 addition). The operating conditions of all the bioreactors are shown in Table 3.3, and Figure 3.1 shows sections of the bioreactors.

Table 3.3 Operating conditions for all the bioreactors (√ = yes and x = no)

Bioreactor	LED light	CO_2 supplementation	pH control	Temperature control
R1	x	√	x	x
R2	√	√	x	x
R3	√	√	x	x
R4	√	√	x	x
R5	√	√	x	x
R6	√	√	x	x
R7	x	x	x	x
R8	√	x	x	x
R9	√	x	x	x
R10	√	x	x	x
R11	√	x	x	x
R12	√	x	x	x

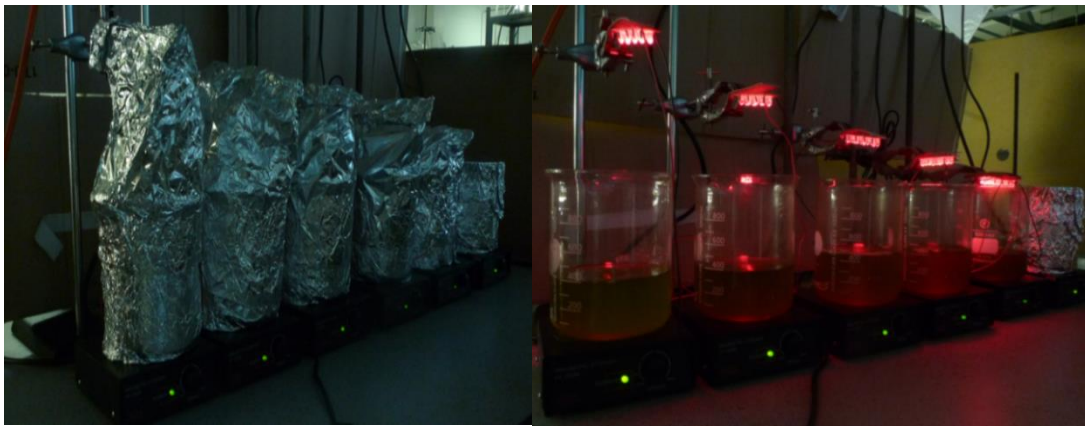

Figure 3.1 Experimental set-up (left: bioreactors covered with aluminium foil; and right: without aluminium foil cover)

Both the bioreactors with and without CO_2 addition were set up and operated concurrently in batch mode, with neither pH nor temperature control. They had the same initial biomass and substrate concentration. Wastewater samples for analytical tests were collected from control bioreactors moving to the other experimental bioreactors starting from the ones with lowest to those with highest irradiance values. The bioreactors with CO_2 addition were placed in one row and those without CO_2 addition in another and serially numbered from R1 to R6 and R7 to R12, respectively, based on increasing irradiance. Aluminium foil was used to isolate the bioreactors from external light sources, concentrate the irradiance, and maximise the amount of photons reaching the algal cells.

The CO_2-aenriched bioreactors were supplied with premixed industrial-grade gas composing of 10% CO_2, 6% O_2 and balance of N_2 (Hsueh *et al.*, 2009), sourced from BOC Gas (with product code 226964-AK-C). The gas was bubbled at constant flow rate of 40 $mL.min^{-1}$, via 6-outlet brass manifold connected to 6 mm diameter silicon tubes. The silicon tubes connected the manifold to 0.5 mm pore gas spargers (Code 226; SUPA Aquatic Supplies Ltd, UK) inside the bioreactors. A control valve at each of the manifold outlets and an airflow meter (FR2A12BVBN; Key Instruments, Trevose, PA) were used to regulate and set the gas flow rate for each CO_2-enriched bioreactor.

In addition, each bioreactor was equipped with a magnetic stirrer (HI-190M, Hanna Instruments, UK) set at about 100 rpm to continuously agitate the culture. The stirring prevented the algal biomass from settling at the bottom of the bioreactors, enhanced gas mixing and continuously exposed the algal cells to irradiance. The gas was supplied to the bioreactors during the light phase of the photoperiod stated in Section 3.2.1.

3.2.5 Analytical tests

Samples were routinely collected from the bioreactors every 48 h and analysed for the following parameters: ammonium (NH_4-N), COD, DO, inorganic carbon (IC), organic carbon (OC), total carbon (TC); anions: nitrite (NO_2^-), nitrate (NO_3^-) and phosphate (PO_4^{3-}). In addition, total suspended solids (expressed as cell dry weight, CDW); optical density (OD) at 560 nm, pH and temperature were also monitored. All samples for chemical analyses were filtered through 0.2 µm filters (Sartorius, UK) prior to measurements and all measurements were carried out in triplicate except for pH.

The growth rates of the microalgal culture were determined using Equation 3.1 by considering the linear part of exponential growth phase of the plot of natural logarithms of CDW values against time of cultivation. The CDW values were correlated with corresponding OD values in Equations 3.2 and 3.3, for bioreactors with and without CO_2 addition, respectively (coefficients of correlation are shown in the parenthesis).

$$\mu_{max} = \frac{1}{t_2 - t_1} \ln\left(\frac{CDW_{t2}}{CDW_{t1}}\right) \quad (3.1)$$

$$CDW_{CO_2} = 0.5535 OD_{560;\, CO_2} - 0.0469 \ (R^2 = 0.98) \quad (3.2)$$

$$CDW_n = 0.9982 OD_{560;\, n} - 0.0017 \ (R^2 = 1.00) \quad (3.3)$$

In Equations 3.1, 3.2 and 3.3, μ_{max} is the maximum specific growth rate; CDW_{t1} and CDW_{t2} are the cell dry weights in $g.L^{-1}$ corresponding to the initial and final times of cultivation t_1 and t_2, respectively. The subscripts *CO_2* denotes artificial CO_2, *n* denotes natural surface aeration, and *560* the wavelengths at which the OD was measured.

3.2.6 Measured parameters

3.2.6.1 Soluble COD

The soluble COD (SCOD) measurements were performed with commercial test kits (25-1500 $mg.L^{-1}$ COD; Merck, Germany, procured from VWR, UK) according to closed reflux, colorimetric method (5220 D.; APHA, 2005) based on manufacturer's instructions as follows. Three mL of filtered sample was added to the test kit and digested for 120 min using pre-heated QBH2 heating block (Grant, UK) set at 150 ± 1°C. The samples were removed and allowed to cool at room temperature for about 10 min after which they were swirled and allowed to cool further at room temperature. The sample concentrations were then measured (in $mg.L^{-1}$) using Spectroquant Spectrophotometer (Merck, Germany).

SCOD removal efficiency was calculated using Equation 3.4.

$$\eta_{COD} = \left(\frac{(SCOD_{t0} - SCOD_t)}{SCOD_0}\right) * 100 \quad (3.4)$$

Where: η_r is the SCOD removal efficiency in %; whereas $SCOD_{t0}$ and $SCOD_t$ are values of SCOD concentration at the start of the experiments and at time t.

3.2.6.2 NH_4-N

Similarly, NH_4-N was measured with commercial test kits (5-150 mg.L^{-1} NH_4-N; Merck, Germany, also procured from VWR, UK) based on the manufacturer's instructions according to phenate method (4500-NH3 F.; APHA, 2005). A 5 mL of reagent NH_4-1 (i.e. substituted phenol) was pipetted into a 10 mL glass vial and followed with 0.1 mL of the filtered sample, at room temperature, and mixed. One level blue microspoon of reagent NH_4-2 (i.e. hypochlorite granules) was then added and the mixture shaken vigorously until the reagent completely dissolved. The sample was allowed to stand for a reaction time of 15 min at room temperature. The sample was then pipetted into a 10 mL glass cuvette (OG 6030, Merck, Germany) and concentration was then measured using a Spectroquant Spectrophotometer (Merck, Germany) pre-mounted with 5-150 mg.L^{-1} auto-selector cell kit. Readings were displayed directly in mg.L^{-1} NH_4-N.

Similarly, NH_4-N removal efficiency was calculated using Equation 3.5.

$$\eta_{NH_4-N} = \left(\frac{(NH_4-N_{t0} - NH_4-N_t)}{NH_4-N_{t0}}\right) * 100 \qquad (3.5)$$

Where: η_{NH_4N} is the NH_4-N removal efficiency in %; NH_4-N_{t0} and NH_4-N_t are the initial and final NH_4-N concentrations, respectively.

3.2.6.3 Anions

Anions were measured using the method of ion chromatography with chemical suppression of eluent conductivity (4110 B.; APHA, 2005) with ICS-1000 Ion Chromatography System equipped with AS40 Automated Sampler and an Ionpac AS14A, 4 x 250mm analytical column (Dionex, USA). An eluent composing of 1mM $NaHCO_3$ and 8mM Na_2CO_3 solution was injected at a flow rate of 1 mL.min^{-1} with an injection loop of 25µL. Five mL of filtered samples was pipetted to 5 mL vials for quantitation of NO_2^-, NO_3^- and PO_4^{3-} in mg.L^{-1}. This method is based on the principles of ion exchange and separation of the test sample in relation to the suppressed conductivity of the eluent with respect to each anion retention time in the analytical column.

3.2.6.4 TOC

TOC analysis was performed with a total organic carbon analyser TOC 5050A equipped with ASI-5000A automated sampler (Shimadzu, Japan) according to high-temperature combustion method (5310 B.; APHA, 2005). Zero grade air was used as the carrier gas, with 25% phosphoric acid solution as inorganic catalyst. Seven mL of filtered sample were pipetted to 10 mL vials. The vials were then mounted onto the automated TOC analyser for analyses.

3.2.6.5 pH

pH was measured with a hydrogen electrode (pH probe) connected to pH meter (Jenway, England) using electrometric method (4500-H^+ B.; APHA, 2005). The probe was calibrated using pH 4 and 7 buffers, based on the manufactures instruction, prior to each set of measurements.

3.2.6.6 DO and temperature

DO and temperature were measured *in situ* with a multi parameter probe connected to a potable DO meter (DO200; VWR International, UK) using membrane electrode method (4500-O G.; APHA, 2005). The DO probe was calibrated for 0% DO using sodium sulphite solution until the meter stabilised and displayed 0% DO concentration. The probe was then exposed to air until the meter displayed 100% DO concentration. The calibration for the DO probe was performed on every sampling day prior to the measurements. Temperature was reading was displayed directly in °C.

3.2.6.7 CDW

CDW was determined from the results of total suspended solids and volatile suspended solids dried at 103 - 105 °C and ignited at 550 °C, respectively, according to the method for the determination of physical and aggregate properties (2540 D. and 2540 E.; APHA, 2005). Fibre glass filters (0.4 µm pore sizes, VWR, UK) were dried in an oven pre-set at 103 - 104 °C for 1 h prior to gravimetric analyses. The filters were then transferred to pre-heated furnace set at 550 °C, for 10 min. The filters were allowed to cool in a desiccator and weighed with a balance (Mettler Toledo, UK). A known volume of microalgal culture was filtered through the pre-dried filters mounted onto a filtration unit connected to a vacuum pump.

The filters (with the retentate) were then dried at 104 °C for 60 min. They were then removed and allowed to cool at room temperature and weighed after cooling. The weights before and after filtration were then used to determine the total suspended solids retained on each filter. The filters were then transferred to the pre-heated furnace mentioned earlier. After 10 min, the filters were removed and allowed to cool in a desiccator at room temperature and reweighed. The last two weights were then used to determine the volatile suspended solids, here referred to as CDW.

3.2.6.8 OD_{560}

OD of the algal culture was measured with UV-1700 Phamarspec spectrophotometer (Shimadzu, Japan) according to multi-wavelength spectrometric method (2120 D.; APHA, 2005) at 560 nm wavelength (Wang *et al.*, 2007) with distilled water as reference. The spectrophotometer was allowed to perform self-check prior to the measurements. After the check, the wavelength value was manually entered into the instrument. About 4 mL of distilled water was then pipetted into transparent plastic cuvette (10 mm path length; VWR, UK). The cuvette was then mounted onto the measurement cell and its absorbance was adjusted to zero. Similar volume of the microalgal culture was then pipetted into another cuvette and mounted onto the spectrophotometer to measure its optical absorbance at 560 nm, here referred to as the optical density (OD_{560}). Whenever the OD value was above 0.5, a dilution with distilled water was applied to the sample and the readings multiplied with the appropriate dilution factor.

3.3 Light measurement

The irradiance was measured as shown in Figure 3.2.

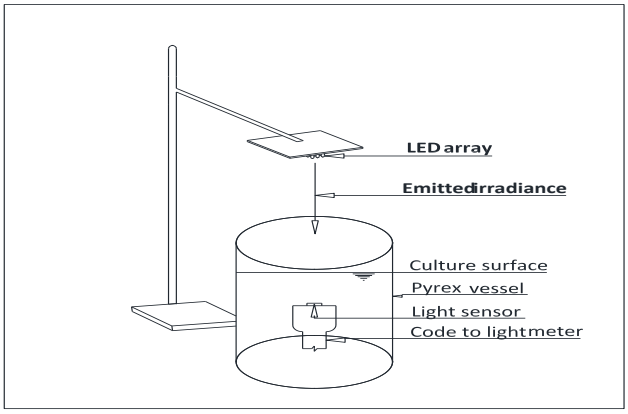

Figure 3.2 Schematic showing point of irradiance measurement

Light measurements were performed with the light sensor placed internally at the centre of the bioreactor (for the culture and distilled water media) with the sensor facing the direction of illumination (Figure 3.2).

3.4 Results and discussion

3.4.1 Light measurement

Figure 3.3 shows the results of LED irradiance measurements carried out with bioreactors with and without aluminium foil cover: in air; filled with either 1 L deionised water or with 1 L microalgal culture (Table A3.1; Appendix). Figure 3.3 shows that higher irradiance values were obtained when the bioreactors were covered with aluminium foil than when they were uncovered due to reflection of stray LED light back into the culture. This supports the idea of covering the bioreactors with aluminium foil during this and subsequent experiments in order to maximise the amount of light utilisation reaching the culture.

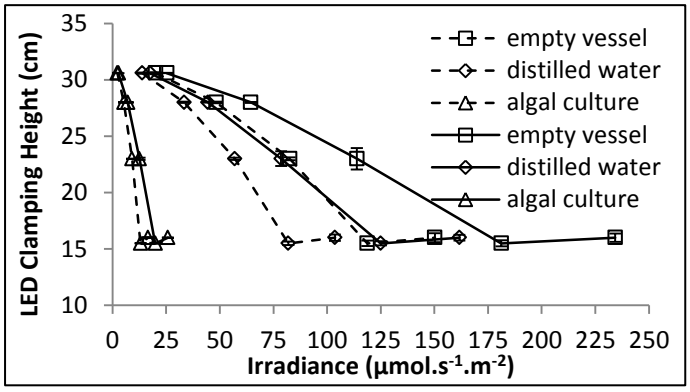

Figure 3.3 Plot of irradiance versus height of LED clamping (solid lines: reactors wrapped with aluminium foil; dashed lines: reactors without aluminium foil)

As expected, the sensor recorded the least amounts of irradiance when the bioreactor vessels were filled with microalgal culture, without foil cover (i.e. 2.78 µmol.s^{-1}.m^{-2} at 30.6 cm; Figure 3.3), indicating light absorbance/attenuation by the suspended microalgal biomass; the amount of irradiance decreases with increasing clamping height. On the one hand, amount of irradiance of about 25.8 µmol.s^{-1}.m^{-2} was recorded in the algal culture at 16 cm clamping height when the bioreactors were covered with aluminium foil (Figure 3.3), and the irradiance value recorded in the bioreactors without aluminium foil cover corresponding to this height was 16.52 µmol.s^{-1}.m^{-2}.

This shows that to achieve a desired minimum irradiance of at least 25 µmol.s^{-1}.m^{-2} which was used in the pair of bioreactors R2 and R8 in the main experiments, the LED had to be clamped no higher than 16 cm and the bioreactors had to be operated with aluminium foil cover. This light measurement experiment provided a criterion for selecting the LED clamping height to achieve the desired least irradiance values that were used in the growth experiments. On the other hand, the maximum irradiance value used in the experiments was the maximum achievable at the shortest practical height above the bioreactors.

3.4.2 Biomass productivity and maximum specific growth rates

Figure 3.4 shows the variation of microalgae-bacterial CDW with time. Highest CDW values were obtained in the bioreactors illuminated with highest amount of irradiance.

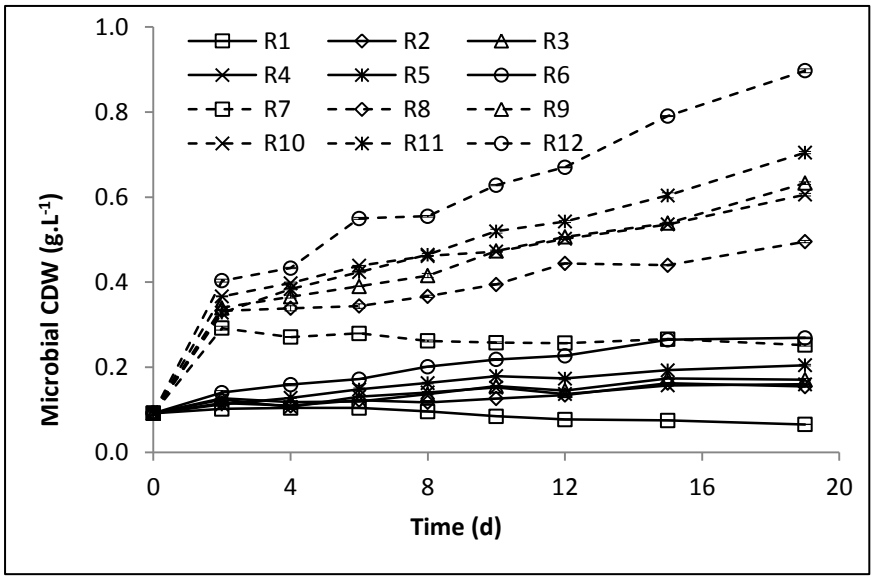

Figure 3.4 Time courses of microbial (i.e. microalgae and bacteria) CDW (continuous lines, with CO_2 addition; dashed lines, without CO_2 addition)

The cell density of the mixed microbial culture increased with the time of cultivation, and the increase in the CDW was greater in bioreactors without CO_2 addition than in those with CO_2 addition (Figure 3.4). This was unexpected as the CO_2 in known to be a growth-limiting substrate in phototrophic organisms. Surprisingly, the CDW value at day 15 for the control reactor with neither CO_2 addition nor illumination was almost the same as that for CO_2-enriched bioreactor with the highest irradiance.

One possible reason for such unusual trend in the CO_2-enriched bioreactors could have been the presence of microalgal species that were intolerant to high CO_2 concentration

considering that the concentration of CO_2 in these bioreactors is about 250-fold that of ambient air (i.e. 10% CO_2 as compared to 0.04% CO_2). This might have exerted an inhibition which would have resulted in prolonged acclimation period in the bioreactors with CO_2 addition. Conversely, low CO_2 concentration in the other bioreactors might have favoured growth of algal strains adapted to environmental levels of CO_2, resulting in higher biomass productivity than the bioreactors with CO_2 addition.

Additionally, the culture in the bioreactors without CO_2 addition did not appear to require any time to acclimate as the cultivation condition is similar to the conditions of the inoculum culture before the start of these experiments. The rapid increase in CDW within the first 2 days (Figure 3.4) in the bioreactors without CO_2 addition supports this viewpoint. The absence of an acclimation period clearly favoured these bioreactors over those with CO_2 addition, such that early inhibition due to high CO_2 concentration probably reduced the microalgal growth in the CO_2-enriched bioreactors. Moreover, the low biomass productivity recorded in the CO_2-enriched reactors might not be unconnected with the low cell density of the starting biomass of the culture (Perez-Garcia *et al.*, 2011a) coupled with intolerance of high CO_2 concentration.

The maximum specific growth rates for all of the bioreactors were determined using Equation 3.1, by considering the linear portion of exponential growth phase from the plot of natural logarithm with time. The maximum growth rates were determined from the equations of lines of best fit on the plots (Figure A3.1; Appendix). The growth rates for both systems increased with increasing irradiance up to irradiance values of 114 to 181 $\mu mol.s^{-1}.m^{-2}$ (Figure 3.5). Interestingly, the growth rates corresponding to such irradiance values are higher in the CO_2-enriched bioreactors than in those without CO_2 addition. However, the maximum value obtained in this study (i.e. 0.06 d^{-1}; Figure 3.5) is much lower than the value of 0.39 d^{-1} reported by Termini *et al.* (2011) microalgal culture predominated by *Scenedesmus* sp, treating settled municipal wastewater.

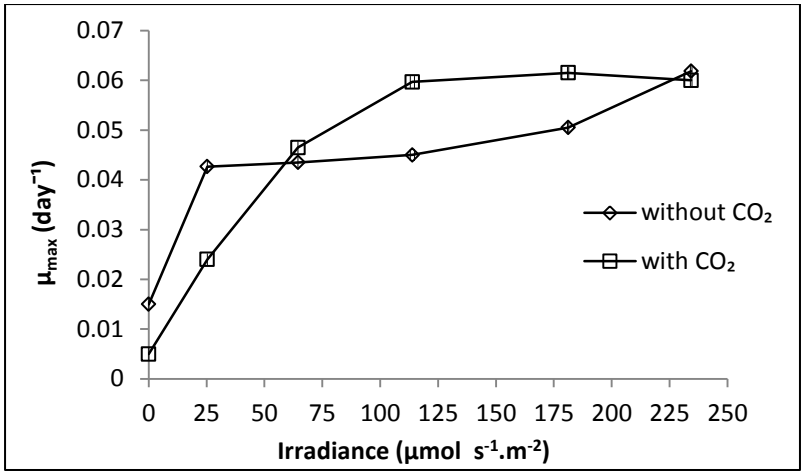

Figure 3.5 Variation of maximum specific growth rates with red LED irradiance for the bioreactors operated in batch mode

Conversely, the maximum CDW values corresponding to maximum irradiance obtained in this study (i.e. ≈ 0.3 and 0.9 $g.L^{-1}$ for bioreactors with and without CO_2 addition, respectively) are much higher than the CDW values reported by Wang *et al.* (2007) cultivated under red LED irradiance of 300 $\mu mol.s^{-1}m^{-2}$. In fact, the maximum values obtained in this study for the CO_2-enriched bioreactors and those without CO_2 addition are, respectively, about 8- and 23-fold higher than the CDW reported by Wang *et al.* (2007) for similar amount of irradiance.

However, the value of red LED irradiance corresponding to the maximum growth rate reported by Wang *et al.* (2007) was 3000 $\mu mol.s^{-1}m^{-2}$, which is about 13-fold higher than the maximum irradiance used in this study. As such, it could be concluded here that even the highest amount of irradiance used in this study might still have limited the productivity of the mixed microalgal culture, thereby resulting in very low deserved growth rates. However, Wang *et al.* (2007) and Termini *et al.* (2011) used isolated microalgal strains which would have had, if any, minimal competition between microbial species in their cultivation systems. In addition, Wang *et al.* (2007) cultivated their alga solely on Zarrouk (nutrient) medium containing, among other chemical constituents, about 583 $mg.(HCO_3^-).L^{-1}$ and 729 $mg.(NO_3^-).L^{-1}$.

3.4.3 Wastewater treatment efficiency

The wastewater treatment efficiency in this study was evaluated in terms of ammonium and SCOD removal efficiencies.

3.4.3.1 Ammonium removal

Figure 3.6 shows the variation of the maximum ammonium removal efficiency with irradiance in all the bioreactors. Each point in the Figure represents the highest removal efficiency achieved in each bioreactor.

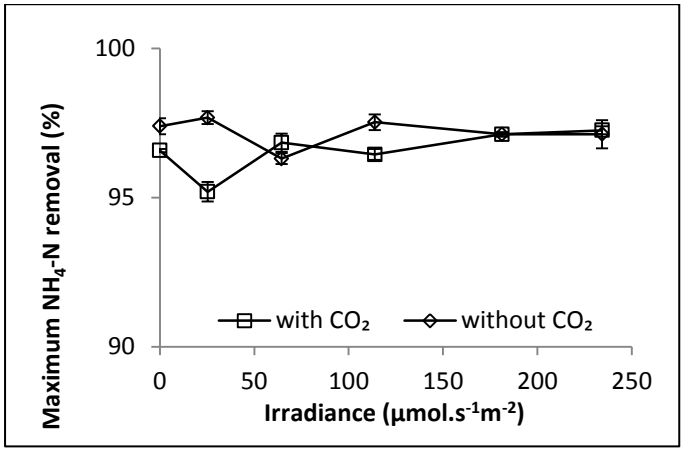

Figure 3.6 Variation of ammonium removal efficiency with red LED irradiance for the bioreactors operated in batch mode

Ammonium removal efficiencies greater than 90% were achieved in all the experimental bioreactors. Up to the irradiance value of 50 µmol.m^{-2}.s^{-1}, CO_2 addition did not appear to have enhanced the ammonium removal efficiency (Figure 3.6). The ammonium removal efficiency achieved in the CO_2-enriched bioreactors exceeded that of the bioreactor without CO_2 addition only at irradiance value of 64.5 µmol.m^{-2}.s^{-1}. From 181.2 µmol.m^{-2}.s^{-1} onwards, ammonium removal appears to be independent of both CO_2 addition and irradiance in the bioreactors (Figure 3.6). The ammonia removal efficiencies found in this study is similar to values reported in the literature in both photobioreactors and conventional algal ponds, e.g. (Silva-Benavides and Torzillo, 2012; Park and Craggs, 2010). Due to possible ammonification of organic nitrogen substances in the treated wastewater, the effluent ammonium concentration exceeded the initial concentration. However, lack of TKN analysis data in the current study might have limited this interpretation.

3.4.3.2 SCOD removal

In contrast to NH_4-N removal, the SCOD removal efficiency of both systems increased with increasing irradiance (Figure 3.7). Each point in Figure 3.7 represents the highest SCOD removal achieved in each bioreactor. A maximum value of more than 75% removal was

achieved in the bioreactors with CO_2 addition. This value is not far from 89% SCOD removal reported by Hammouda *et al.* (1995) in a domestic wastewater treatment system dominated by *C. vulgaris* and *Scenedesmus* sp operated in batch mode, illuminated with fluorescent lamps and supplemented with nutrients. Much higher SCOD removal was observed in the bioreactors with CO_2 addition than in the bioreactors without CO_2 addition.

However, it is not clear whether the high SCOD removal in the CO_2-enriched bioreactors was due to the inorganic carbon supplementation. Nevertheless, it may be concluded that 'optimum' SCOD removal was achieved at an irradiance value lower than the maximum used in this study (Figure 3.7).

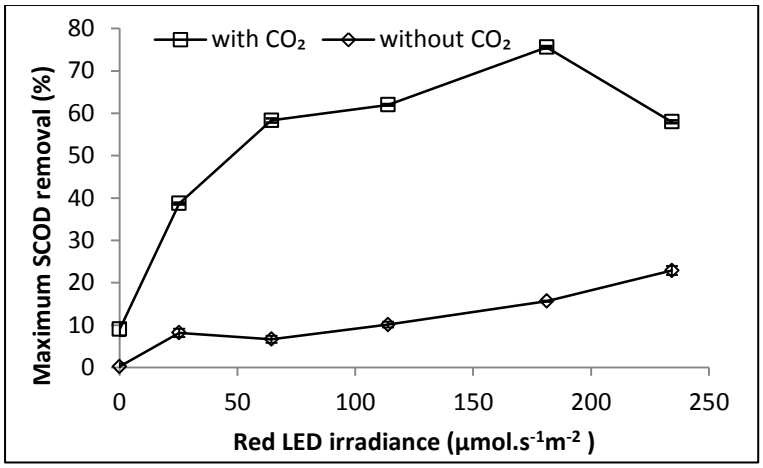

Figure 3.7 SCOD removal efficiency versus red LED irradiance in the bioreactors

Interestingly, SCOD removal efficiency of about 10% and less than 1% were recorded in the control bioreactors (R1 and R7) with and without CO_2 addition, respectively. This observation contrasts well with ammonium removal in which almost identical values were obtained in the control bioreactors. The low level of SCOD removal which was observed in the control bioreactors may be due to presence of microalgal species such as *C. vulgaris*, (and some bacteria), that can grow heterotrophically in the dark (Perez-Garcia *et al.*, 2011a; Ogbonna *et al.*, 2001) and consume SCOD substrates.

3.4.3.3 Phosphate and nitrite accumulation

High phosphate and nitrite accumulations were recorded in both the bioreactors with and without CO_2 addition (Figure 3.8); with maximum concentration of these parameters in the control bioreactors. The initial phosphate concentration in the inoculated wastewater was

12.6 mg.PO_4-P.L^{-1}, whereas nitrite was not detected. This seems to be in excess of algal phosphorus requirement considering the low amount of phosphorus in algal biomass (Powell *et al.*, 2009). The mechanism responsible for phosphate accumulation in both systems is unclear. Nevertheless, phosphate accumulating organisms (PAO) were probably absent in the bioreactors (Saito *et al.*, 2004). However, pH values higher than 7 recorded in the bioreactors without CO_2 addition do not corroborate this argument since such organisms usually thrive in acidic condition (Saito *et al.*, 2004).

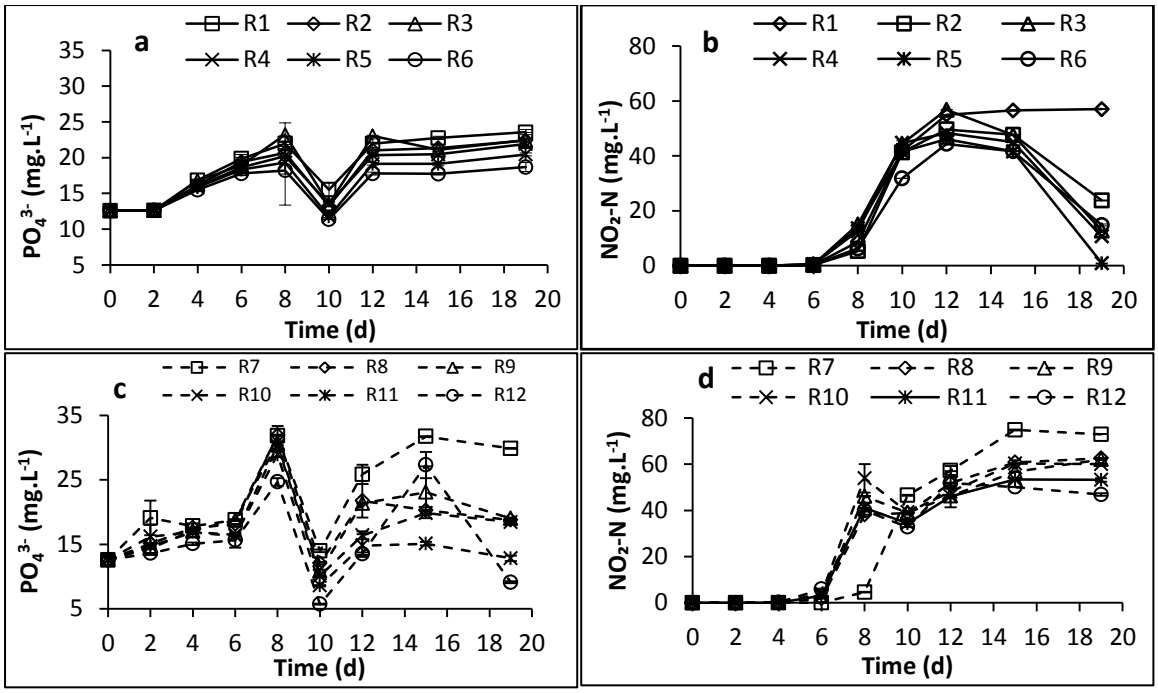

Figure 3.8 Time courses of phosphate and nitrite concentrations in bioreactors with CO_2 addition (a, b), and without CO_2 addition (c, d)

Considerable amounts of nitrite started to appear from day 6 onwards in both bioreactors with and without CO_2 addition (Figure 3.8b and d). Initially, these accumulations seem to be independent of CO_2 addition as they are similar in both bioreactors up to day 15. The nitrite accumulation pattern was almost identical in both of the control bioreactors even up to day 19 (Figure 3.8b and d). It remained fairly constant in the CO_2-enriched control and all bioreactors without CO_2 addition, but decreased sharply in all the CO_2-enriched bioreactors regardless of LED light intensity. This sudden decrease is more pronounced in CO_2-enriched R5 (down to about 1 mg.NO_2-N.L^{-1}) than in the other bioreactors (15-24 mg.L^{-1}). This is further supported by the NO_3-N concentration of up to 43 mg.L^{-1} recorded in this bioreactor at day 19. One disadvantage of having NO_2-N in wastewater treatment is that it interferes

with COD test measurement because it exerts more COD in the test samples, at concentration higher than 2 $mg.L^{-1}$, thereby affecting the accuracy of this quality parameter.

Figure 3.8a and c shows the orthophosphate concentrations recorded in both the bioreactors with and without CO_2 addition, respectively. Phosphate concentrations higher than the initial value were recorded in all of the bioreactors. This may not be unconnected with release of phosphate into the mixed liquor due to possible biodegradation of phosphate-rich compounds in the wastewater. Higher phosphate concentration was recorded in the bioreactors without CO_2 (up to about 32 $mg.L^{-1}$; Figure 3.8c) compared to those with CO_2 addition (about 23 $mg.L^{-1}$; Figure 3.8a). The sudden decrease in phosphate concentration from day 8 to day 10 possibly resulted from lack of microbial activity due to failure of the AC-DC adaptor used in supplying electrical power to the light sources; this took about 1 h to fix.

Although studies have been undertaken on ammonia oxidation via nitrite accumulation in sequencing batch bioreactors (Aslan *et al.*, 2009), on partial nitrification of ammonia in DO-limited activated sludge system (Jianlong and Ning, 2004), and on inhibitory effect of nitrite on biological phosphorus uptake under aerobic conditions (Yoshida *et al.*, 2006; Saito *et al.*, 2004), this literature mainly concerns nitrite accumulation in non-algal systems. No studies have been reported on nitrite and phosphate accumulation in mixed microalgal culture treating municipal wastewater.

However, most of the available studies are related to biofilms rather than suspended microalgae (e.g. Nijhof and Klapwijk, 1995). Nitrite may accumulate in aquatic systems due to high equilibrium concentration before it is further oxidised to nitrate or due to slow nitrite oxidation rate (Philips *et al.*, 2002). The causes and effects of nitrite accumulation in aquatic systems are poorly understood, but factors such as pH, DO, phosphate, etc., may play important roles in nitrite accumulation due to disruption in steps in nitrification and/or denitrification (Philips *et al.*, 2002). The above systems reported in the literature are similar to microalgal systems with respect to aeration, i.e. their aerobic mode of operation. As such, ammonia-oxidising bacteria may be present in the cultures used in the current study which might have partially oxidised ammonia to nitrite with consequent inhibition of nitrite-oxidising bacteria leading to high nitrite accumulation (Jianlong and Ning, 2004).

This is contrary to the understanding that nitrite oxidation proceeds more rapidly than ammonia oxidation in DO-rich systems, thereby preventing nitrite accumulation (Jianlong and Ning, 2004) because high amount of nitrite (up to about 61 mg.NO_2-N).L^{-1} was recorded on day 15 in bioreactors without CO_2 addition (Figure 3.8d). Coupled effects of high CO_2 and light appears to facilitate complete nitrification leading to low NO_2-N (but high NO_3-N) concentration. This observation is supported by the remarkable decrease in NO_2-N concentration (and increase in NO_3-N concentration; data not shown) in the illuminated CO_2-enriched bioreactors (day 19; Figure 3.8b). On the other hand, the high CO_2 and red LED light may have selected different phototrophic populations capable of consuming NO_2-N from day 15 onwards. This could have been confirmed had the experiments lasted longer.

High DO and pH, up to 9 mg.L^{-1} and 9, respectively, were recorded in the bioreactors without CO_2 addition (Figure 3.9).

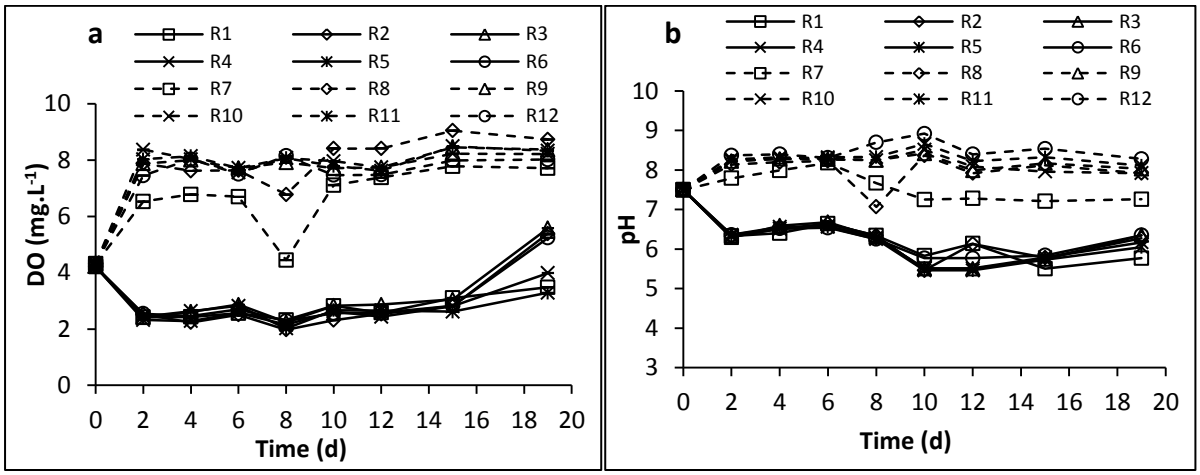

Figure 3.9 Time courses of dissolved oxygen and pH in all of the bioreactors (solid lines: with CO_2 addition; dashed lines: without CO_2 addition)

In contrast, DO and pH values as low as 1.98 mg.L^{-1} and 5.4 were recorded in bioreactors with CO_2 addition. The low pH values of these bioreactors might have created unfavourable conditions that have limited the growth of algal species in the inoculum, leading to much lower productivity than in bioreactors without CO_2 addition (Park and Craggs, 2010). Stress due to sudden change from pH 7 in the inoculum down to pH 6, resulting from carbonic acid formation from CO_2 addition appears to have inhibited microbial growth at the early stage of the experiments. This observation is supported by the remarkable difference in CDW values (0.141 and 0.404 g.L^{-1}, on day 2; Figure 3.4) in bioreactors with CO_2 addition and

those without CO_2 addition, respectively. Apparent inhibition of microbial growth rate by high CO_2 concentration might have resulted in low algal photosynthesis which consequently led to lower DO and pH in the bioreactors with CO_2 addition since high DO and pH are a function of algal photosynthesis.

Clearly, the pH and DO concentration were much higher in bioreactors without CO_2 addition than in those with CO_2 addition and would have had different consequences on the microbial populations of the two systems. Therefore, this study confirms that there is a critical need to regulate pH in any subsequent experiments, and a need to determine whether or not this parameter, as well as DO, played a role in the variable and poorly understood nitrite and/or phosphate accumulation characteristics. Temperature ranged from 22 to 31 °C in a similar pattern in all bioreactors (Figure 3.10a and b) from the beginning to the end of the experiments.

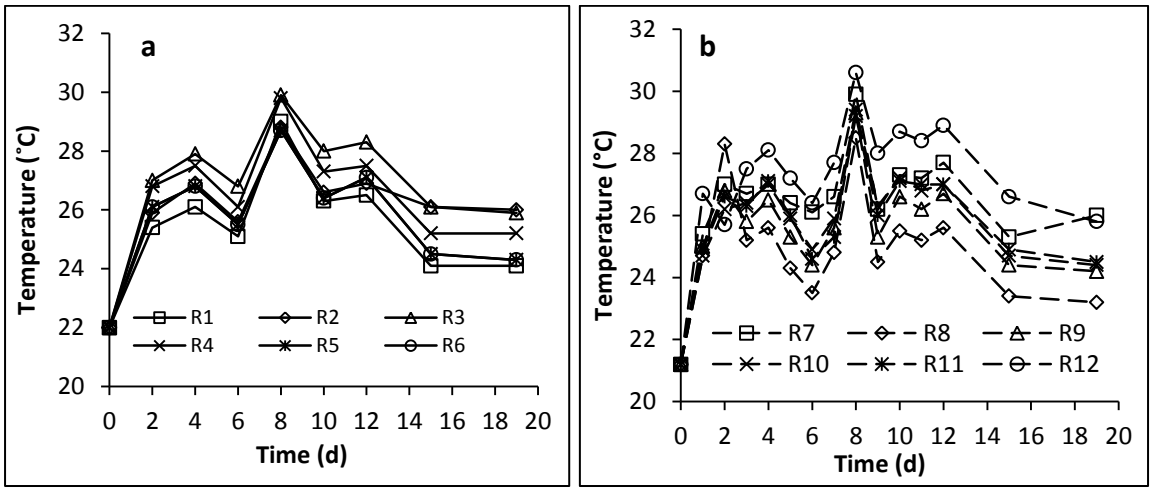

Figure 3.10 Time courses of temperature in all of the bioreactors: (a) with CO_2 addition, and (b) without CO_2 addition

This upper range of temperature is not unusual in algal systems as *Chlorella* sp. was reported to be tolerant to high temperature up to 40 °C, both in large-scale outdoor PBR and at bench-scale (Ong *et al.*, 2010; Sung *et al.*, 1999).

Chapter 4

Optimisation of red light-emitting diodes irradiance for illuminating mixed microalgal cultures treating municipal wastewater

4.1 Introduction

This chapter presents the results obtained from Phase II experiments. Red LEDs with identical specification with those presented in Chapter 3 were used as light source. However, synthetic rather than real municipal wastewater was used as substrate in these bioreactors in order to minimise temporal variation of the wastewater characteristics, and to allow for better comparison with the Phase III experiments presented in Chapter 5. These experiments were conducted in up-scaled microalgal photobioreactors made of transparent Plexiglas, for 30 d.

The objective of the experiments was to determine the optimum amount of irradiance needed to illuminate the mixed microalgal culture treating modified synthetic municipal wastewater (MSMW), with a view to using the optimised irradiance in developing the HMAS system (presented in Chapter 5). Light regimes higher than those presented in Chapter 3 were used in this study. Furthermore, illumination and mixing were provided internally as opposed to the external illumination used in the previous study conducted in 1 L bioreactors.

4.2 Materials and Methods

4.2.1 Stirred-tank photobioreactor (STPBR) design

Internally-illuminated STPBR made of transparent Plexiglas, were used in this study. Illumination was provided radially from the centre of the STPBR by LED (N45AT, Maplin Electronics) emitting red light at 660 nm characteristic wavelength. The STPBR was 30 cm deep and 30 cm in diameter, with a total volume of about 21 L. It has a central chamber for housing the LED arrays on Vero matrix boards, herein referred to as the core. Figure 4.1 shows the components of the STPBR.

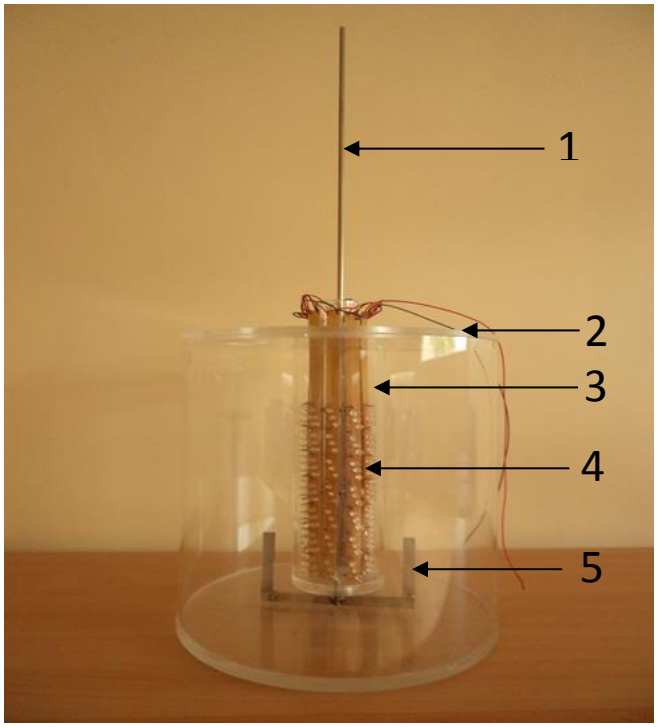

Figure 4.1 The STPBR showing: (1) stirrer shaft, (2) lid holding the LED chamber, (3) LED chamber, (4) LED core, and (5) stirring blade

The STPBR consisted of a 2-cm-diameter Plexiglas cylinder mounted within a 9-cm-diameter Plexiglas cylinder, both being glued to the lid of the vessel at the top and to a 9-cm-diameter horizontal Plexiglas plate at the bottom, which formed the central chamber. Two centimetre diameter holes were cut at the centre of the bottom horizontal plate and the lid to allow free insertion of 0.5-cm-diameter stirrer shaft from the bottom of the LED chamber, through the 2-cm-diameter mounted cylinder, to the top of the STPBR above which a stirrer motor rested on a centrally drilled wooden frame (Figure 4.3).

The bottom outer wall of the STPBR was 3 cm deeper than the central chamber, creating a free space at the bottom between the base plates of the chamber and the STPBR to accommodate the end blade of the overhead mechanical stirrer. Zero to 12 LED-mounted Vero matrix boards were glued vertically round a circular Plexiglas frame, equidistant to each other. Power was supplied to the LED using a variable AC-DC power supply adaptors (PSM 2/2A 2-Channel; RS Components, UK) while mixing was provided using an overhead mechanical stirrer (RW 20; IKA, UK).

The LED core was designed and constructed separately from the central chamber for easy maintenance. The STPBR had a light path of 10.5 cm from the wall of the LED chamber to the outer vertical wall of the STPBR, measured horizontally between internal distances, and a surface-to-volume ratio of about 0.14 cm^{-1}. The LED core was designed to illuminate the STPBR up to a maximum water depth of 28 cm, giving a working volume of about 16 L, and allowing for about 2 cm degassing head space. Three STPBR (i.e. SR 1, SR 2 and SR 3), each illuminated with different irradiance (Table 4.1), were used in the study. A similar bioreactor operated in the dark (SR 0), served as a control. Figure 4.2 shows the detailed drawing used in fabricating the STPBR vessel.

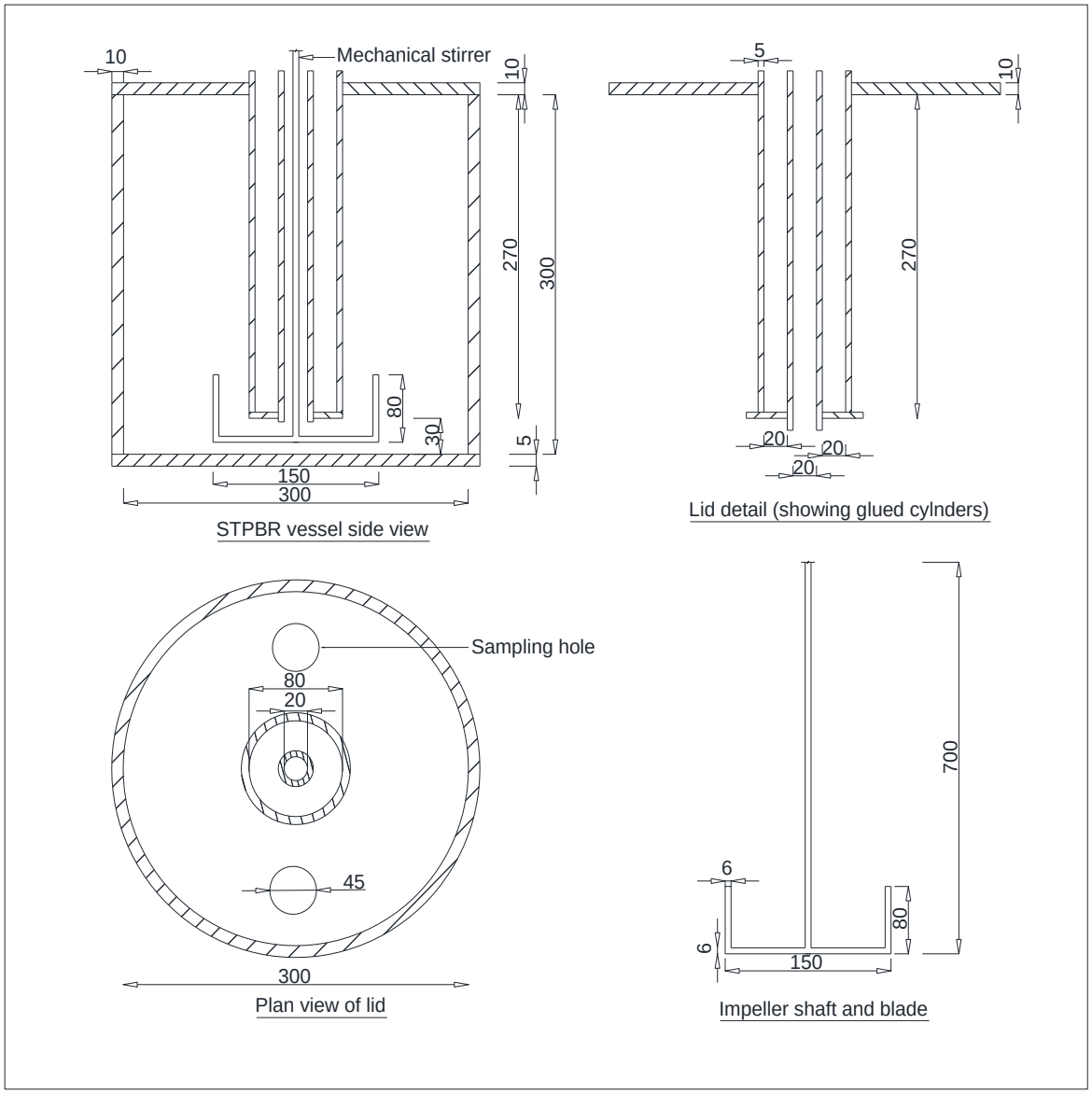

Figure 4.2 Detailed drawing of the STPBR (all dimensions in mm)

4.2.2 Experimental set-up

4.2.2.1 Irradiance

All the bioreactors were wrapped with aluminium foil to exclude room light, concentrate the supplied light, and minimise photon loss. The control bioreactor, SR 0, was therefore maintained in the dark throughout the experimental period (Figure 4.3). The measurements were performed with the STPBR covered with aluminium foil under different fill conditions (air, distilled water, and microalgal culture) and at varying distance starting from the wall of the LED chamber to at least the maximum STPBR light path length.

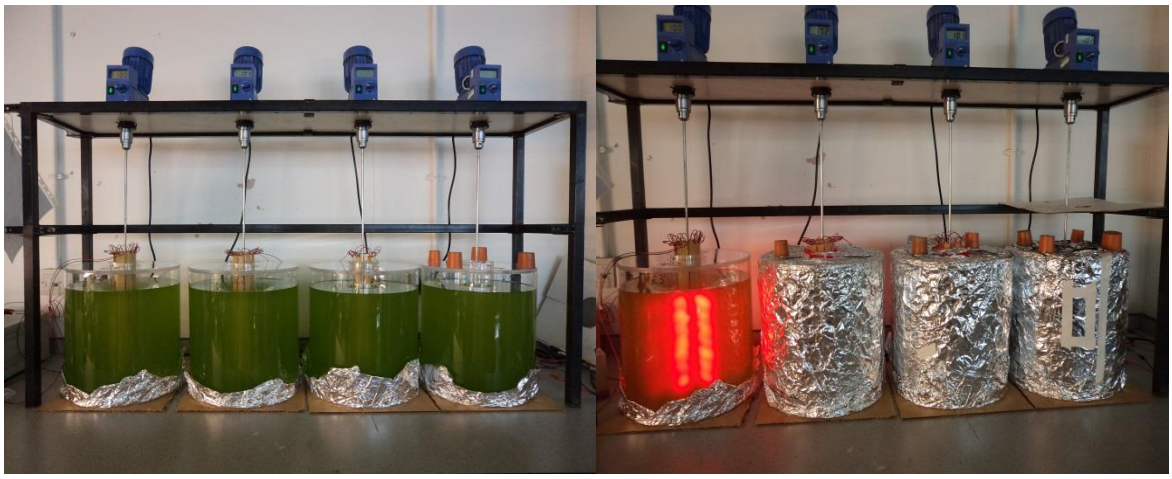

Figure 4.3 Experimental set-up showing unlit bioreactors (left), and lit bioreactors (right)

The values of average irradiance, number of LED and other components as well as the electrical power consumed by the STPBR are given in Table 4.1.

Table 4.1 LED and power details for the bioreactors

Bioreactor	Irradiance (µmol.s^{-1}.m^{-2})	Vero boards	LEDs	Power (W)
Control (SR0)	0	0	0	0
STPBR1 (SR1)	429.9 (0.8)	6	126	5.04
STPBR2 (SR2)	582.7 (3.2)	9	189	7.56
STPBR3 (SR3)	730.8 (1.5)	12	252	10.1

4.2.2.2 Modified synthetic municipal wastewater

MSMW adapted from Bracklow *et al.* (2007) was used in the current study. It was modified to mimic an anaerobically digested wastewater. The wastewater was autoclaved at 120 °C for 15 min in an Autoclave (Rodwell Scientific Instruments, UK) to dissolve its chemical constituents. It was subsequently allowed to cool at room temperature prior to its use in the

experiment. Both the composition and characteristics of the wastewater are given in Table 4.2.

Table 4.2 Modified synthetic municipal wastewater composition and characteristics

Composition		Characteristics*	
Constituents	**($mg.L^{-1}$)**	**Parameter**	**($mg.L^{-1}$)****
Peptone	17.40	COD	395 (7.8)
Yeast extract	52.20	NH_4-N	53.3 (1.7)
Glucose	61.00	TC	177.9 (0.3)
NH_4-acetate	317.60	IC	n/d
KH_2PO_4	5.85	PO_4^{3-}	9.07 (0.3)
$MgNH_4PO_4$	7.25	NO_2-N	n/d
K_2HPO_4	5.25	NO_3-N	0.05 (0.02)
Urea	91.70	DO	8.40 (0.01)
NH_4Cl	12.80	pH	6.75 (0.00)
$FeSO_4 \cdot 7H_2O$	5.80	Temperature	20.8 (0.0)

*(x) standard deviation for duplicate samples; ** unit does not apply to pH and temperature
n/d = not detected

4.2.2.3 Nutrient media

Due to the possibility that the lack of nutrient supplementation might have limited microalgal growth in Phase I experiments, a Modified Bold's Basal Media (MBBM) for freshwater algae was used in the current study. However, in view of the ammonium content of the wastewater shown in Table 4.2 (characteristics), $NaNO_3$ was excluded from the chemical constituents of the MBBM in order to achieve a nitrate content representative of a pretreated wastewater, as opposed to the usual practice of growing algae in the laboratory solely on nutrient media with high nitrate concentration. Nitrogen was therefore provided by the ammonium content.

Similarly, the orthophosphate compounds in the MBBM were also excluded in order to achieve a phosphate concentration representative of real municipal wastewater. Phosphate compounds were also excluded from the MBBM as they already formed part of the modified synthetic wastewater composition (Table 4.2). In addition, Table 4.3 shows the MBBM used as nutrient supplement in the experimental culture.

Table 4.3 MBBM for freshwater algae used in the STPBR as part of growth medium

Stock number*	Constituent	Concentration ($g.L^{-1}$)
(2)	$MgSO_4.7H_2O$	7.50
(3)	NaCl	2.50
(6)	$CaCl_2.2H_2O$	2.50
(7)	Trace elements solution	
	$ZnSO_4.7H_2O$	8.82
	$MnCl_2.4H_2O$	1.44
	MoO_3	0.71
	$CuSO_4.5H_2O$	1.57
	$Co(NO_3)_2.6H_2O$	0.49
(8)	H_3BO_3	11.42
(9)	EDTA	50.0
	KOH	31.0
(10)	$FeSO_4.7H_2O$	4.98
	H_2SO_4 (98%, v/v)	1.0 mL
	Medium	**per Litre**
	Stock solutions (2), (3) and (6)	10.0 mL each
	Stock solutions (7) through (10)	1.0 mL each

Composition from CCAP, Dunstaffnage Marine laboratory, UK; *stocks number 1, 4 and 5 were excluded

The stock solution of trace elements (i.e. constituents under stock number (7)) was autoclaved as described in Section 4.2.2.2, to dissolve the chemical substances in order to increase their availability to the algae. Each numbered stock solution was made up to 1 L with deionised water in volumetric flask and stored in separate glass bottles at 4 °C, for 1 month.

4.2.2.4 Inoculum

The synthetic municipal wastewater was inoculated with mixed culture of microalgae (and bacteria?). The algal culture was obtained from Phase I experiments (Chapter 3). The culture was washed twice with synthetic wastewater and centrifuged at 1000 g for 20 minutes at 22 °C (APHA, 2005). It was then maintained in 1 L Pyrex beaker under red LED illumination and agitated with a magnetic stirrer (Hanna Instruments, UK) prior to the experiments. The inoculum was not washed with phosphate buffer in order not to expose the algae to high phosphate concentration which would have resulted in luxury uptake of P (Powell *et al.*, 2011), and consequently affect PO_4-P uptake during the experiments. Rather, it was washed with the modified synthetic wastewater.

4.2.2.5 Experimental culture preparation

The culture media used in the experiments consisted of the inoculum, the modified synthetic municipal wastewater concentrate, and the MBBM. These constituents were mixed with distilled water based on the volumes shown in Table 4.4 order to obtain the experimental culture.

Table 4.4 Constituents per 16 L of the experimental culture

Constituents	Volume (L)
Inoculum	0.200
Distilled water	15.26
Modified wastewater	0.316
MBBM stock	
(2) + (3) + (6)	0.160
(7)	0.016
(8)	0.016
(9)	0.016
(10)	0.016

Note: see Table 4.3 for definition of numbers in the parentheses

The culture was based on centrifuged microalgal biomass with CDW of 399.3 $mg.L^{-1}$, to achieve an initial average CDW of about 73 $mg.L^{-1}$. A culture of about 64 L was prepared in an 84 L container, from which 16 L was supplied to each bioreactor.

4.2.3 Bioreactor operation and monitoring

All the experimental bioreactors were operated in batch mode with pH control at ambient temperature (20 ± 2 °C) and under continuous illumination (Lee and Lee, 2001a; Borchardt and Azad, 1968), for 30 days. Aqueous solutions of hydrochloric acid (HCl) and sodium hydroxide (NaOH) were appropriately used to control pH within the desired range for algal growth (i.e. pH 7.0 to 8.5; Park and Craggs, 2010) in all bioreactors. Overhead mechanical stirrers were used to provide mixing and operated at 100 ± 1 rpm and 60 ± 1, corresponding to experimental stage with and without and CO_2 addition, respectively.

Premixed industrial-grade gas composing of 10% CO_2, 6% O_2 and 84% N_2 (BOC Gas, UK) was bubbled into all bioreactors at a flow rate of 100 $mL.min^{-1}$. The bioreactors were maintained under natural surface aeration up to day 23. The gas was then supplied into the bioreactors from day 24 to day 30, as described in Section 3.2.4.

Samples were collected every 24 h during the first week, and subsequently every 48 h for physical and chemical analyses. Additional samples were collected twice a week, fixed with 98 - 100% ethanol and stored at -20 °C (Eland *et al.*, 2012) for biological analyses and the results are presented in Chapter 6.

4.2.4 Analytical tests

Samples collected from the bioreactors where analysed for physical and chemical parameters as detailed in Chapter 3 (Sections 3.2.5 and 3.2.6). In addition, total Kjeldahl nitrogen (TKN) was also quantified using titrimetry according to Macro-Kjeldahl method (4500-Norg B.; APHA, 2005). Ten mL of sample was pipetted to Kjeldahl flasks followed by addition of 2 Kjeltabs containing 0.3 g K_2SO_4 and 0.5 g $CuSO_4.5H_2O$, and 14 mL H_2SO_4 (98% w/v).

The samples were digested for 120 minutes in TKN digestion rack (Gerhardt, UK), with fumes collected in a bottle containing NaOH solution (10% w/v) and allowed to cool in the instrument to further remove acid fumes. The samples were then distilled using Vapodest (Gerhardt, UK) with 50 mL indicating boric acid solution and NaOH solution (40% w/v). The NaOH was automatically supplied by the instrument, to volatilise ammonia. The samples were then titrated with N/50 H_2SO_4 to end point. The titre values were finally used to compute the amount of TKN available in the test samples (4500-Norg B.; APHA, 2005).

All samples for chemical analyses were filtered through 0.2 µm filters (Sartorius, UK) prior to measurements, and analyses were performed in replicates.

4.3 Results and Discussion

4.3.1 Light measurement

The study began with measurement of irradiance in air, water and different dilutions of the microalgal culture with a view to evaluate possible light attenuation which might affect performance of the STPBR. The results of the measurements are shown in Figure 4.4.

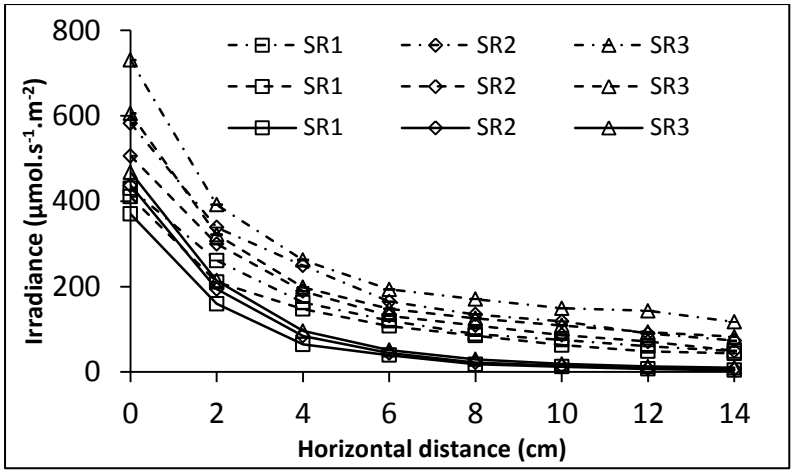

Figure 4.4 Plot of horizontal light attenuation in the PBR (dashed dot: in air; dashed lines: distilled water; solid lines: 82 mg.(microbial CDW).L^{-1})

Irradiance decreased exponentially with increasing horizontal distance, measured from the LED in the STPBR for both air and liquid fill conditions (Figure 4.4). Interestingly, the irradiance values on the wall of the LED core (i.e. at 0 cm in Figure 4.4, a point of maximum irradiance) decreased with increasing media densities; having a highest value in air and the lowest in the algal culture. This is because of light obstruction caused by thin film of water or algal between the light sensor and the wall of Plexiglas housing the light source. The choice of the initial biomass concentration of the experimental culture was therefore based on the evaluation of the light attenuation with respect to the microalgal CDW shown in Figure 4.4.

4.3.2 Specific growth rate, biomass productivity and optimum irradiance

The microbial specific growth rates were calculated based on the variation of CDW with time, using Equation 3.1 (Section 3.2.5), while biomass productivity was computed from CDW as the amount of biomass produced daily. Both the biomass productivity and maximum specific growth rate (Figure 4.5) increased with increasing irradiance up to an irradiance of 582.7 µmol.s^{-1}.m^{-2}. Both parameters subsequently declined at the highest irradiance value. However, the microbial growth and productivity might have reached their optimum values at this irradiance due to lack of more irradiance values higher than the maximum used in the current study.

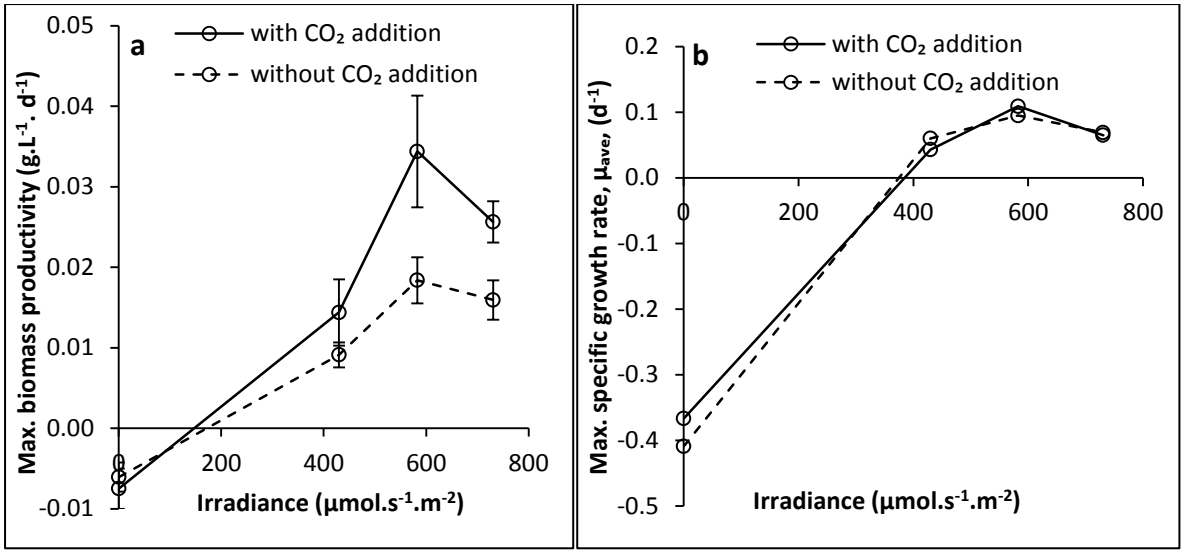

Figure 4.5 Microbial (a) biomass productivity and (b) maximum specific growth rate versus irradiance in PBR (CO_2 was added to the bioreactors for 7 days)

Highest maximum specific growth rate and biomass productivity of 0.109 d^{-1} and 0.034 $g.L^{-1}.d^{-1}$, respectively, were achieved in this research. However, growth rates as high as 0.40 d^{-1} (Wang *et al.*, 2007) for pure culture of *S. platensis*, and 135% (i.e. equivalent to 1.35 d^{-1}) for *C. vulgaris* under red LED illumination with temperature control (25 ± 0.5 °C; Yan *et al.*, 2013), as well as biomass productivity of 0.25 $g.L^{-1}.d^{-1}$ and growth rate of 0.39 d^{-1} for *Scenedesmus* grown in a tubular PBR treating settled activated sludge effluent (Termini *et al.*, 2011) have been reported in the literature. The relatively low values in both growth rate and biomass productivity obtained in the current study might be due to inorganic carbon limitation observed in the bioreactors prior to CO_2 addition. This might have masked the effect of the subsequent inorganic carbon supplementation on the microalgal culture.

Furthermore, the finding in the current study is contrary to that of Wang *et al.* (2007) who reported maximal growth rate of the cyanobacteria *S. platensis* at highest irradiance of 3000 $\mu mol.s^{-1}.m^{-2}$, under red LED illumination. However, the mixed microbial culture used in the current study may have exhibited different metabolic and growth mechanisms. Nevertheless, the finding in the current study suggests that intermediate level of irradiance was optimum for microalgal growth under the experimental conditions. Interestingly, lack of illumination has apparently limited microalgal growth considering the declining CDW (Figure 4.6a) for the control bioreactor despite some amount of organic carbon present in the

mixed liquor (Figure 4.6b) which may have favoured algal heterotrophic metabolism. This suggests the dominance of obligate photoautotrophs in the microalgal culture (Lee, 1999).

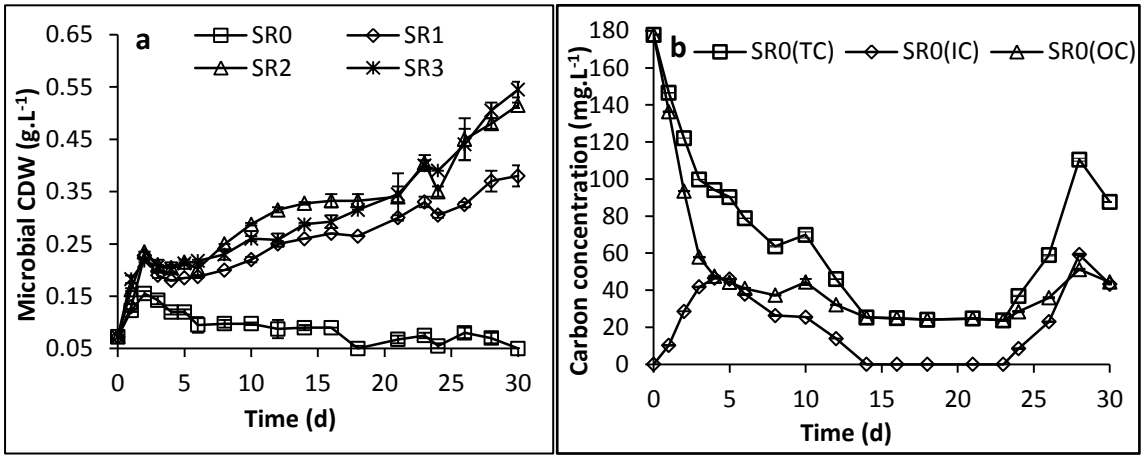

Figure 4.6 Time courses of (a): microbial CDW for all PBR, and (b) TC, IC, and OC concentrations for the control bioreactor

4.3.3 SCOD removal

The SCOD removal efficiencies of all of the bioreactors are presented in Figure 4.7.

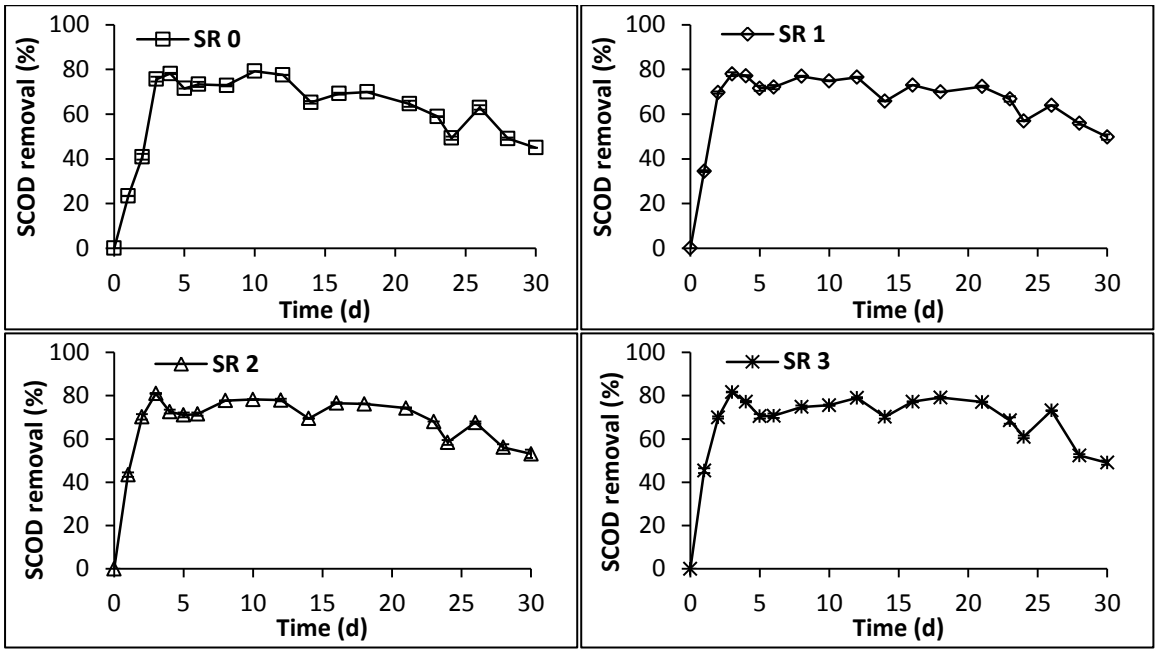

Figure 4.7 Time courses of SCOD removal efficiencies in STPBR at different LED irradiance

The SCOD removal efficiency increased with time up to a maximum value on day 3 in each of the bioreactors. Initially, SCOD was removed at faster rate than at later times. After 24 h, the SCOD removal efficiency appeared to follow the order SR 3 > SR 2 >> SR 1 >>> SR 0. Up

to day 3, the SCOD removal efficiency increased with increasing irradiance after which it suddenly declined up to day 5. It then increased up to day 12 and subsequently remained fairly constant up to day 21 in all bioreactors, except for the slight decrease on day 14. On day 21, the SCOD removal efficiency declined substantially in all bioreactors up to the beginning of CO_2 addition (on day 24). It then increased briefly for the first 2 days of CO_2 addition and subsequently declined up to the end of the study period. Generally, the SCOD removal efficiency differed only marginally between the bioreactors. This observation is supported by result of statistical analysis on the SCOD removal efficiency which revealed insignificant difference between all of the STPBR, including the control (p = 0.435; two-way ANOVA).

Despite the marginal differences in the SCOD removal, highest removal efficiency of about 82% was achieved in SR 3, operated at an irradiance value of 730.8 $\mu mol.s^{-1}.m^{-2}$ (Figure 4.7). This value was then followed by about 81% SCOD removal efficiency in SR 2. In contrast to biomass productivities and maximum specific growth rates, 'optimum' SCOD removal efficiency was achieved in SR 3 (rather than in SR 2).

However, a relatively high SCOD removal efficiency of up to 75% was achieved in the control bioreactor (Figure 4.7: SR 0). One possible explanation for this result could be the presence of aerobic bacteria in the algal inoculum since same algal culture was used in all of the bioreactors, including the control. Such bacterial community in SR 0 might have aerobically degraded the available organic carbon leading to high observed SCOD removal. In addition, microalgal species capable of living heterotrophically on organic carbon substrates (Ogbonna *et al.*, 2001) were probably responsible for the SCOD removal in the control bioreactor since certain algal species use organic carbon as substrate (Pearson, 2005).

4.3.4 Ammonium and phosphate removal

Ammonium and phosphate removal efficiencies for all of the bioreactors are presented in Figure 4.8. Both ammonium and phosphate removal efficiencies varied with irradiance. CO_2 addition appeared to have substantially enhanced ammonium removal even in the control bioreactor (Figure 4.8a).

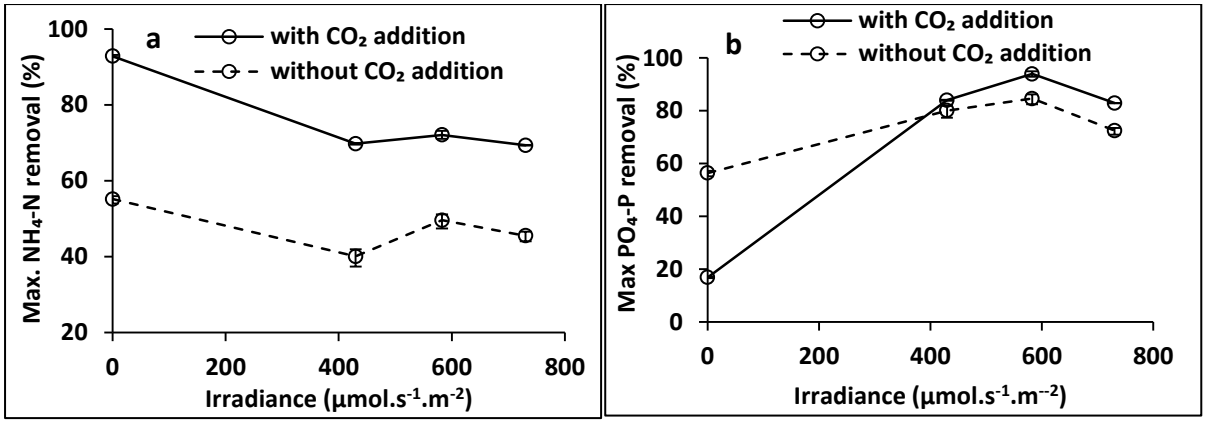

Figure 4.8 Maximum (a) ammonium and (b) phosphate removal efficiencies in STPBR under different levels of LED irradiance

However, this was not the case with phosphate removal efficiency which appears to be marginally enhanced by CO_2 addition in LED-illuminated STPBR but not in the control bioreactor (Figure 4.8b). This is shown by higher phosphate removal efficiency in the control bioreactor of 56.4% without CO_2 addition, compared to 17% in the control bioreactor with CO_2 addition (Figure 4.8b).

Interestingly, the highest phosphate removal efficiencies of about 94 and 85% were achieved with and without CO_2 addition, respectively, in the STPBR operated at medium irradiance (Figure 4.8b). Ammonium removal efficiencies also followed similar pattern, considering the illuminated STPBR and ignoring the removal efficiency of the control bioreactor, giving values of about 72 and 50%, with and without CO_2 addition, respectively (Figure 4.8a). These results followed a similar pattern to those of the growth parameters presented in Section 4.3.2.

However, ammonium removal efficiencies in the control bioreactor were higher than those obtained in the illuminated STPBR. This may possibly have been due to partial nitrification proceeding at higher rate in the control bioreactor than in the illuminated STPBR which may be due to inhibitory effect of the red light on NOB in the STPBR. This viewpoint is supported by the corresponding highest maximum nitrite concentration (Figure 4.10) and near lowest nitrate concentration (Figure 4.9b) being recorded in the control reactor.

4.3.5 Nitrite accumulation

Nitrite concentrations were recorded in the illuminated STPBR up to a maximum of about 50 mg.NO_2-N.L^{-1} in the STPBR operated at high irradiance (SR 3), or perhaps more reliably, a maximum of 49 mg.NO_2-N.L^{-1} recorded in the STPBR with low irradiance (SR 1) as SR 3 NO_2-N concentration on day 28 appears to be an outlier (Figure 4.9a).

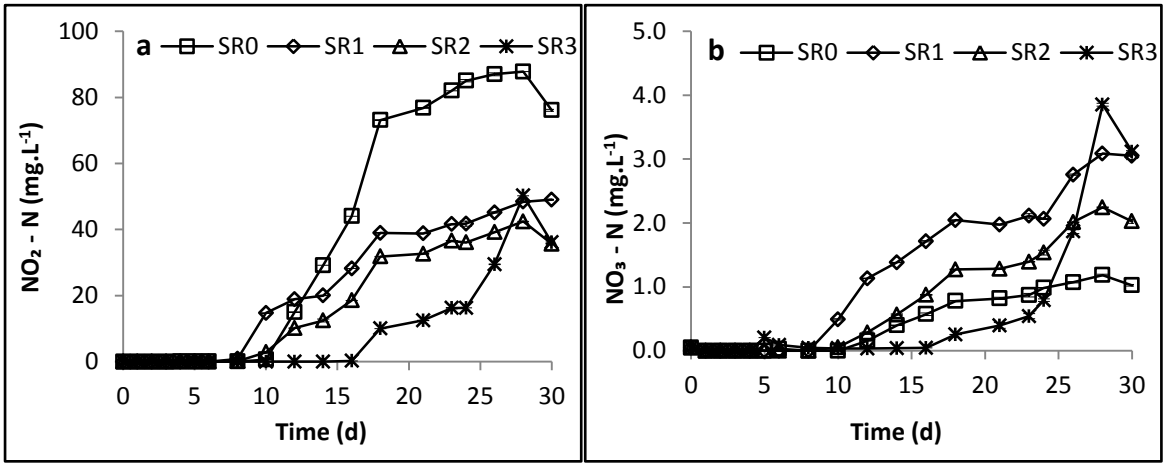

Figure 4.9 Time courses of (a) nitrite-nitrogen (NO_2–N), and (b) nitrate-nitrogen (NO_3–N) concentrations in batch- operated STPBR at different levels of LED irradiance

Interestingly, higher concentration of about 88 mg.NO_2-N.L^{-1} was recorded in SR0. The NO_2-N concentration consistently accumulated with time and may have been light-dependent as it decreased with increasing irradiance (Figure 4.10). Partial nitrification was probably responsible for this nitrite accumulation, as suggested by the relatively low NO_3-N concentrations shown in Figure 4.9b. This may possibly be due to imbalance in AOB and/or NOB activities considering the coupled nature of ammonia and nitrite oxidation in the nitrification process (Philips *et al.*, 2002).

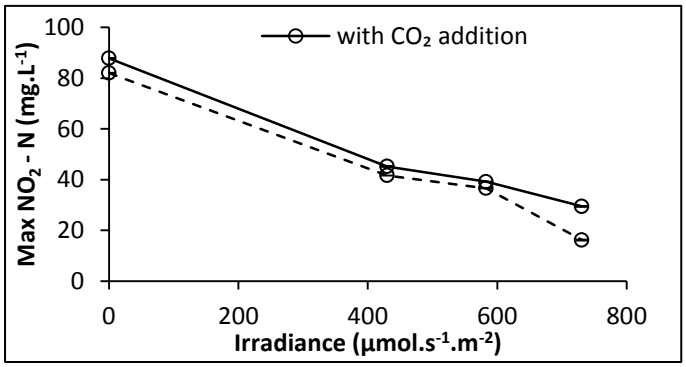

Figure 4.10 Variation of maximum NO_2-N concentration with LED irradiance

Another possibility could be that the accumulated nitrite might have partly resulted from mineralisation of organic nitrogen in the synthetic wastewater chemical constituents such as urea and peptone. This is supported by effluent ammonium concentrations higher than the initial with corresponding TN concentration in the SR (Table A4.6 and Figure A4.1; Appendix). However, lack of TKN analysis data in the current study might have limited this interpretation. High concentrations of nitrite have been reported as having toxic effects on aquatic organisms, especially under non-steady-state conditions (Philips *et al.*, 2002), which is condition existing in microalgal systems operated in batch mode. As such, nitrite toxicity might have affected the nitrogen removal efficiency, and by extension, the overall performance, of the STPBR.

However, the exact cause of this unexpected nitrite accumulation remains unclear. Nevertheless, researchers on bacterial systems have been focussing attention on partial nitrification or nitrite accumulation due to its potential in offering cost savings through minimisation of the oxygen needed for artificial aeration and/or organic carbon required for wastewater treatment, and in nitrogen removal via conventional denitrification process (Sinha and Annachhatre, 2007).

Chapter 5

Effect of MLVSS and SRT on the wastewater treatment efficiency of microalgal STPBR operating at optimum irradiance

5.1 Introduction

This chapter presents the results of Phase III experiments conducted using the STPBR which was defined in Chapter 4. The light source used in these experiments were the same as in the previous study but with slight modifications that brought the irradiance values in all the STPBR to the same optimum level determined in Phase II experiments. The detail on the modification of the light source is presented in Section 5.2.4. Modified synthetic municipal wastewater, based on the composition presented in Section 4.2.2.2 was used as feed substrate for the current experiments. The experiments were conducted without pH or temperature control.

In contrast to Phase I and II experiments, a mixture of microalgae and activated sludge was used to inoculate the STPBR in the current study, with the sole objectives of evaluating the effect of the optimum irradiance, SRT, and MLVSS on wastewater treatment efficiency. These objectives were set in order to develop the HMAS system introduced in Chapter 1, sharing the characteristics and advantages of the individual microalgae and activated sludge systems. The inoculum composition was based on an estimated initial microalgae-bacteria ratio. The STPBR were operated at controlled MLVSS values achieved by the use of clarifiers which facilitated biomass settling and recycling into the STPBR.

5.2 Materials and Methods

5.2.1 Synthetic wastewater

The MSMW used in the STPBR was prepared based on the composition shown in Table 4.2 The concentrated wastewater was prepared and autoclaved at 120 °C for 15 minutes (Rodwell Scientific Equipment, UK) and stored at 4 °C, for about 2 months. MBBM solutions were prepared and added to the synthetic wastewater before use, as described previously

(Section 4.2.2.3). The characteristics of the wastewater used in this study are shown in Table 5.1.

Table 5.1 Composition and characteristics of the MSMW

Composition of Concentrate		Characteristics of diluted concentrate	
Constituents	**Concentration ($g.L^{-1}$)**	**Parameter**	**Concentration ($mg.L^{-1}$)***
Peptone	1.740	SCOD	254 (1.7)
Yeast extract	5.220	NH_4-N	88.1 (1.2)
Glucose	6.100	Total carbon	391.4 (5.9)
NH_4-acetate	31.76	Inorganic carbon	n/d
KH_2PO_4	0.585	PO_4^{3-}	12.4 (0.1)
$MgNH_4PO_4$	0.725	NO_2-N	n/d
K_2HPO_4	0.525	NO_3-N	0.02 (0.00)
Urea	9.170	DO	3.50 (0.01)
NH_4Cl	1.280	pH	5.70 (0.00)
$FeSO_4 \cdot 7H_2O$	0.580	Temperature (°C)	22.1 (0.1)

Note: *unit not applicable to pH and temperature, and values in parentheses are standard deviations

The algal culture growth medium (ACGM) was prepared from a mixture of MBBM, portion of the MSMW concentrate (Table 5.1), and distilled water, and this was fed continuously into the STPBR with peristaltic pumps (520S; Watson Marlow, UK) based on the operating conditions shown in Table 5.2.

Table 5.2 Operating conditions for the STPBR run at 4 d HRT

Bioreactor conditions				ACGM Feedstock composition (% v/v)			
Bioreactor	V (L)	Q ($L.d^{-1}$)	MLVSS ($mg.L^{-1}$)	MBBM	MSMW	Distilled water	Total
STPBR 1	14.92	3.73	50	1.4	1.0	97.6	100
STPBR 2	14.92	3.73	300	1.4	1.0	97.6	100
STPBR 3	15.44	3.86	600	1.4	1.0	97.6	100

5.2.2 Inoculum

The STPBR were inoculated with mixed culture of microalgae and activated sludge at an initial microalgae-bacteria ratio of 90:10, estimated through flow cytometry (detailed in Chapter 6). The algal culture was obtained from Phase II experiments. The culture was centrifuged as described previously (Chapter 3). Aerobic activated sludge (AS) was obtained from the AS tank of Tudhoe Mill Sewerage Works, Spennymoor, County Durham, UK.

The AS was allowed to settle for 2 h at 22 ± 1 °C under quiescent condition to concentrate the sludge, after which the supernatant liquid was decanted and disposed of. The sludge was then mixed with the microalgal culture based on the aforementioned ratio, and

maintained for 3 d in one of the STPBR under red LED irradiance of 582.7 µmol.m^{-2}.s^{-1}, at 16:8 light-dark cycles, prior to the experiments. A single 500 ml batch dose of the ACGM (Table 5.2) was used as feed substrate.

5.2.3 Carbon dioxide

Premixed industrial-grade gas (about 95% pure), composing of 25% CO_2 and 75% N_2 (155924-L-C; BOC, UK) was supplied into the STPBR as described previously (Chapter 3), but at a flow rate of 25 mL.min^{-1}. The gas was supplied to the STPBR only during illumination periods. The premixed gas used in this study was slightly different from that of the previous experiments because O_2 was deliberately excluded in the mixture in order to avoid artificial oxygenation with a view of evaluating the ability of microalgae to satisfy bacterial DO requirements, based on a criterion of achieving a minimum DO concentration of 2 mg.L^{-1} in the STPBR.

5.2.4 Illumination and modification of light source

The same light sources used in Phase II experiments were also used to illuminate the STPBR in the current study, at an average optimum irradiance of 582.7 µmol.m^{-2}.s^{-1}. This irradiance value was determined previously by Mohammed *et al.* (2013b) using the STPBR described in Section 4.2.1. After the light optimisation study presented in Chapter 4, the irradiance values of 429.9 and 730.8 µmol.m^{-2}.s^{-1} were both changed to 582.7 µmol.m^{-2}.s^{-1}. To achieve this, the 6, 9 and 12 Vero matrix boards in the LED cores of the STPBR with low, medium and high irradiance values, respectively (Table 4.1) were changed so that all STPBR contained 9 boards (i.e. 189 LED) in their core.

5.2.5 Selection of MLVSS values

The MLVSS values used in the current study were selected following evaluation of light attenuation at various concentrations of microalgae-activated sludge mixtures at the ratio stated in Section 5.2.2. Light measurement of transmitted irradiance passing through the experimental microalgal culture was performed with the light sensor placed horizontally at the wall of the STPBR, facing the direction of illumination. The STPBR was wrapped with aluminium foil except the position of the light sensor. Different MLVSS concentrations were used for the light measurement. The result of this measurement (Table 5.3) formed the basis for the selection of the main experimental MLVSS values which were chosen as follows.

Table 5.3 Measured irradiance values at the wall of the STPBR

Culture dilution[a]	MVLSS ($g.L^{-1}$)	Measured irradiance ($\mu mol.s^{-1}.m^{-2}$)
Original	0.423	0.09 (0.01)
1:2	0.190	2.85 (0.12)
1:3	0.140	4.65 (0.05)
1:4	0.110	7.45 (0.05)
1:6	0.050	15.44 (0.03)
1:10	0.030	39.34 (0.11)

Note: a, culture diluted from the original with MLVSS = 0.423 $g.L^{-1}$; values in parenthesis are standard deviations

The measured irradiance decreased with increasing MLVSS due to light attenuation resulting from high microbial cell density (Table 5.3). Almost complete light attenuation (99.98%) occurred at MLVSS value of 0.423 $g.L^{-1}$ allowing only 0.09 $\mu mol.s^{-1}.m^{-2}$ to pass through the experimental culture. On the other hand, up to the irradiance value of 15.44 $\mu mol.s^{-1}.m^{-2}$ (Table 5.3) was measured at the STPBR wall for the MLVSS value of about 0.050 $g.L^{-1}$.

Consequently, 50 $mg.L^{-1}$ was chosen as the first MLVSS value, and was used in STPBR 1. The second MLVSS value was empirically chosen to be 6-fold the first value, i.e. 300 $mg.L^{-1}$, using rule of thumb, and was used in STPBR 2. Similarly, the third MLVSS value, which was used in STPBR 3, was chosen to be greater than 423 $mg.L^{-1}$ in order to operate this STPBR at near complete light attenuation. Hence, an MLVSS value of 600 $mg.L^{-1}$ was used in this STPBR, which is 12- and 2-fold the MLVSS in STPBR 1 and STPBR 2, respectively.

5.2.6 STPBR set-up and operation

STPBR, operating at same level of irradiance, were used to treat the ACGM in the laboratory. Three different MLVSS concentrations of 50, 300 and 600 $mg.L^{-1}$ were used in STPBR 1, STPBR 2, and STPBR 3, respectively as the main control parameter. The STPBR were run at 4 d HRT, and 16:8 light-dark cycles, analogous to UK summer time day-night cycles, for 64 days. Clarifiers were used to settle and return slurry into the STPBR to maintain the MLVSS at desired levels. The settled slurry was manually returned to the STPBR daily after determination of its MLVSS through OD measurements and gravimetric analyses, as described previously (Chapter 3). Mixing was provided by a single rectangular impeller, 150 mm x 80 mm, rotating at 100 ± 1 rpm, driven by an overhead stirrer (IKA, UK). Noteworthy, an AS bioreactor was also set-up but its data is not presented due to non-performance and to avoid unfair comparison. Figure 5.1 shows the STPBR experimental set-up.

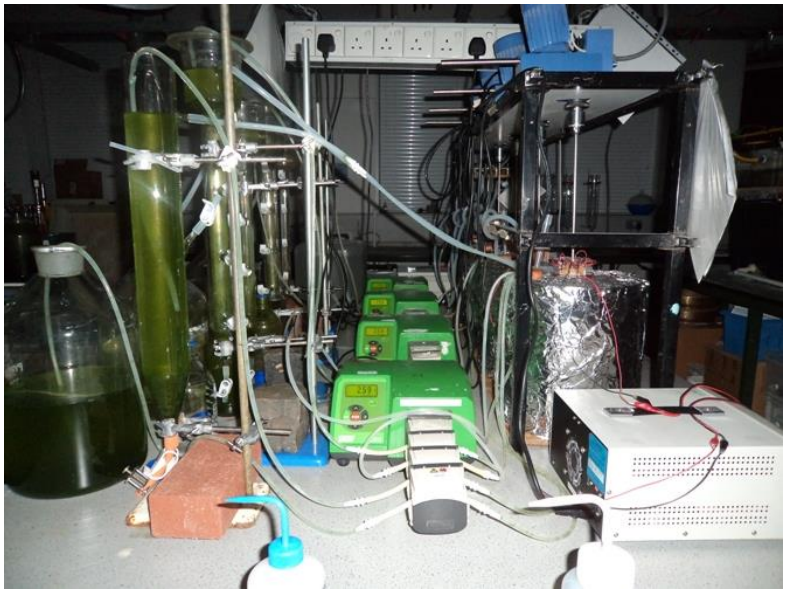

Figure 5.1 STPBR experimental set-up

5.2.7 Test for reference concentration of CO_2 used to determine net carbon uptake rate

To evaluate the carbon uptake of the HMAS (Section 5.3.2), a reference CO_2 concentration was required, and this was determined using a simple test as follows. An STPBR was set-up having the same condition as the main experiments except for the microbial inoculum and illumination, which were omitted. The same premixed gas (Section 5.2.3) was continuously bubbled into the reactor at 25 mL.min^{-1} (25% CO_2, v/v in N_2), for 4 d, until the ACGM was saturated with dissolved CO_2. The saturation concentration was confirmed through daily TOC analyses of samples collected from the reactor, in hexuplicate. The pH and temperature of the ACGM were 6.23 ± 0.01 and 20 ± 1 °C.

The collected samples were filtered through 0.2 µm filter, and analysed for IC concentration using TOC analysis as described previously (Section 3.2.6.4). The average value of the IC concentration was used as a reference for calculating net carbon uptake rate (as mg of equivalent CO_2 L^{-1}.d^{-1}), using Equation 5.1.

$$U_{CO_2} = (IC_{ACGM} - IC_{STPBR_t})\frac{M_{CO_2}}{M_C} \quad (5.1)$$

Where U_{CO_2} is the microalgal equivalent net CO_2 uptake rate (as mg of equivalent CO_2 L^{-1}.d^{-1}); IC_{ACGM} and IC_{STPBR_t} are the peak concentrations of IC in the algal culture growth medium and in the inoculated STPBR (in mg.L^{-1}) at time t; and M_{CO_2} and M_C are the molar masses of CO_2 and elemental carbon (in g.mol^{-1}).

5.2.8 Analytical tests

Samples were collected from the STPBR during each 4 d HRT cycle, and analysed for the parameters stated in Sections 3.2.5 and 3.2.6 (Chapter 3), according to Standard Methods (APHA, 2005), except for NH_4-N. In this case, NH_4-N was measured using Ammonium Ion Selective Electrode (3051) connected to Ion Meter (DR359Tx; EDT Instruments, UK). The ISE was calibrated with five different NH_4Cl concentrations covering the expected range of the experimental samples (i.e. from 5 to 500 $mg.L^{-1}$), according to the manufacturer's instruction. Prior to each set of measurements, the NH_4-N probe was immersed into a high concentration ammonium solution for about 30 min until a stable reading was obtained. Measurements were performed starting from samples with high concentration to the ones with low concentrations, according to manufacturer's recommendations. The electrode was rinsed with deionised water between measurements.

In addition to the offline measurements for DO, pH and temperature using the instruments and methods described previously (Chapter 3); these parameters were also monitored in real-time, at steady-state. DO was monitored using Model D100 OxyProbes whereas pH was monitored using Model S400 ProcessProbes, both connected to Model 30 direct display units, (Broadley James, UK). The direct display units were connected to two-channel Voltage, Current and Resistance Converters (EL037; Pico Technology Ltd., UK). Temperature was monitored using stainless steel jacketed Pt100 probes (Type K; RS Components Ltd, UK) which were connected to four-channel Thermocouple Converters (EL041; Pico Technology Ltd., UK).

All the Converters were then connected to a Data Logger (EL005 EnviroMon; Pico Technology Ltd., UK) using telephone cables (4P2C) and finally to a desktop computer (PC) using a serial cable. Each Converter was configured separately until it was detected by both the Data Logger and the PC. All of the instruments were then daisy-chained and set for online data monitoring. Data was automatically saved on the PC with the aid of preinstalled Data Logging Software (EnviroMon, Version 5.21.4; Pico Technology, UK). The data was finally retrieved manually to a memory stick. The above instruments were configured according to the manufacturer's instruction available in a user manual. Figure 5.2 shows the data logging system connected to a PC.

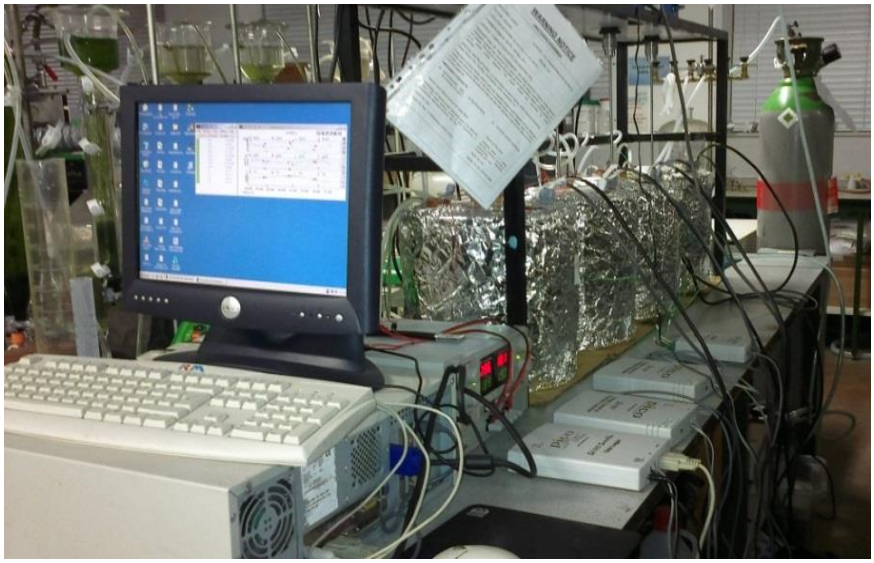

Figure 5.2 The real-time data logging system

5.3 Results and Discussion

5.3.1 STPBR continuous operation

5.3.1.1 SCOD removal and bacterial oxygen requirement

SCOD removal efficiencies with corresponding IC concentration for the STPBR are shown in Figure 5.3.

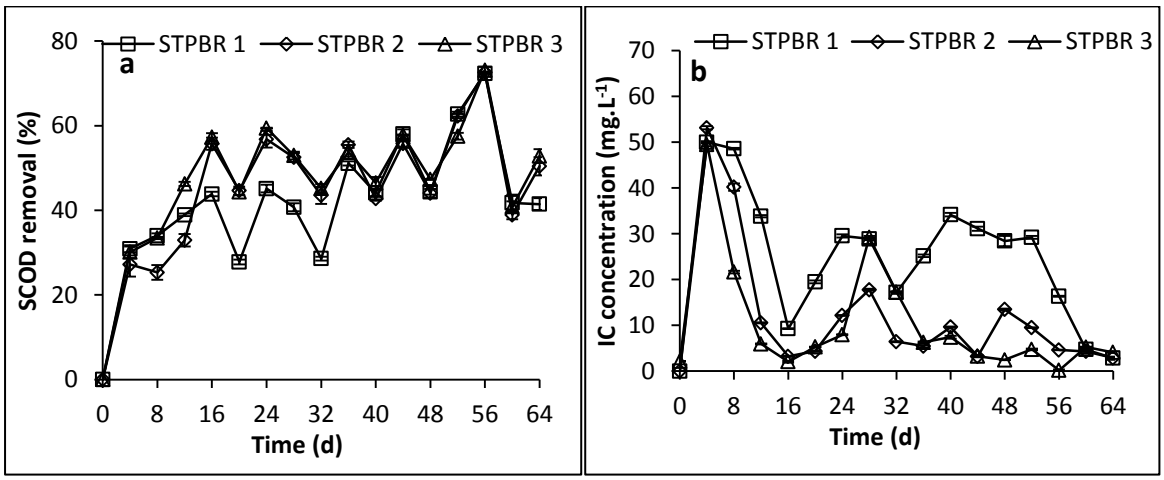

Figure 5.3 Time courses of (a) SCOD removal efficiencies, and (b) IC concentration in the STPBR operated at 582.7 µmol.s^{-1}.m^{-2} red LED irradiance

A maximum SCOD removal efficiency greater than 70% was achieved in all STPBR (Figure 5.3a). The SCOD removal efficiencies in the STPBR were not significantly different (p = 0.495; one-way ANOVA); these results followed a similar pattern to the SCOD removal efficiencies

presented in Section 4.3.3. However, separate statistical analysis on the SCOD removal efficiencies from day 16 through day 36 revealed significant difference (p = 0.045; one-way ANOVA). Maximum SCOD removal achieved in the STPBR ranged from 72% in STPBR 1 to 73 % in both STPBR 2 and STPBR 3 (with average SCOD removal efficiencies ranging from 44% in STPBR 1 to 50% in STPBR 3, with average SCOD removal in STPBR 2 falling between these values).

In addition, the overall highest SCOD removal efficiency of the STPBR are at the lower end of the range quoted for conventional AS systems treating municipal wastewater, which can be up to 90% or even higher (Tandukar *et al.*, 2007). A possible reason for this relatively low SCOD removal efficiency in the STPBR could be the acidic conditions which formed in the STPBR, as reflected by pH values below 7 (Figure 5.4b). This suggests reduced algal activity resulting from possible light attenuation due to high MLVSS. Another possible reason for obtaining lower pH was due to low available oxygen in the liquid and facultative aerobic bacteria started producing acid at oxygen limiting condition.

Considering the pH values (Figure 5.4b), it may be possible that the amount of CO_2 added to the STPBR was too high to control pH within the optimum range needed for algal growth, i.e. $7 < pH \leq 8$ (Park and Craggs, 2010). However, IC concentration in Figure 5.2b does not support this assumption as the mixed liquor should have had more residual IC (i.e. HCO_3^-) to reduce the pH. This was possibly because CO_2 addition was manually controlled in the current study, unlike, for instance, in the case of Park and Craggs (2010) where CO_2 supply was automated based on culture pH dynamics.

Another possibility might be due to increase in CO_2 concentration in the mixed liquor during dark cycle which might have reduced the pH. Since samples were collected during light cycle, the extra IC resulting from microbial respiration would not have been included. Imbalance in CO_2 uptake and production (by algal respiration and bacterial activity and CO_2 gas addition) might have created acidic pH. Nevertheless, the use of CO_2 addition to control pH as applied to this treatment system (which involved the use of monochromatic LED as light source) requires further investigation. This may help in better understanding of the full potential of this newly introduced HMAS.

5.3.1.2 DO, pH, and temperature dynamics in the STPBR

Real-time data of average hourly variation of DO, pH and temperature for all the STPBR are presented in Figure 5.4. These parameters were monitored for 24 h, at steady-state (assumed to be in steady state on day 44, after the 11th HRT cycle; Figure 5.3). Microalgal activity appears to be higher in STPBR 2 than in the other two STPBR as evidenced by the highest DO concentrations predominating in this STPBR, compared to STPBR 1 and STPBR 3 (Figure 5.4a).

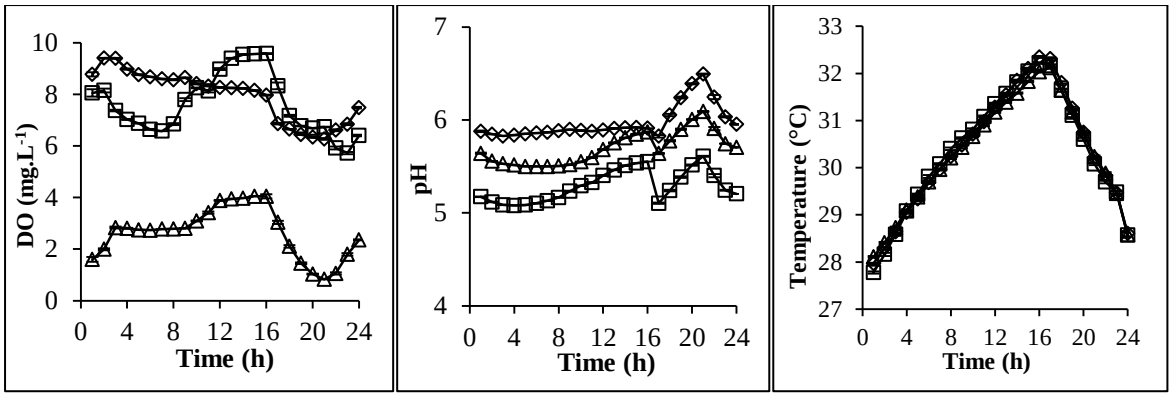

Figure 5.4 Steady-state average 24-h real-time DO, pH and temperature profiles in the STPBR operated at same level of red LED irradiance: □ STPBR 1, ◊ STPBR 2 and Δ STPBR 3 (first 16 h with light, and subsequent 8 h in the dark)

This observation is supported by the highest pH values also being recorded in STPBR 2 (Figure 5.4b). All the hourly pH values recorded in the STPBR were below 7 (Figure 5.4b), suggesting acidic conditions occurred in all STPBR. The acidic pH values may not be unconnected with the relatively low removal of dissolve PO_4-P in all the STPBR (Figure 5.6).

Nevertheless, the resulting DO concentrations (Figure 5.4a) did not show a lack of oxygenation, however, as the stirrer shaft was not sealed, some DO would have dissolved from the ambient air through the liquid vortex created by mechanical mixing due to a gap between the stirrer shaft and the STPBR lid. This observation might explain the relatively low SCOD removal efficiency recorded in the STPBR, compared to conventional AS treating similar waste stream, since DO produced by algae through oxygenic photosynthesis was reportedly more useful in bacterial metabolism than atmospheric oxygen from surface aeration (Shilton and Harrison, 2003).

Furthermore, the acidic pH might have created conditions unfavourable for microbial growth (Figure 5.4b). Additionally, the CO_2 concentration of the added gas (i.e. 25 $mL.min^{-1}$; 25% v/v, in N_2) might have inhibited microbial activity. Inhibition of microalgae at CO_2 concentrations greater than 20% was reported in the literature (Yun *et al.*, 1996). However, CO_2 inhibition was possibly not significant in the current study, considering that lowest MLVSS gave lowest pH due to the higher dissolved CO_2 but was still efficient at SCOD removal, especially in STPBR 2 and 3 which would have had lower CO_2 due to higher algal concentration. Interestingly, bacterial oxygen requirement was apparently satisfied through photosynthetic oxygenation as reflected by DO concentrations greater than 2 $mg.L^{-1}$, measured in all the STPBR (Figure 5.4a). About 1 to 3 $mg.DO.L^{-1}$ is typically needed in AS system in order to maintain aerobic conditions and satisfy bacterial oxygen requirements for COD removal (Metcalf and Eddy, 2003).

There was similar pattern of temperature variation across the STPBR (Figure 5.4c). Temperature increased almost linearly from about 28 °C at the start of illumination to a maximum of about 32 °C at the end of the light cycle. It then declined to about 29 °C at the end of the dark cycle. This relatively high temperature might have adversely affected the performance of the STPBR if the algal populations had been unable to acclimate quickly enough to the relatively quick temperature rise. In contrast, effective operation at temperatures higher than 32 °C, has been demonstrated in full-scale algal PBR (Ong *et al.*, 2010).

Furthermore, the temperature characteristics encountered in this study may be beneficial if the STPBR were to be operated outdoors during winter. The beneficial effect of higher temperatures, arising from LED energy dissipation, might stimulate microbial activities and their associated biochemical reactions (Paterson and Curtis, 2005).

5.3.1.3 Ammonium removal efficiency

Ammonium removal efficiencies of the STPBR were calculated as percentage ammonium removal (Figure 5.5).

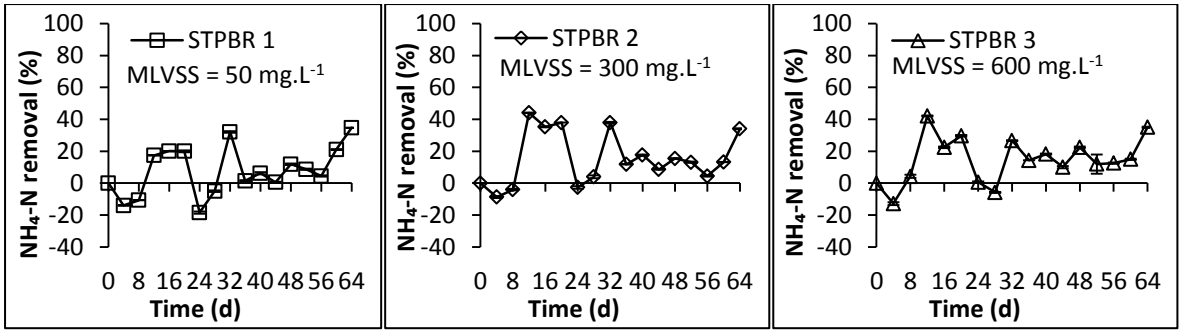

Figure 5.5 Time courses of NH_4-N removal efficiencies in the STPBR operated at 582.7 µmol.s^{-1}.m^{-2} red LED irradiance

The NH_4-N removal efficiencies varied with MLVSS concentrations, as shown by different patterns of removal for the different STBPR. The negative values of the removal efficiency may indicate release of ammonia through possible ammonification of the urea and/other organic nitrogen compounds in the synthetic wastewater. Maximum NH_4-N removal efficiencies of 32, 44 and 42% were achieved in STPBR 1, 2 and 3, respectively. However, these NH_4-N removal efficiencies are much lower than, for example, 83.3% achieved in a pilot-scale HRAP operated at 4 d HRT, with CO_2 addition (Park and Craggs, 2011), the value of 80% reported by Silva-Benavides and Torzillo (2012) in batch culture of *C. vulgaris* grown on nutrient media, and the 90% removal achieved by Camargo-Valero and Mara (2007a) in pilot-scale maturation ponds under ambient supply of CO_2.

However, NH_4-N removal efficiencies similar to the ones obtained in the current study were reported in the literature. For example, Aslan and Kapdan (2006) reported about 50 % NH_4-N removal efficiency in a batch culture of *C. vulgaris* treating synthetic wastewater.

5.3.1.4 Phosphate removal efficiency

Phosphate (PO_4-P) removal efficiencies for the STPBR are shown in Figure 5.6. The PO_4-P removal efficiency varied with time. Generally, low PO_4-P removal efficiencies were achieved in the STPBR. Despite an apparent luxury uptake (Powell *et al.*, 2009; Carberry and Tenney, 1973) of about 5.4, 6.6, and 7.3 mg.PO_4-P.L^{-1}, corresponding to removal efficiencies of 44, 52 and 53% in STPBR 1, 2 and 3, respectively, in the first HRT cycle (day 0 to day 4), this initial removal efficiency was only exceeded in STPBR 1 on day 48 (about 55%; Figure 5.6).

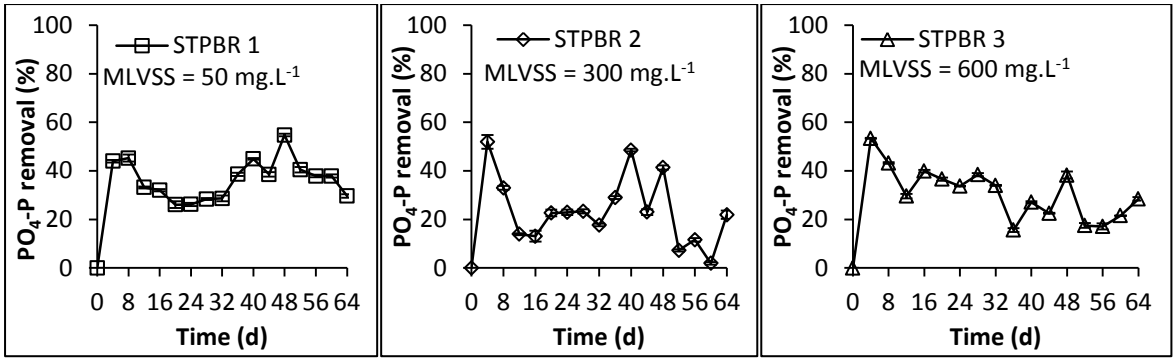

Figure 5.6 Time courses of phosphate removal efficiencies in the STPBR operated at 582.7 µmol.s^{-1}.m^{-2} red LED irradiance

STPBR 1 also appears to be generally more efficient in removing PO_4-P from the wastewater than the other STPBR. This was probably due to the apparently higher rate of biomass growth rate in STPBR 1 resulting from the higher level of irradiance caused by the lower MLVSS (50 mg.L^{-1}). However, the STPBR generally exhibited low PO_4-P removal as compared to higher values achieved in conventional systems reported in the literature. For instance, Aslan and Kapdan (2006) reported PO_4-P removal efficiency ranging from below 30% to a maximum of 78%. Nevertheless, the PO_4-P removal efficiencies generally found in the current study (especially in STPBR 1) are higher than those achieved by Aslan and Kapdan (2006), which were mostly below 30%.

5.3.1.5 Variation of MLVSS with SRT

Operating the STPBR at controlled MLVSS resulted in different SRT ranging from a minimum value of 3.9 d in STPBR 1 to a maximum value of about 6.2 d in STPBR 3. A median SRT of 4.62 was achieved in STPBR 2, which was operated at controlled MLVSS of 300 mg.L^{-1}. The SRT increased with increasing MLVSS across all the STPBR. These findings show that light attenuation has a relatively minor effect on microbial growth rates in the STPBR. Due to the absence of light limitation in STPBR 1, it appears to have slightly higher microbial growth rate than the other two STPBR. Although the SRT values suggest similar microbial growth rates, there were notable differences in the STPBR. Additionally, there was no biomass recycling in STPBR 1 throughout the experimental period due to MLVSS production higher than 50 mg.L^{-1}. Another clarifier was added to STPBR 1 to aid further settling of biomass and to facilitate more wastage in order to maintain this STPBR at the desired MLVSS of 50 mg.L^{-1}.

The biomass concentration in STPBR 2 (i.e. 300 $mg.L^{-1}$) appears to be the relative optimum for operating the STPBR under the experimental light regime because higher algal activity as reflected by higher DO concentration and higher pH values compared to the other two STPBR were observed in this bioreactor. It can, therefore, be concluded that extremes of biomass concentration should be avoided when operating the STPBR at irradiance values of 582.7 $\mu mol.s^{-1}.m^{-2}$ or lower, in order to avoid possible light attenuation. This observation may also apply to pilot- and full-scale hybrid algae-activated sludge systems incorporating internal monochromatic light sources. Although STPBR 1 produced biomass at a slightly faster growth rate than the other two STPBR, low microbial cell density may not be suitable for operating the STPBR, i.e. conditions with MLVSS concentration of 50 $mg.L^{-1}$ or lower.

Additionally, an optimum amount of MLVSS may be useful in mutual cell shading thereby preventing possible photoinhibition in algal photobioreactors operating at high irradiance, close to the intensity of full sunlight or even higher, which may result in photooxidative bleaching of photosynthetic pigments, leading to inactivation or permanent damage of PSII pigment, particularly under prolonged continuous illumination (Long *et al.*, 1994).

5.3.2 Net carbon uptake rates

Carbon uptake rates (CUR) in the STPBR were evaluated based on the variation of inorganic carbon concentration in the mixed liquor, through TOC analysis, assuming that the change in IC concentration was mainly due to algal assimilation (ignoring contribution in IC concentration in the mixed liquor due to microalgal respiration and bacterial activity). The calculated CUR values are, therefore, net rather than gross. However, this assumption would have possibly underestimated the net CUR of the STPBR. Nevertheless, the IC measurements were performed during light cycles and algal photosynthesis might have consumed the CO_2 produced through bacterial degradation of organic matter, and that microbial respiration was probably minimal. The net CUR was calculated using Equation 5.1 (Section 5.2.7). Figure 5.7 shows the amount of inorganic carbon taken up in each of the STPBR.

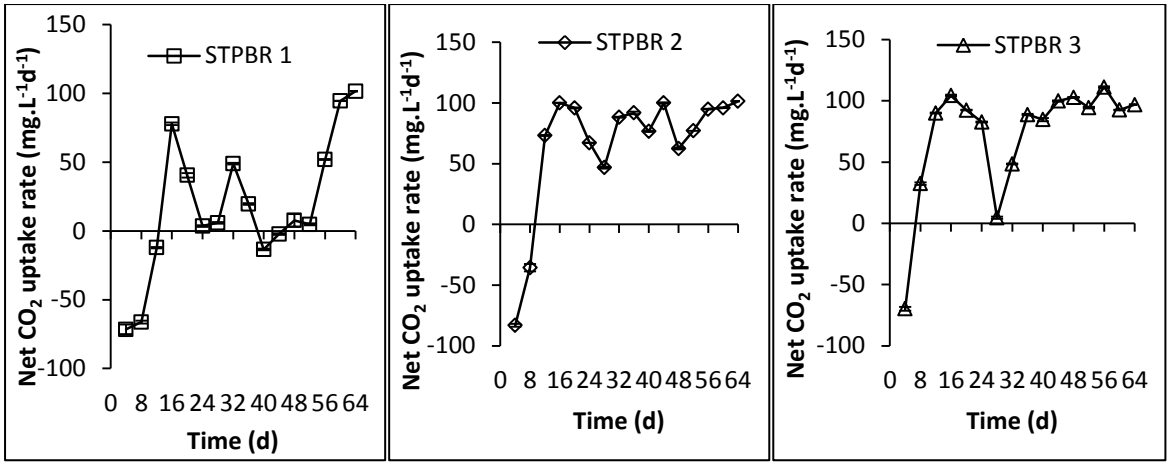

Figure 5.7 Time courses of net carbon uptake rates at different MLVSS concentrations

The negative values of the net CUR (Figure 5.7) in the first 3, 2 and 1 HRT cycles in STPBR 1, 2 and 3, respectively, were possibly due to the background IC concentration in the microalgal inoculum that was used to seed the STPBR. The other negative values in STPBR 1 (day 40 to day 44) may indicate lack of CO_2 uptake in this STPBR. The net CUR were more stable in STPBR 2 and 3 than (from day 16 onwards) than in STPBR 1. The net CUR appeared to stabilise in STPBR 1 only at the end of the experimental period (day 64; Figure 5.7).

Generally, the net CUR varied with time across the STPBR with maximum values of about 102, 100 and 111 $mg.L^{-1}.d^{-1}$ achieved in STPBR 1, 2 and 3, respectively (Figure 5.7). Although higher net CUR was recorded in STPBR 1 compared to STPBR 2, a reverse trend can be observed when the net CUR is generally considered in these two STPBR. Average net CUR values of about 33, 85 and 85 $mg.L^{-1}.d^{-1}$ were achieved in STPBR 1, 2 and 3, respectively.

Considering the average maximum values of the net CUR achieved in both STPBR 2 and 3, and the marginal differences in the overall maximum net CUR recorded in all the STPBR, there was no definite pattern of the net CUR variation with respect to light attenuation. As such, there seemed to be no clear relationship between the net CUR and photosynthetic activity in the STPBR under the operating red LED irradiance of 582.7 $\mu mol.s^{-1}.m^{-2}$.

Compared to CUR reported in the literature, the highest value found in this study is lower than 0.846 $g.L^{-1}.d^{-1}$ CO_2 fixation rate for *C. sorokiniana* reported by Ogbonna *et al.* (1999) in an internally-illuminated PBR with integrated artificial-solar light collection and distribution system, at 5% CO_2 (v/v) concentration. However, the above microalga was grown in a high-

nutrient media which cannot feasibly be applied to full-scale systems and, therefore, such fixation rates may rather be achievable only in principle.

5.3.3 Electrical power consumption

The electrical power consumed by each of the STPBR at 4 d HRT (i.e. 64 h) is shown in Table 5.4.

Table 5.4 Electrical power requirements for the STPBR operated at 4 d HRT

Bioreactor	Transmitted irradiance ($\mu mol.s^{-1}.m^{-2}$)	Equivalent power (W)	Power (kWh)
STPBR 1	45	0.58	0.0374
STPBR 2	7.5	0.10	0.0062
STPBR 3	3.8	0.05	0.0032

The power consumed by each of the STPBR was used to evaluate the energy required to remove 1 kg of SCOD from the wastewater (Section 5.3.4). The energy calculation was based on equivalent power consumed in illuminating the STPBR with reference to the amount of measured transmitted irradiance on the wall of the STPBR in order to account for the variation in MLVSS across STPBR. The equivalent power was the difference between that of transmitted irradiance through air and the transmitted irradiance through microbial culture.

For example, the transmitted irradiance for STPBR 1 in Table 5.4 was obtained by subtracting 15.44 $\mu mol.s^{-1}.m^{-2}$, the transmitted irradiance obtained at MLVSS of 50 $mg.L^{-1}$ (Table 5.3) on the reactor wall, from 60.3 $\mu mol.s^{-1}.m^{-2}$, the irradiance obtained in empty STPBR wall (Table A4.1; Appendix). The corresponding equivalent power value for STPBR 1 was then calculated proportionately using the power of 7.56 W for 582.7 $\mu mol.s^{-1}.m^{-2}$, i.e. the irradiance on the LED core (Table 4.1). The transmitted irradiance and their corresponding power values (Table 5.4) for STPBR 2 and 3 were proportionately calculated by dividing those obtained in STPBR 1 by 6 and 12, respectively (based on the factor of increase in MLVSS across the STPBR earlier presented in Section 5.2.5).

On the other hand, the total SCOD removed in the STPBR (Table 5.5) were determined by adding SCOD removed through conversion of the bubbled CO_2 to glucose by algal photosynthesis (assuming 80% of the added CO_2 was assimilated by algae, Table A5.4; Appendix) to the amount removed based on maximum SCOD removal efficiency obtained in the STPBR (Table A5.5; Appendix).

5.3.4 Energy requirement for SCOD removal

Since energy is required to remove a given amount of pollutant from a known volume of wastewater, it is important to evaluate the energy efficiency in relation to the performance of a given treatment system. Therefore, the efficiency of the current HMAS was evaluated based on the electrical energy required by the STPBR in removing a given amount of SCOD at the operating HRT and photoperiod. The amount of energy required to remove 1 kg of SCOD, based on the maximum treatment efficiency achieved in the STPBR, is given in Table 5.5.

Table 5.5 Energy required for SCOD removal in the STPBR

Bioreactor	SCOD removed (kg)	Energy (kWh(kg.SCOD)$^{-1}$)
STPBR 1	0.0671	0.56[a]
STPBR 2	0.0672	0.10[a]
STPBR 3	0.0673	0.05[a]
AS	-	1.00[b]

Note: 'a' denotes values found in current study and 'b' obtained from Ahammad *et al.* (2013)

Importantly, the energy requirement in Table 5.5 was solely evaluated based on the power required to illuminate the LED in the STPBR operating at 4 d HRT and the corresponding photoperiod of 64 h (based on the light-dark cycle of 16:8). It is well known that artificial aeration with its associated energy requirements constitutes about 80% of the overall operational costs of aerobic wastewater treatment processes, e.g. the AS system, (Driessen and Vereijken, 2003). Since about 1 kWh of electrical power is required to remove 1 kg of COD in conventional aerobic wastewater treatment systems (Ahammad *et al.*, 2013), this implies that about 0.8 kWh of energy is expended on provision of artificial aeration in, for example, the AS system to remove 1 kg of COD.

Interestingly, the current HMAS exhibits greater potential towards energy savings as well as reduction in the overall operational cost of municipal wastewater treatment as reflected by its energy efficiency (Table 5.5). It achieved up to 95% energy saving, compared to conventional AS system.

Chapter 6

Effect of 'optimum' irradiance and system mode of operation on microbial dynamics in photobioreactors treating municipal wastewater

6.1 Introduction

This Chapter presents the results of microbiological analyses carried out on selected samples from Phase I and II experiments, to estimate the proportion of microalgae and bacteria present in the PBR treating municipal wastewater. The analyses employed the application of two microbial techniques: FCM and/or qPCR. These methods are fast and accurate, and can be repeated easily on prepared, fixed and preserved samples.

FCM was used to estimate the proportion of photosynthetic (assumed to be microalgae in this study) and non-photosynthetic (assumed to be bacteria) microorganisms in samples collected from the PBR, based on chlorophyll fluorescence, represented by two distinct colours, i.e. green for photosynthetic and red for non-photosynthetic microorganisms (see Figures A5.2 and A5.3; Appendix). FCM has the advantage of counting all phototrophs, both cyanobacterial and microalgal cells; cyanobacteria are prokaryotic and are also targeted by qPCR. However, there is a problem of overlap between negative/non-photosynthetic and positive/photosynthetic controls/samples during gating of the counted cells on the captured image (Figure A5.3; Appendix), and this slightly underestimates the microbial proportion.

On the other hand, qPCR was used to estimate the number of gene copies of both microalgae (targeted as eukaryotic), and bacteria (targeted as prokaryotic, including cyanobacteria), based on amplification of their targeted ribosomal ribonucleic acids (18S rRNA for prokaryotic, and 16S rRNA for eukaryotic organisms). However, a limitation of the qPCR technique is the possible overestimation of bacterial gene copy numbers due to the presence of 16S rRNA in eukaryotic chloroplasts, cyanobacterial and bacterial DNA (Giovannoni *et al.*, 1988). This can lead to false-positive signals (Knapp and Graham, 2004), leading to overestimation of the bacterial numbers in the tested samples.

Due to wide variability in eukaryotic microalgal gene copy numbers between species (Zhu *et al.*, 2005), the data obtained through qPCR analysis would be more accurately expressed as gene copy per gram of microalgal biomass, than gene copy per microalgal cell. Despite that limitation, bacterial qPCR data can be expressed as gene copy per cell. Both the bacterial and microalgal qPCR data obtained in this study are presented as gene copy per gram biomass, for accuracy and ease of comparison. Accepting the limitations of these microbial techniques, lack of cheaper and more robust alternative methods necessitated the application of these methods in this research. Moreover, either of the above techniques can be used as an alternative to conventional chlorophyll measurement methods.

Depending on the strength of correlation between the data obtained from the above two microbial techniques, the end result can serve as a guide in adopting either of these methods in combination with, or as an alternative to, the generic microalgal growth measurement methods (with special regard to mixed microbial cultures), such as gravimetry and simple photometry, bearing in mind analytical cost and time required for sample preparation, and the numerical analyses undertaken. However, the selectivity of the microbial techniques, compared to generic methods such as gravimetry, may favour the use of the former methods over the latter.

Application of these techniques was particularly helpful to the development of the HMAS, as they can be used as an accurate tool in evaluating the microbial dynamics with respect to the optimum irradiance, and PBR mode of operation (i.e. batch or continuous). Evaluation of cell numbers through microbial analyses could serve as a strategy for checking and possibly preventing process failure, since bacteria may rapidly out-number microalgae, or perhaps vice-versa, depending on the prevailing growth conditions. This is due to the fact that bacteria have higher growth rates than microalgae, possibly due to their simpler cell structure and DNA replication (Campbell *et al.*, 2000). This may help in better understanding of the performance of the HMAS with respect to both bacterial and microalgal dynamics.

The above microbiological analyses were performed by Miss Lucy Eland, a fellow PhD candidate at the School of Civil Engineering and Geosciences, Newcastle University, UK, on behalf of the author. Her involvement included the sample collection from the PBR, sample preparation, and running of both the FCM and the qPCR, in the laboratory. This approach

was taken, rather than the author develop these skills directly, due to the level of work and time involved in establishing reliable quantitative results from these techniques (Miss Eland had established these skills over a considerable period of time).

Although the majority of analyses were carried out by Miss Eland, the author undertook some sample collection, preparation and some FCM analysis. This approach, which enabled sample to be run with Miss Elands' own samples, was the only effective option, in terms of actual cost and time investment, for the author to conduct these analyses with the current project, particularly since these analyses were beyond the scope of the original research plan. Consequently, the additional data added greatly to the information provided by data obtained from the measurements of traditional wastewater treatment parameters.

6.2 Materials and Methods

6.2.1 Sample collection

Samples were collected from the PBR in 50 mL screw-cap centrifuge tubes (VWR, UK), at the initial, middle and final stages in Phase II, and at 8-d interval in Phase III experiments. The sample quantity collected in each experimental phase depended on the biomass concentration in each photobioreactor during sampling, with the sample volume decreasing towards the end of each experimental period, due to greater microbial growth and productivity.

6.2.2 Flow cytometry

In order to carry out the FCM, the collected samples were prepared and fixed with paraformaldehyde (PFA) fixative as follows.

6.2.2.1 Preparation of PFA fixative

PFA fixative was prepared as follows. 44.5 mL of sterile distilled water (autoclaved at 121 °C for 15 min) was heated at 60 °C followed by the addition of 10X phosphate buffered saline (PBS) and 1 drop of 10 M NaOH. 2 g of powdered PFA was then added to the heated solution, and the mixture was stored on ice, and the pH of the solution was adjusted to 7.2, using dilute HCl. The solution was then filtered through 0.2 µm filter, and the filtrate frozen for subsequent use in sample preparation.

6.2.2.2 Sample preparation and fixation

A 1 mL of sample was added to a 2 mL Eppendorf tube (Eppendorf, Germany), and centrifuged at 13,000 g for 3 min, using Micro Centaur Centrifuge (MSE, UK). The above procedure was repeated until enough cell pellets (about 50 µL volume) was obtained in the Eppendorf tube. The supernatant liquid was then removed with a mini pipette and the biomass pellet resuspended and washed twice by addition of 1 mL PBS and vortexed using a vortex mixer (Velp Scientifica, Europe), and centrifuged as earlier mentioned.

The biomass pellet was then resuspended in 0.25 mL PBS and 0.75 mL PFA fixative, and vortexed. The cells suspension was incubated overnight, for about 15 h at 4 °C. The cell pellet was centrifuged again as above and washed once more with 1 mL PBS, vortexed and recentrifuged. The cells were eventually resuspended in a 1:1 mixture of PBS and absolute ethanol, and stored at - 20 °C for subsequent FCM analysis.

6.2.2.3 Flow Cytometer set-up and operation

The Flow Cytometer (5 Laser LSR II; BD Biosciences, USA) was set-up according to the manufacturer's recommendations as follows. The cytometer and the PC, with BD FACSDiva Software (Version 6.1.3; BD Biosciences, USA), were switched on and left for 30 min, allowing the laser to stabilise. The cytometer fluidics was then crosschecked using the software to ensure it was at sufficient level for running the test. The cytometer column was then cleaned by running distilled water, which immediately drained into the waste collection tank connected to the machine. A data storage file (with sample labels) was then created in the Diva software.

After completing the above procedure, the stored PFA fixed cells were thawed and resuspended by the addition of 1 mL PBS and vortexing. A 1 mL of the cell suspension was then transferred into a 5 mL polystyrene tube (Partec, Germany), and mounted onto the cytometer. The sample was run through the machine by clicking acquisition button in the software until 10,000 cells were counted, based on the presence or absence of fluorescence detected by the cytometer. Prior to sample run, samples were vortexed to break cell clumps but those remaining were removed by filtering through a 30 µm CellTrics green coloured filter (Partec, Germany), to avoid blockage of the cytometer column. The data was then

immediately acquired by the machine and automatically saved to file, and subsequently accessed and analysed offline.

6.2.2.4 Cell counts

Both negative (activated sludge; Section 5.2.2) and positive (isolated microalgal strains; Table 6.1) control samples were used to set up the gating of the 5 Laser LSR II Flow Cytometer with 488-710/50 Laser (laser-band pass/tolerance; BD Biosciences, USA). The gating was set up to reflect the pattern observed in both the negative and the positive control samples. The isolated microalgal strains (grown in sterile conditions) were obtained from the Schools of Civil Engineering and Geosciences (CEG) and Marine Science and Technology (MAST), Newcastle University, UK.

Table 6.1 Microalgal strains used as positive samples in FCM analysis

Species	Type of microalga	Source
C. vulgaris	Eukaryotic	CEG
Scenedesmus quadricauda	Eukaryotic	CEG
Synechococcus	Blue-green	CEG
Dunaliella viridis	Eukaryotic	MAST
Tetraselmis sp.	Eukaryotic	MAST

The microalgal and bacterial cell counts, data acquisition and analysis were performed on a BD LSR II workstation using the BD FACSDiva Software which was linked to the FCM database of the 5 Laser LSR II flow cytometer (located at the FCM Suite of Newcastle University Medical School at the Newcastle Centre for Life).

6.2.3 Real-time qPCR

In order to carry out qPCR on the aliquots collected from the PBR, sample volumes were calculated to give a corresponding CDW of 0.0025 g of biomass required to extract enough DNA for a qPCR reaction, and samples prepared according to Eland *et al.* (2012), adapted from the manufacturer's recommendations, as specified below.

6.2.3.1 Sample preparation for DNA extraction

Sample volumes appropriate for DNA extraction (Table A6.1; Appendix) were transferred into 50 mL screw-cap sterile centrifuge tubes and centrifuged at 4200 rpm for 120 min, using Sigma 3 – 16P (Sigma, Germany). The supernatant liquid was decanted and disposed ,

and the cell pellets transferred into 2 mL Eppendorf tubes, and frozen at – 20 °C for subsequent DNA extraction.

6.2.3.2 DNA extraction

The prepared samples were thawed, and DNA was extracted from the cells using QiagenDNeasy Blood and Tissue kits (Qiagen, Germany) according to the manufacturer's instruction, as modified for use on mixed microalgal cultures by Eland *et al.* (2012), as follows. The reagents used for the DNA extraction, as well as spin column and collection tubes, were all supplied with the QiagenDNeasy kits, except ethanol. The samples were transferred to a number of 2 mL Eppendorf tubes and centrifuged at 13,000 g, for 3 min. The supernatant liquid was carefully removed followed by the addition of 180 µL Buffer ATL and 20 µL proteinase K solutions. The mixture was vortexed, and mixed overnight at 56 °C, in a Unitron CH4103 incubator-shaker (Infors AG, Switzerland).

The incubated samples were then vortexed for 15 s followed by the addition of 200 µL Buffer ATL and 200 µL absolute ethanol. The mixed samples were then transferred to Qiagen DNeasy Mini Spin column and centrifuged at 6,000 g, for 1 min. As a precaution, this step was sometimes repeated to facilitate the passage of all the liquid through the spin column membrane. Both the collection tube and permeate passing the membrane were discarded. The spin column was then placed in a new collection tube and 500 µL of AW1 reagent was added to the column and centrifuged at 6,000 g, for 1 min. The tube and permeate and were again discarded. A 500 µL of AW2 reagent was then added to the column and centrifuged at 20,000 g, for 3 min.

The collection tube and permeate were discarded, and the column placed in a sterile 2 mL microcentrifuge tube. A 200 µL of elution buffer was then added to the membrane of a spin column and incubated at room temperature for 1 min, and centrifuged at 6,000 g, for 1 min, to elute the extracted DNA, which collected in collection tube. This step was repeated for another elution which was also collected in the same tube, giving a total elution volume of 400 µL.

6.2.3.3 Real-time qPCR reactions

As required, DNA standards were prepared prior to carrying out the qPCR reactions on the eluted samples. A eukaryotic primer standard was made using a purified and sequenced

microalgal band from DGGE band, using a primer set EUK1A and EUK516r according to Eland *et al.* (2012) as follows. Initially, PCR was carried out on the band DNA followed by agarose gel electrophoresis on a 1.5% gel without the addition of a DNA stain. About 11 µL PCR product was then loaded on the gel, and electrophoresis current applied (200 V for 4.5 h). The first PCR and marker lanes were then cut out of the gel and stained. The cut portion was viewed to check for correct size of target fragment, using the marker ladder.

The desired gel was then cut out and the large gel replaced into its space. The unstained band parallels were then cut out with reference to the stained gel, as a guide. The bands were placed in weighing tubes and weighed to determine the weight of the gel fragments. This was followed by clean-up, with extra stage to dissolve the gel using the gel extraction spin protocol and Qiagen PCR purification kits, with QC buffer and isopropanol. The amount of DNA in the suspension was assessed using ND-1000 Spectrophotometer (NanoDrop Inc., USA); and the number of DNA fragments contained in 1 µL of the standard solution was computed using Equation 6.1.

$$N_{G_c} = \left(\frac{C_{DNA}}{M_f}\right) \times 6.023 \times 10^{23} \quad (6.1)$$

Where N_{G_c} is the gene copy number per µL of sample DNA; C_{DNA}, the concentration of DNA (in g.µL^{-1}); M_f, the molar weight of fragment (i.e. amplicon + primers; in g.mol^{-1}); and 6.023 X 10^{23}, the Avogadro number (in molecules.mol^{-1}). M_f is defined in Equation 6.2 as follows.

$$M_f = 660 \times N_{bp} \quad (6.2)$$

With N_{bp} as the number of base pairs in each fragment; and 660 is the weight of a fragment (in Daltons, Da). Similarly, a prokaryotic standard solution available in the laboratory was used for the bacterial qPCR. The eukaryotic standard was made through the cloning method.

To check for inhibition of the qPCR reaction, test runs were carried out based on serial dilutions, and no inhibition was detected. Therefore, 1:10 dilution was applied to the DNA extracts, using Qiagen molecular-grade nuclease-free water. A 5 µL of SsoFast EvaGreen Supermix (SsoFast mix) qPCR reagent was added to 0.5 µL each of forward and reverse primers, and 2 µL of nuclease-free water, per each qPCR reaction. A mixture of these reagents based on the ratio of the stated volumes, enough for all qPCR reactions, was made;

and a Qiagen QIAgility robot was used to dispense 8 µL of the mixture and 2 µL of the extracted DNA to each of the wells on a 96-well plate.

All of the qPCR reactions were carried out using SsoFast mix and the reactions were performed on a CFX C1000 Thermal Cycler with a CFX96 real-time system adaptor (Bio-Rad, Hercules, USA). All of the qPCR reactions were performed in triplicate, as recommended by Bio-Rad, using primers obtained from the literature as shown in Table 6.2.

Table 6.2 Details of primers used in the qPCR reactions

Primer	Sequence (5'→3')	Function	Specificity	Base pairs	Reference
BAC338F	ACTCCTACGGGAGGCAG	Forward	Bacteria	708	Yu *et al.* (2005)
BAC1046R	CGACARCCATGCANCACCT	Reverse	Bacteria	708	Huse *et al.* (2008)
EUK345F	AAGGAAGGCAGCAGGCG	Forward	Eukarya	149	Zhu *et al.* (2005)
EUK499R	CACCAGACTTGCCCTCYAAT	Reverse	Eukarya	149	Zhu *et al.* (2005)

The qPCR programme was set-up as follows. For the *eukaryot*es, each qPCR reaction began with initial enzyme activation at 95 °C for 10 min, denaturation at 95 °C for 30 s, annealing at 55 °C for 30 s, and extension at 60 °C for 30 s. The qPCR reaction continued in a similar manner for 39 more cycles. On the other hand, each qPCR reaction for the *prokaryotes* began with initial enzyme activation at 95 °C for 5 min, denaturation at 95 °C for 45 s, annealing at 62 °C for 45 s, and extension at 72 °C for 45 s. The reactions continued in a similar manner for 39 more cycles. Additionally, the melt curves for both the eukaryotes and prokaryotes were separately tested at 65 to 95 °C for 5 s, at temperature increment of 0.5 °C.

6.2.4 Data analysis

The number of photosynthetic and non-photosynthetic cells (presented as microalgal and bacterial, from Section 6.3 onwards), counted by FCM analysis was obtained from the FACSDiva software, as a percentage value. In order to compare the dynamics of these two microbial groups in the PBR, the eukaryotic and prokaryotic cell numbers obtained from qPCR reactions (also presented as microalgal and bacterial, in the same sections) were also expressed in percentage units. These two percentage estimates were then correlated in order to determine whether the data obtained from these two microbiological methods are strongly or weakly related. Pearson's correlation was performed on the data using SPSS software (version 19; IBM Corp., USA).

6.3 Results and Discussion

Since the FCM analysis was only carried out on Phase III experimental samples, the results of this microbial technique obtained from this experimental phase, and the qPCR results are presented first in Section 6.3.1. Consequently, the qPCR results for Phases II experiments are presented later in Section 6.3.2.

6.3.1 Phase III experimental samples

6.3.1.1 Microbial dynamics: FCM and qPCR

The STPBR were set up with an initial M:B of about 90:10 (Figure 6.1), as estimated using FCM. This parameter was used to evaluate the microbial dynamics in the STPBR, from the analyses carried out on replicated samples.

Considering the FCM analysis, the proportions of bacteria and microalgae varied in a similar pattern in all the STPBR (Figure 6.1a, c and e).

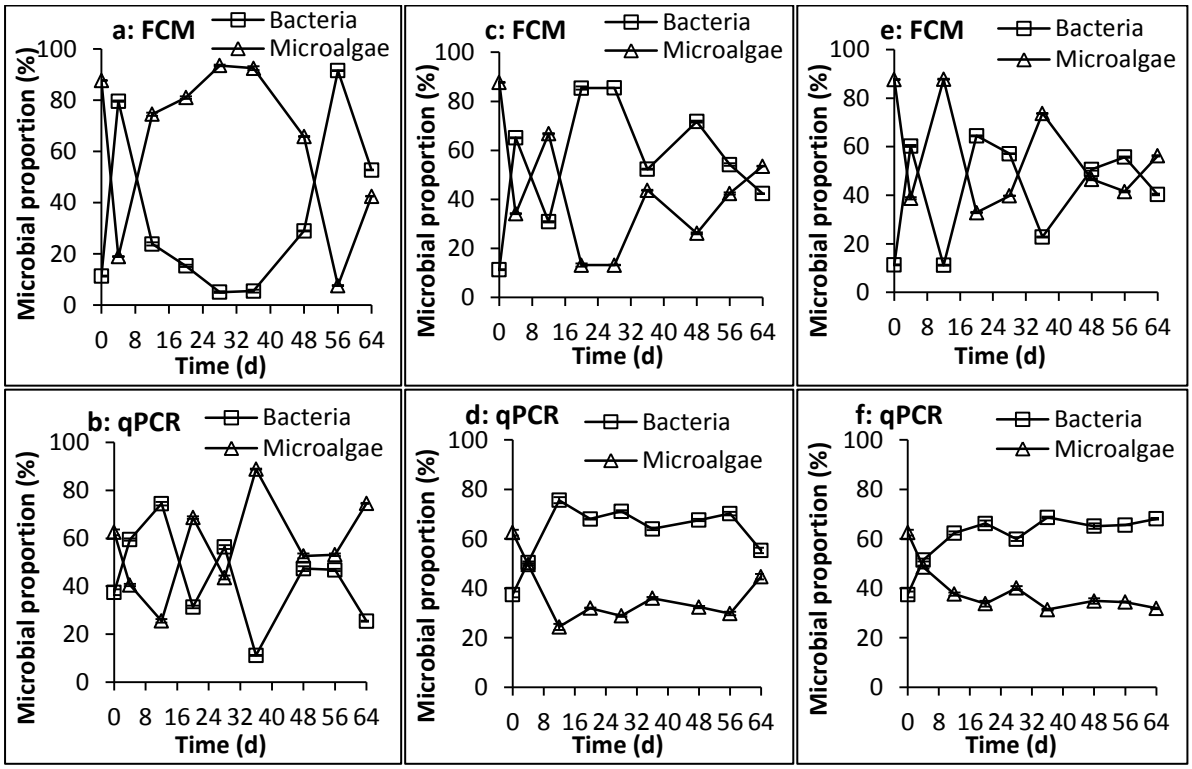

Figure 6.1 FCM and qPCR time courses of microbial proportions in (a, b), STPBR 1; (c, d), STPBR 2; and (e, f), STPBR 3. All STPBR operated at 582.7 µmol.s^{-1}.m^{-2} red LED irradiance and 4-d HRT

There was a sharp decrease in the M:B ratio from its starting value to a value of 50:50 in all the STPBR in the first HRT cycle, i.e. the intersection of the two lines between day 0 and day

4 in Figure 6.1a, c and e, indicating an equal proportion of these two microbial communities. The 50:50 M:B composition occurred at other times in the STPBR: three times in STPBR 1; four times in STPBR 2 and six times in STPBR 3; this trend followed the order STPBR 3 > STPBR 2 > STPBR 1. This shows the dominant class changes regularly, indicating a highly dynamic population, particularly in STPBR 3.

The M:B decreased further to about 20:80, 30:70 and 40:60 in STPBR 1, 2 and 3, respectively, at the end of the first HRT cycle (day 4; Figure 6.1a, c and e), indicating the bacteria were growing at faster rate than microalgae. This resulted in decrease in microalgal population with corresponding increase in bacterial population across the STPBR (day 4 in Figure 6.1a, c and e).

Due to a change in microbial growth dynamics, the microalgal population eventually exceeded that of bacteria on day 12 in all STPBR, leading to M:B of about 80:20, 70:30, and 90:10 in STPBR 1, 2 and 3, respectively (Figure 6.1a, c and e). This is interesting, especially for STPBR 1 and 2 as these M:B are the inverse of those recorded on day 4 in these two STPBR. In STPBR 3, the M:B value recorded on day 12 (i.e. 90:10; Figure 6.1e) is, however, much greater than that recorded on day 4 (M:B = 40:60) in STPBR 3, suggesting microalgae growing faster in this STPBR compared to other STPBR. A possible reason for the faster microalgal growth in STPBR 3 might be due to the microalgal community growing heterotrophically, at a faster rate than in the other STPBR.

The M:B ratio increased continuously in STPBR 1 up to day 28 when it reached a highest value of about 90:10 (Figure 6.1a). After remaining at this level until day 38, it then decreased rapidly to its lowest value of about 10:90 on day 56, and eventually approached 50:50 at the end of the experiment. In STPBR 2, however, there was a decrease in the M:B ratio on day 20, reaching a lowest value of about 10:90 (Figure 6.1c). The M:B remained fairly constant in STPBR 2 up to day 28, and subsequently increased approaching 50:50, at the end of the experiment. STPBR 3 showed microbial dynamics similar to that in STPBR 2 from day 20 onwards (Figure 6.1e). The M:B decreased to about 30:70 on day 20; it then increased to about 70:30 on day 36, and approached 50:50 towards the end of the experiments.

Generally, higher microalgal growth rate was observed in STPBR 1 compared to the other STPBR (Figure 6.1a, c, and e). This is reflected by the number of times the initial M:B (i.e. 90:10) was exceeded in this STPBR (days 28 to 36 in Figure 6.1a). The initial M:B was exceeded slightly only once in STPBR 3 but never in STPBR 2. This clearly shows that the microalgae have exceeded the bacteria in STPBR 1, more times than in the other STPBR (i.e. five times in STPBR 1, three times in STPBR 3; and only twice in STPBR 2; Figure 6.1a, c, and e). In contrast, the bacterial community appears to have grown faster, and become more stable within STPBR 2 compared to the other STPBR. STPBR 2 appears to have had conditions more favourable for bacterial growth compared to the other STPBR.

Considering the molecular analysis data, variation in M:B shown by the qPCR data (Figure 6.1b, d and f) was actually very similar to FCM data, in the first HRT cycle, across the STPBR. However, qPCR analysis gave an initial M:B ratio much lower than that obtained by FCM analysis (about 40:60; Figure 6.1b, d and f); this was probably due to overestimation of the bacterial cell numbers (Table A5.3; Appendix), resulting from the inclusion of cyanobacteria in prokaryotic gene copy numbers. Additionally, the 50:50 ratio was only found to reoccur frequently in STPBR 1 (almost six times; Figure 6.1b) but much less in STPBR 2 and 3 (Figure 6.1d and f).

Nevertheless, the microbial dynamics depicted by the qPCR data in STPBR 1 is fairly consistent with the microbial dynamics depicted by FCM data; the initial M:B was exceeded on three occasions, though not strictly at the same time shown by FCM data (on days 20, 36 and 64; Figure 6.1b). Moreover, the lowest M:B value of 10:90 was achieved, through qPCR, 20 days earlier than achieved through FCM (day 36 in Figure 6.1b, compared to day 56 in Figure 6.1a).

Interestingly, the qPCR results consistently showed higher bacterial numbers than microalgae in STPBR 2 and 3, from day 12 onwards, giving an average M:B of about 30:70 (Figure 6.1b, d and f); this implies the presence of more bacteria than microalgae in these two STPBR. The data from the two different methods appeared to agree more in STPBR 2 than in the other STPBR, with the pattern of microbial dynamics agreeing for most of the experiment. Interestingly, high bacterial numbers in STPBR 2 and 3 supports the higher

SCOD removal efficiency reported earlier in these STPBR, compared to STPBR 1 (Section 5.3.1.1).

6.3.1.2 Correlation of FCM with qPCR data

In order to evaluate the relationship between the results obtained from the two different microbial analysis techniques, simple linear correlation analysis was carried out on the FCM and qPCR data, using IBM SPSS. The strength of the relationship was evaluated based on Pearson correlation coefficients (Figure 6.2). The correlation plots were used to explain further the pattern displayed by the FCM and qPCR data of the microbial cell numbers, expressed as M:B (in decimal rather than as ratios).

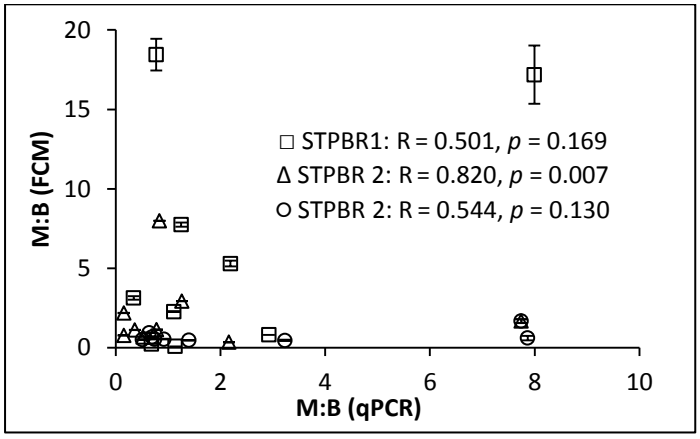

Figure 6.2 Correlation plots of the M:B values obtained from the two microbial analyses with M:B expressed as a fraction (100% M:B = 1.0)

Both the FCM and the qPCR data were positively correlated across the STPBR, with STPBR 2 showing the strongest correlation, as reflected by its correlation coefficient of 0.82. Additionally, the M:B values from both FCM and qPCR in STPBR 2 are significantly different at the 1 % level (p = 0.007; Figure 6.2), suggesting highest agreement between the M:B values calculated from the data obtained from the two microbial techniques in this STPBR. No significant difference was observed in STPBR 1 and 3 (with p values of 0.169 and 0.130, respectively; Figure 6.2). This finding supports the apparent observed stability in microbial dynamics, especially with regard to the bacterial dominance in STPBR 2, discussed earlier. In conclusion, the microbial analyses data revealed temporal changes in the microbial population composition in the STPBR which were probably a result of the conditions established in each STPBR.

6.3.2 Phase II experimental samples

6.3.2.1 Microbial dynamics: qPCR data

As the PBR in Phase II experiments were not inoculated with AS, but only with mixed microalgal culture, all had same starting biomass concentration, and were operated in batch mode under controlled pH, it may be interesting to compare the microbial dynamics of the Phase II experiments with that in Phase III. Potentially, this could be useful in evaluating the effect of PBR mode of operation and optimum irradiance on microbial dynamics in these experimental phases. However, only qPCR data was available from Phase II experiments, and fewer (though stage-representative) samples were analysed. Nevertheless, the comparison could shed more light on the microbial dynamics between the two experimental phases, especially the M:B values obtained under 'natural' and engineered conditions. Figure 6.3 shows the microbial proportions obtained from qPCR analyses, with the three data points representing the beginning, middle and end of Phase II experiments.

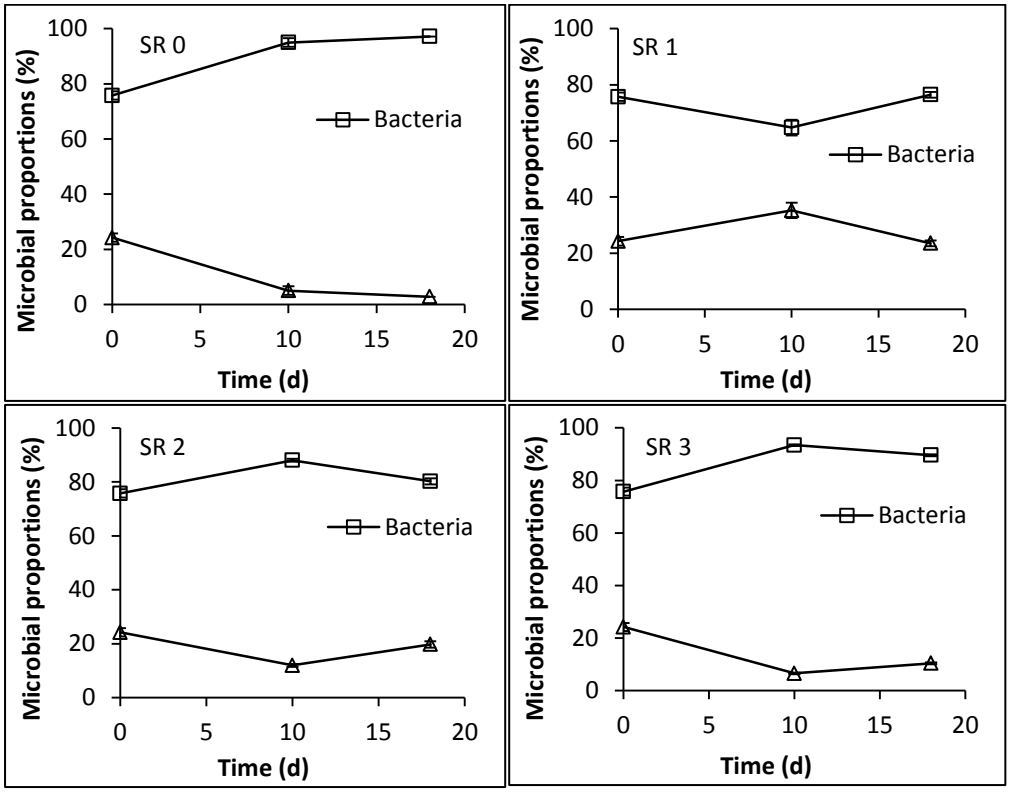

Figure 6.3 qPCR microbial proportions in Phase II experimental PBR (SR 0, 1, 2, and 3)

The PBR in Phase II experiments had initial M:B of about 20:80, as estimated by qPCR analysis (day 0 in Figure 6.3). Bacteria appeared to have grown faster than microalgae in all the PBR, including the control bioreactor (SR 0), maintaining higher cell numbers throughout.

The bacterial population increased slightly in all the PBR (and the control) up to the middle of the experiments, except in SR 1 (day 10 in Figure 6.3). After day 10, there was a slight decrease in bacterial population in SR 2, and 3, to the end of the experiments.

On the other hand, there was decrease in bacteria in SR 1 with corresponding increase in microalgae at the middle of the experiments. Subsequently, the pattern of the microbial dynamics was reversed, up to the end of the experiments, leading to increase in bacteria with corresponding decrease in microalgae, in SR 1. The microbial dynamics yielded average M:B ratios of about 10:90, 30:70, 20:80, and 10:90, in SR 0, 1, 2, and 3, respectively.

Furthermore, fairly the same average microbial proportions were obtained at the two extremes of illumination regime (i.e. in the dark and at the highest irradiance); suggesting probable light limitation, on the one hand, and photoinhibition, on the other. Additionally, the PBR operated at low and medium irradiance (i.e. the optimum value determined in Chapter 4) had nearly the same average microbial proportions. Interestingly, the microbial dynamics appeared to be more stable in the PBR operated at medium irradiance, giving average M:B ratio of about 20:80.

6.3.3 Comparison of results from the two experimental phases

One fundamental relationship between these two experimental phases is that all STPBR in Phase III were operated at the same irradiance level (that of SR 2 in Phase II). Comparing Figure 6.1 and Figure 6.3 reveals an apparent similarity in the stability of the bacterial population in SR 2 (average M:B = 30:70) and STPBR 2 (average M:B = 20:80), suggesting bacterial dominance over microalgae in both PBR. Therefore, irradiance probably determines the eventual population composition.

However, this similarity may have been clearer, despite the fact that SR 2 and STPBR 2 were operated in different modes (i.e. batch vs. continuous mode of operation), if same number of samples had been analysed in both photobioreactors. Nevertheless, the microbial dynamics in both Phase II and III suggests more bacteria than microalgae, confirming the higher growth rate of prokaryotic organisms compared to eukaryotic ones under the levels of irradiance used.

Figure 6.4 shows the microbial gene copy (cell) numbers of Phase II and III photobioreactors, obtained from qPCR analysis. The cell enumeration data shows bacterial dominance over microalgae in all the PBR in both experimental phases throughout the experimental period, except in STPBR 1 in Phase III.

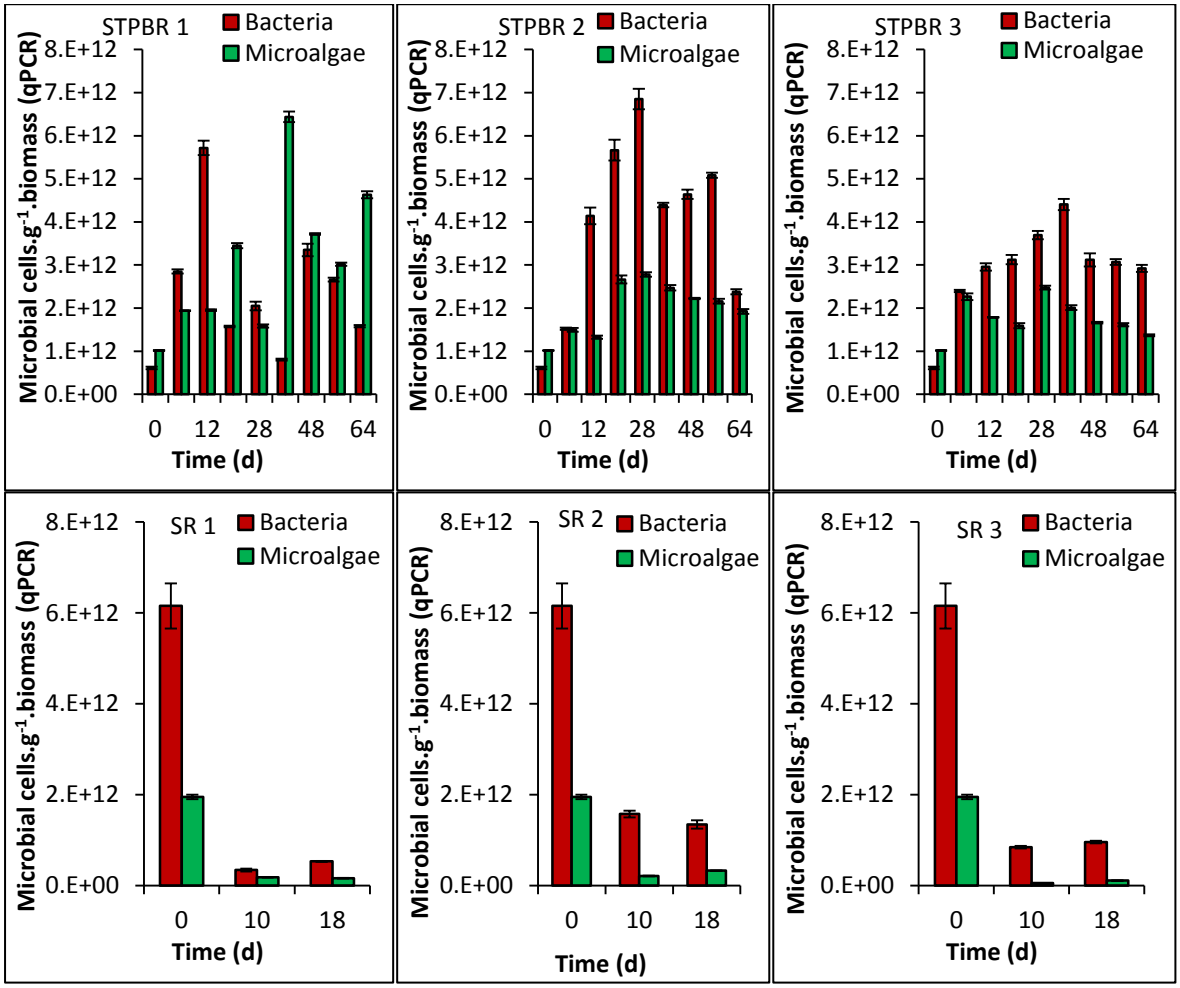

Figure 6.4 Time courses of microbial cell numbers of Phase III (STPBR 1, 2 and 3, see Chapter 5) and Phase II (SR 1, 2 and 3; see Chapter 4) experiments

Considering Phase III microbial cell numbers (STPBR 1, 2 and 3; Figure 6.4), the bacterial cell count reached its peak on day 12 (5.72 x 10^{12}.g^{-1}.biomass), day 28 (6.85 x 10^{12}.g^{-1}.biomass) and day 36 (4.40 x 10^{12}.g^{-1}.biomass) in STPBR 1, 2 and 3, respectively, with the highest bacterial population in STPBR 2. In contrast, the microalgal cell count reached its maximum on day 36 in STPBR 1 (6.44 x 10^{12}.g^{-1}.biomass), and on day 28 in both STPBR 2 (2.78 x 10^{12}.g^{-1}.biomass) and 3 (2.47 x 10^{12}.g^{-1}.biomass), with the highest microalgal population in STPBR 1.

Furthermore, the microbial dynamics observed in Phase II PBR was very similar to that of Phase III, with bacteria dominating within the PBR throughout the experimental period (SR 1, 2 and 3; Figure 6.4). This is interesting since the inoculum used in Phase II experiments lacked activated sludge. One possibility could be that bacteria were present in the microalgal culture since the culture originated from environmental sample collected from sewage treatment works. Another possibility could be overestimation of the bacterial numbers since cyanobacteria are prokaryotes and are targeted by qPCR. The algal inoculum was dominated by bacteria probably because cyanobacteria were present in the culture and relatively growing at faster rate.

However, neither class of microorganism maintained its initial population size in the middle and end of the experiments due to lower growth rates and possible net die-off in these batch systems. Nevertheless, highest microbial cell counts were achieved in SR 2: 1.58 x 10^{12}.g^{-1}.biomass bacteria, 2.14 x 10^{11}.g^{-1}.biomass microalgae and 1.35 x 10^{12}.g^{-1}.biomass bacteria, 3.30 x 10^{11}.g^{-1}.biomass microalgae at the middle and end of the experiments, respectively; suggesting better microbial growth conditions compared to SR 1 and 3.

Interestingly, SR 2 was operated at 582.7 µmol.m^{-2}.s^{-1} which was found to be the optimum irradiance for operating the PBR (see Chapter 4), and subsequently adopted in developing the HMAS system presented in Chapter 5.

Chapter 7

General Discussion

7.1 Introduction

This Chapter presents a general discussion on the findings of the current research. The discussion focusses on the SCOD, NH_4-N, and PO_4-P removal efficiencies achieved in the three experimental phases in relation to each other, with reference to system performance, and in relation to the existing (relevant) wastewater treatment principles and practices. The discussion also highlights the relative merits of the different modes of PBR operation; CO_2 addition, pH control, and up-scaling. It also emphasises the potential of the newly introduced HMAS system with regard to the red LED illumination, the need for light optimisation in hybrid microalgal systems, potential for energy saving in a prototype full-scale HMAS system; strengths and limitations of the HMAS system, and strategies for improvement.

7.2 Wastewater Treatment Efficiency

Efficiency is an important parameter for evaluating the performance of any given wastewater treatment system. In this research, the performance of the systems used to treat municipal wastewater was evaluated in the three experimental phases in terms of removal efficiencies for organic matter (as SCOD), ammonia (as NH_4-N), and phosphorus (as PO_4-P). The performance of any given wastewater treatment system depends partly on its process and operational conditions, the treatment system performing differently under different conditions.

In Chapter 3, carbon dioxide supplementation resulted in enhanced SCOD removal efficiency in a mixed microalgal culture operating at bench-scale at low light regimes (25 to 250 $\mu mol.m^{-2}.s^{-1}$), treating real municipal wastewater. Additionally, there was considerable difference between the maximum SCOD removal efficiencies achieved by the different bioreactors (i.e. at different irradiance levels). However, there was only a marginal difference between the efficiencies achieved in bioreactors with and without inorganic

carbon supplementation in terms of NH_4-N removal. This is not unusual since at irradiance values lower than saturation level, CO_2 concentration has been reported to have negligible effects on photosynthetic efficiency (Hall and Rao, 1999).

In terms of PO_4-P removal efficiency, the 1-L photobioreactors used in the current study (Chapter 3) were not very effective in removing phosphate from the wastewater. In contrast to NH_4-N removal, PO_4-P was found to accumulate in all the small-scale bioreactors, including the controls. It was not clear whether the high concentrations of PO_4-P in the wastewater (about 13 to 32 $mg.L^{-1}$ orthophosphate concentration) stressed the microalgae, since over supply of phosphorus has been reported to be no panacea to this nutrient limitation, and can even result in stress, and consequently limit algal growth (Grobbelaar, 2004). Interestingly, very low levels of PO_4-P removal is a common characteristic of natural algal wastewater treatment systems, such as WSP (Powell *et al.*, 2009; Mbwele, 2006); this common feature also appears to apply to 'artificial' algal systems, such as the bench-scale bioreactors (involving the use of LED as light source) used in the current research.

SCOD removal efficiencies fairly similar to those recorded in the bench-scale PBR, were also achieved in up-scaled PBR (Chapter 4) operating at light regimes higher than those used in the bench-scale bioreactors. Operating the up-scaled PBR at higher irradiance levels also resulted in high SCOD removal efficiency (> 70%), however, this was not higher than the SCOD removal efficiencies achieved at bench-scale. Nevertheless, problems with up-scaling still remain a major challenge in PBR operation, especially in large-scale algal biomass production (Grobbelaar, 2010), and the same problems might have affected the 16-L PBR used in the current research.

In contrast to the bench-scale bioreactors, in which SCOD removal efficiencies varied widely with irradiance, the up-scaled PBR achieved very similar maximum SCOD removal efficiencies. One interesting observation common to the two PBR systems was that the SCOD removal efficiency increased with increasing irradiance up to an irradiance value lower than the maxima used in both systems. That is, maximum SCOD removal efficiencies were not achieved at the highest irradiance values used in the two studies. The irradiance values showing best performance were apparently considered as the *optima* for operating the PBR, under the experimental conditions employed in this research.

Another remarkable difference between the 1-L and the batch STPBR was that carbon dioxide addition clearly enhanced NH_4-N removal efficiencies in the STPBR (including the control bioreactor used in the study). In addition, maximum NH_4-N removal was clearly achieved at optimum irradiance. A similar trend was also observed with phosphorus removal, however, an inverse trend was observed in the control STPBR, with higher phosphorus removal being achieved in the control without inorganic carbon supplementation.

Interestingly, very high PO_4-P removal efficiencies were achieved in the STPBR, with a maximum of 94% removal being observed at optimum irradiance. This contrasts strikingly with the 1-L photobioreactors. This finding also agrees with earlier reports that up-scaling causes substantial changes in microalgal PBR operation and biomass production (Grobbelaar, 2010), use of monochromatic light sources (Mohammed *et al.*, 2013b; Wang *et al.*, 2007) coupled with inorganic carbon supplementation (Park and Craggs, 2010) could enhance microalgal growth, productivity and wastewater treatment efficiency, and consequently offset some of these disadvantages.

In Chapter 5, continuously operating STPBR (also referred to as HMAS systems in this research), running at 'optimum' red LED irradiance (i.e. 582.7 $\mu mol.m^{-2}.s^{-1}$) and controlled MLVSS (i.e. 50, 300 and 600 $mg.L^{-1}$), treating synthetic municipal wastewater, achieved high SCOD removal efficiency greater than 70% (Mohammed *et al.*, 2013a). Although the experimental HMAS systems were operated in continuous mode, the SCOD removal efficiencies found in the study were similar to those achieved in batch-operated STPBR (Phase II experiments). Additionally, the SCOD removal efficiencies in the HMAS systems were not significantly different; which is also similar to the trend observed for SCOD removal efficiency in Phase II experimental STPBR.

Compared to the batch-operated photobioreactors, the HMAS systems, operating continuously at 4-d HRT, achieved much lower NH_4-N removal efficiency, with the maximum value of 44% when MLVSS was controlled at 300 $mg.L^{-1}$. This maximum value of NH_4-N removal efficiency, found in the HMAS, is much lower than those achieved by conventional algal wastewater treatment systems at a range of HRT values, e.g. by Park *et al.* (2011), in an HRAP at the same HRT; Silva-Benavides and Torzillo (2012), in batch operated PBR; and

Camargo-Valero and Mara (2007a), in a maturation pond (at a mean HRT of 17.5) succeeding a primary facultative pond (with HRT of 60 d); all of these showing greater than 80% removal. Nevertheless, values of NH_4-N removal efficiencies similar to those found in the HMAS have also been reported in the literature, e.g. Aslan and Kapdan (2006).

In terms of phosphorus removal efficiency, the HMAS systems performed below expectation, as reflected by the low PO_4-P removal efficiency achieved by the continuously operating STPBR (a maximum of about 55% at MLVSS of 50 $mg.L^{-1.}$). Compared to the other two batch-operated systems, the continuously operating HMAS systems had much lower PO_4-P removal efficiencies, which was possibly due to acidic conditions, or probable stress (to the microbial community) caused by the initially high orthophosphate concentration of about 13 $mg.L^{-1}$. The low phosphate removal efficiency of the HMAS might not be unconnected to the STPBR mode of operation, which is similar to that of conventional algal ponds, considering that low phosphate removal is a typical characteristic of algae-based WSP (Powell, 2009).

Another possible reason for the low phosphate removal in the HMAS systems might be lack of microbial species responsible for phosphate removal (e.g. phosphate accumulating organisms, PAO) in the STPBR. PAO depend on cyclic conditions of high and low carbon availability to become dominant within the reactor biomass (Oehmen *et al.*, 2007), and the constant carbon loading used in this study would not have favoured their growth above that of normal heterotrophs.

The batch-operated STPBR were similar to the HMAS systems in terms of scaling, composition of the microalgal growth medium, and usage of optimum irradiance. In contrast, the HMAS systems differed from the batch PBR in the composition of inoculum used, the mode of operation and control, and the level of irradiance used. Despite the differences between these two systems, similar SCOD and NH_4-N removal efficiencies were achieved. Interestingly, the continuous mode of operation appeared to eliminate nitrite accumulation, which was commonly observed in both the small-scale and up-scaled batch-operated systems.

In contrast, the HMAS differed greatly from the batch operated 1-L PBR in terms of scale, mode of operation, inoculum and feed substrate composition. Despite these differences, there were also some similarities in the level of treatment efficiencies, especially with

respect to SCOD and ammonia removal. However, the HMAS performed below expectation, though in a similar manner to the 1-L bioreactors, in terms of phosphorus removal from the synthetic municipal wastewater. Nevertheless, the HMAS has not been tested with pretreated real municipal wastewater, e.g. effluent from anaerobic ponds/bioreactors treating domestic sewage. This needs further investigation.

7.3 Microbial Dynamics in Microalgal Photobioreactors

Before this research, there were no publications reporting the proportion of bacteria and microalgae in photobioreactors treating municipal wastewater in the laboratory. However, studies have been undertaken to identify the bacterial groups involved in nitrogen transformation in WSP, using PCR and DGGE (Camargo-Valero *et al.*, 2009b). Since wastewater treatment in WSP and related wastewater treatment systems is achieved through the symbiotic relationship of bacteria and algae (Humenik and Hanna-Jr, 1971) , it is important to evaluate the temporal dynamics of these microorganisms with reference to growth conditions. This can help in better understanding of the dynamics, and effective design of artificial algae-based wastewater treatment systems. However, determination of the microbial species present in the HMAS and other PBR systems was outside the scope of this research but may need further investigation.

In this research, microbial dynamics was evaluated with respect to inorganic carbon supplementation, and amount of irradiance/level of light attenuation (Chapter 6). Since the quantification of microalgae and bacteria in PBR with a view to evaluating microbial dynamics has received limited attention to date, direct comparison of the current research with previously published work may be difficult.

Operating microalgal STPBR in batch and continuous modes resulted in temporal variation of microalgae-bacteria (M:B) ratio, with bacteria dominating throughout the experimental period, in most cases. In terms of cell counts, bacterial numbers decreased from 10^{12} to 10^{11} per gram of biomass in batch STPBR operating at low and high red LED irradiance, whilst bacterial numbers were steady at 10^{12} per gram of biomass, in the STPBR operating at a medium level of irradiance. The continuously operating STPBR showed similar microbial dynamics. In view of the bacterial dominance in the STPBR, a minimum M:B ratio of 90:10 was recommended for starting up a HMAS system. This will help in avoiding the risk of

having an LED-lit activated sludge system resulting, from complete bacterial dominance over microalgae, and realisation of the potential of the HMAS system from thriving algae-bacteria symbiosis.

Microalgal dynamics has been reported to be greatly influenced by the amount of light penetrating facultative ponds, with flagellated algae occupying near surface strata (Pearson, 2005). As such, apparent bacterial dominance over microalgae in the HMAS was probably related to light attenuation in STPBR 2 and 3 considering the MLVSS concentrations of these reactors (300 and 600 $mg.L^{-1}$), which is higher than algal biomass concentration in facultative ponds (Sperling and Chernicharo, 2005). Although the STPBR were relatively mixed at high speed (i.e. 100 rpm), the level of attenuation coupled with apparent stress resulting from acidic conditions (pH lower than 7) in STPBR 2 and 3 might have limited microalgal growth, and consequently led to bacterial dominance. Therefore, operating the STPBR at biomass concentrations, where light attenuation would be reduced, needs to be investigated.

7.4 Future Potential of the HMAS System

Development of the HMAS system began with a study investigating the use of red LED for real municipal wastewater treatment, at bench-scale (Phase I; Chapter 3). This was then followed by coupling up-scaling and irradiance optimisation in microalgal STPBR, treating synthetic municipal wastewater at pilot-scale (Phase II; Chapter 4). Finally, the system was developed and tested with mixed inoculum of algae and AS (Phase III; Chapter 5). The newly developed HMAS can be considered as a sustainable wastewater treatment option due to its ability to couple wastewater treatment with carbon sequestration, and provide overall net energy savings.

The HMAS system (through concomitant use of algal and bacterial activities) was able to capture considerable amount of CO_2 during pilot-scale municipal wastewater treatment in the laboratory. It also eliminated the need for external aeration by satisfying bacterial oxygen requirements through algal photosynthesis driven by the energy-efficient light source, i.e. 660 nm low-cost and low-power light emitting diodes (Mohammed *et al.*, 2013a). Combining the characteristics of the individual microalgae system and the activated sludge

system, the resulting hybrid system achieved energy savings by eliminating artificial aeration, whilst maintaining high levels of SCOD removal.

The concept of the HMAS system could be extended to larger pilot-scale, or even full-scale, wastewater treatment system through the set-up and operation of bioreactor system to treat municipal sewage. The bioreactor would be inoculated with a mixed culture of microalgae and activated sludge, and illuminated internally with vertical red LED arrays. Concentrated sources of carbon dioxide, in the form of flue gas (Van Den Hende *et al.*, 2010; Brown, 1996) obtained from cement production plant, or even from a fossil fuel powered plant (Zeiler *et al.*, 1995), could be used as an inorganic carbon supplement in the wastewater. The readily available nutrients in the wastewater would eliminate the need for commercial fertilisers as source of nutrients (Yun *et al.*, 1997).

Alternatively, red LED arrays could be used to illuminate an outdoor pilot-scale HRAP, enclosed under gas- and water-proof transparent plastic membranes or Plexiglas. The transparent cover material would eliminate inputs from rain, maintain a carbon dioxide-enriched atmosphere, and facilitate natural solar irradiance during the day. On cloudy days, the LED light could supplement natural solar radiation, or be used solely at night. .

Throughout this research, the performance of the HMAS, and the other batch-operated PBR might have been affected by the composition of the synthetic microbial growth medium that was used (i.e. the ACGM), as this was not optimised systematically by experimentation. There may have been limitations from the concentrations of some components, especially with regard to orthophosphate and ammonium ions, which could be considered as representing the lower range of some industrial wastewaters, such as brewery effluent (e.g. (Driessen and Vereijken (2003)).

Although some efforts were made to modify both the synthetic wastewater and/or the nutrient media used in the three experimental phases, with a view to mimic real pretreated municipal wastewater, and to avoid the use of standard algal growth medium (commonly used in algal research and reported in the literature), especially in photobioreactors, the modified wastewater chemical composition is not ideal and would benefit from further improvement. In addition, the HMAS has not been tested with pretreated real municipal

wastewater, e.g. effluent from anaerobic ponds/bioreactors treating domestic sewage, and this requires further investigation.

Additionally, further improvement in performance efficiency could be investigated by setting-up a number of the HMAS systems in series, operating at lower HRT, and using wastewater with lower phosphate and ammonium content, as feed substrate. This, and other improvement strategies such as use of wide gas sparger at reactor bottom and feedback supply of carbon dioxide, may help in realising the full potential of the HMAS system, and demonstrate feasibility for coupling enhanced carbon capture with wastewater treatment at full-scale.

7.5 Optimised conditions for the HMAS

One of the research objectives set out to propose optimised conditions for designing and operating the HMAS system for effective municipal wastewater treatment. The proposed conditions are based on the overall findings of this research and provide general guidance and initial values for HMAS systems. Therefore, the following observations from this research serve as optimum conditions for designing and operating the HMAS systems. These include use of:

(i) narrow band light sources with wavelengths falling within the range of maximum light absorption band of major photosynthetic pigments (*chlorophyll* a and b) i.e. 660 nm wavelength provided by the red LED.

(ii) internal illumination with arrays of LED positioned vertically to maximise photon energy utilisation and minimise light attenuation through absorption and scattering by water molecules and suspended particles.

(iii) optimum light intensity (181 – 583 $\mu mol.m^{-2}.s^{-1}$) determined through optimisation studies of PBR operating as batch and continuous modes, respectively.

(iv) nutrient concentrations within microbial tolerable limits, e.g. the phosphate and ammonium concentrations, 13 and 88 $mg.L^{-1}$, respectively, used in the algal growth medium appeared to be high for achieving most effective wastewater treatment efficiency in the HMAS.

(v) SCOD was tolerated within the range 83 to 395 $mg.L^{-1}$

(vi) supplementation with carbon dioxide, e.g. 10 - 25% (v/v) in the gas feed at flow rate of 100 and 25 $mL.min^{-1}$, respectively, to avoid carbon limitation and enhance microbial growth and biomass productivity.

(vii) inoculum with relatively high initial microalgae-bacteria ratio (e.g. M:B ratio of 90:10), possibly determined through flow cytometry.

Chapter 8

Conclusions and Recommendations

8.1 Conclusions

This research demonstrated the feasibility of using red LED as light source for a mixed microalgal culture treating real municipal wastewater at bench-scale under low light regimes. In addition, coupling carbon sequestration with wastewater treatment resulted in an enhanced microalgal growth rate, with high ammonium and SCOD removal efficiencies, greater than 90% and 75%, respectively. Interestingly, both maximum ammonia removal and specific growth rate of 0.062 d^{-1} were achieved at a low irradiance value of 181.2 $\mu mol.s^{-1}.m^{-2}$. This irradiance value was apparently the optimum for operating the batch bench-scale PBR, under low light regimes. However, consistently high phosphate and nitrite concentrations might have caused toxic effects on the microbial population, and consequently affected the overall performance of the bench-scale PBR. This observation and the relatively low microalgal growth rates were further investigated at pilot-scale, under higher red LED light regimes.

Carbon dioxide addition to mixed microalgal cultures treating modified synthetic municipal wastewater resulted in approximately a two-fold increase in biomass productivity in the pilot-scale red LED-illuminated STPBR, with the reactor operating at the medium irradiance level exhibiting the highest specific growth rate and biomass productivity of 0.109 d^{-1} and 0.034 $g.L^{-1}.d^{-1}$, respectively. However, the inorganic carbon limitation observed in these STPBR prior to CO_2 addition probably limited the growth and productivity of the mixed microalgal culture, and consequently affected the overall performance of these STPBR. In addition, nitrite accumulation might also have generated toxic effects on the microbial population and possibly reduced the beneficial effect of inorganic carbon supplementation on the microalgal culture.

Results from this research suggest that both microalgal growth rate and biomass productivity are not always directly proportional to irradiance in a batch PBR system.

Importantly, intermediate level of irradiance (i.e. 582.7 µmol.s^{-1}.m^{-2}) apparently resulted in optimum growth and productivity of the mixed microalgae-bacteria culture. The result of this light optimisation study served as a prerequisite in developing the hybrid microalgae-activated sludge wastewater treatment system for operation under continuous loading conditions (Chapter 5). It also demonstrates the limitations of using batch systems for wastewater treatment and for characterising the full potential of microalgal STPBR.

In terms of treatment performance, SCOD removal efficiency greater than 70% was achieved in the hybrid microalgae-activated sludge (HMAS) systems, with energy saving from the elimination of artificial aeration, since bacterial oxygen requirements were satisfied through DO levels that were provided by photosynthetic oxygenation. Additionally, controlling MLVSS concentration could serve as a potential measure for minimising light attenuation in microalgal photobioreactors treating municipal wastewater. MLVSS of 300 mg.L^{-1} with corresponding SRT of about 4.6 d was found to be optimal for operating the STPBR at 582.7 µmol.s^{-1}.m^{-2} red LED irradiance. This study demonstrates the potential of using microalgae to couple carbon capture with municipal wastewater treatment in a HMAS system possessing shared characteristics of both activated sludge and advanced high-rate algal ponds. It also demonstrates the potential for scaling up the process to treat municipal wastewater at larger scale.

Basic microbial composition and cell numbers were successfully estimated using FCM and qPCR analyses. In most cases, results revealed a dominance of bacteria over microalgae. The data from the two techniques, obtained from STPBR operating at MLVSS values ranging from 50 to 600 mg.L^{-1} (i.e. STPBR 1, 2 and 3, see Chapter 5) were positively correlated (*r* ranging from 0.5 to 0.82), whilst similarity between data from the two microbial analyses obtained at MLVSS of 300 mg.L^{-1} was statistically significant at 1% level (r = 0.82 and p = 0.007). Average M:B ratios of about 30:70 and 20:80 were obtained in photobioreactors operating at optimum red LED irradiance, under batch and continuous modes of operation, respectively. In order to prevent system failure, it is therefore recommended that hybrid microalgae-bacteria systems be set-up with initial M:B ratio of at least 90:10, as determined by FCM.

The current study demonstrated the feasibility of starting-up an HMAS system, operating under 582.7 µmol.m^{-2}.s^{-1} irradiance, with a high microalgae-bacteria ratio, and achieving good wastewater treatment efficiency without running the risk of complete bacterial dominance. Such conditions should help in maintaining algal activity, which would in turn satisfy much of the bacterial oxygen requirement through oxygenic photosynthesis. Lastly, either of the microbial analysis methods investigated here could be used successfully to monitor and study microbial growth and dynamics in combined algae-bacteria systems (e.g. HMAS), treating municipal wastewater. Nevertheless, there is still a need to improve the application of qPCR, possibly through the use of more specific eukaryotic primers that can target, for example, *Chlorophyta*, in qPCR reactions. The problem associated with large microbial cell size in FCM analysis may, however, remain a limitation of this method in the near future. Finally, some optimised conditions for designing the HMAS system were proposed (Section 7.5) based on the observations and findings in this research.

8.2 Recommendations for future work

In order to improve the performance efficiency of hybrid microalgae activated sludge wastewater treatment system, further study is needed to better understand its full capability. This may involve testing LED with different wavelengths within the red band of the visible light spectrum, as well as other colours such as white and blue or their combination. Although the HMAS system showed effective performance at 4-d HRT, lower and higher HRT, 2 and 8 d, as well as higher SCOD concentrations (e.g. 700 - 1000 mg.L^{-1}) need to be investigated. This may help in determining the best HRT and COD loading for operating the HMAS systems, with a view to realising its wastewater treatment efficiency. In addition, smaller HRT values (e.g. 1 or 2 d) can be tested simultaneously with multiple STPBR operating in series, as well as MLVSS concentrations lower than 300 mg.L^{-1}, where light attenuation could be minimised may constitute a future work (especially using MLVSS control strategy such as that used in the current research).

System complexity, in terms of number of uncontrolled variables (e.g. inoculum composition, SRT, and variation of MLVSS across STPBR), did not permit the operation of single suitable control for all the HMAS STPBR. This necessitated comparison of the performance and energy efficiency of the tested STPBR with published activated sludge literature only. In addition, resource constraints (i.e. limited number of reactor vessels, LED arrays, etc)

prohibited the setting up of a suitable control bioreactor concurrently with each STPBR under the same operational conditions. This aspect needs further investigation in future work.

Although this research did not set out to characterise the microbial species present in the experimental PBR, identification of both microalgal and bacterial communities present in HMAS illuminated with red LED or other artificial light sources may help in better understanding of the system microbial dynamics, especially in relation to phosphate removal efficiency.

References

Abeliovich, A. and Azov, Y. (1976) 'Toxicity of ammonia to algae in sewage oxidation ponds', *Applied and Environmental Microbiology,* 31(6), pp. 801-806.

Abis, K. L. and Mara, D. D. (2003) 'Research on waste stabilisation ponds in the United Kingdom - initial results from pilot-scale facultative ponds', *Water Science and Technology,* 48(2), pp. 1-7.

Abis, K. L. and Mara, D. D. (2005) 'Primary facultative ponds in the UK: the effect of operational parameters on the performance and algal populations', *Water Science and Technology,* 51(12), pp. 61-67.

Ahammad, S. Z., Zealand, A., Dolfing, J., Mota, C., Amstrong, D. V. and Graham, D. W. (2013) 'Low-energy treatment of colourant wastes using sponge biofilters for personal care product industry', *Bioresource Technology,* 129pp. 634-638.

APHA. (2005), *Standard methods for the examination of water and wastewater,* 21st ed, APHA.

Aslan, S. and Kapdan, I. K. (2006) 'Batch kinetics of nitrogen and phosphorus removal from synthetic wastewater by algae', *Ecological Engineering,* 28(1), pp. 64-70.

Aslan, S., Miller, L. and Dahab, M. (2009) 'Ammonia oxidation via nitrite accumulation under limited oxygen concentration in sequencing batch reactors', *Bioresource Technology,* 100(2), pp. 659-664.

Atomi, H. (2002) 'Microbial enzymes involved in carbon dioxide fixation', *Journal of Bioscience and Bioengineering,* 94(6), pp. 497-505.

Azad, H. S. and Borchardt, J. A. (1970) 'Variations in phosphorus uptake by algae', *Environmental Science and Technology,* 4(9), pp. 732-743.

Badger, M. R. and Price, G. D. (1994) 'The role of carbonic anhydrase in photosynthesis', *Annual Review of Plant Physiology and Plant Molecular Biology,* 45pp. 369-392.

Barber, J. (1987) 'Photosynthetic reaction centres: a common link', *Trends in Biochemical Sciences,* 12pp. 321-326.

Becker, E. W. (1994), *Microalgae biotechnology and microbiology,* Cambridge, UK, Cambridge University Press.

Bergh, A. A. and Dean, P. J. (1972) 'Light-emitting diodes', *Proceedings of the IEEE,* 60(2), pp. 156-223.

Bergh, A. A. and Dean, P. J. (1976), *Light-emitting diodes,* Oxford University Press, Oxford.

Blankenship, R. E. (2002), *Molecular Mechanisms of Photosynthesis,* Blackwell Science Ltd, United Kingdom.

Bogan, R. H. (1961) 'Removal of sewage nutrients by algae', *Public Health Reports,* 76(4), pp. 301-308.

Borchardt, J. A. and Azad, H. S. (1968) 'Biological extraction of nutrients', *Water Pollution Control Federation,* 40(10), pp. 1739-1754.

Bracklow, U., Drews, A., Vocks, M. and Kraume, M. (2007) 'Comparison of nutrients degradation in small scale membrane bioreactors fed with synthetic/domestic wastewater', *Journal of Hazardous Materials,* 144(3), pp. 620-626.

Brown, L. M. (1996) 'Uptake of carbon dioxide from flue gas by microalgae', *Energy Conversion and Management,* 37(6-8), pp. 1363-1367.

Camargo-Valero, M. A. (2008) *Nitrogen Transformation Pathways and Removal Mechanisms in Domestic Wastewater Treatment by Maturation Ponds.* PhD thesis. The University of Leeds, United Kingdom.

Camargo-Valero, M. A. and Mara, D. D. (2007a) 'Nitrogen removal in maturation ponds: tracer experiments with ^{15}N-labelled ammonia', *Water Science,* 55(11), pp. 81-85.

Camargo-Valero, M. A. and Mara, D. D. (2007b) 'Nitrogen removal via ammonia volatilization in maturation ponds', *Water Science,* 55(11), pp. 87-92.

Camargo-Valero, M. A. and Mara, D. D. (2010) 'Ammonia volatilisation in waste stabilisation ponds: a cascade of misinterpretations?', *Water Science and Technology,* 61(3), pp. 555-561.

Camargo-Valero, M. A., Mara, D. D. and Newton, R. J. (2009a) 'Nitrogen removal in maturation WSP ponds via biological uptake and sedimentation of dead biomass*', 8th IWA Specialist Group Conference on Waste Stabilisation Ponds.* Belo Horizonte, Brazil, 26-29 April, 2009. pp. 1-9.

Camargo-Valero, M. A., Read, L. F., Mara, D. D., Newton, R. J., Curtis, T. P. and Davenport, R. J. (2009b) 'Nitrification-denitrification in WSP: a mechanism for permanent nitrogen removal in maturation ponds*', 8th IWA Specialist Group Conference on Waste Stabilisation Ponds.* Belo Horizonte/MG, Brazil, 26-29 April 2009. pp. 1-9.

Campbell, N. A., Mitchell, L. G. and Reece, J. B. (2000), *Biology: Concepts & Connections,* 3rd ed, Longman, San Francisco.

Carberry, J. B. and Tenney, M. W. (1973) 'Luxury uptake of phosphate by activated sludge', *Water Pollution Control Federation,* 45(12), pp. 2444-2462.

Carlsson, A. S., van-Beilen, J. B., Moller, R. and Clayton, D. (2007) *Macro- and micro-algae: utility for industrial applications* [Online]. Available at: http://epobio.net/pdfs/0709AquaticReport.pdf (Accessed: 15-01-2011).

Ceballos, B. S. O., Konig, A., Lomans, B., Athayde, A. B. and Pearson, H. W. (1995) 'Evaluation of a tropical single-cell waste stabilisation pond system for irrigation', *Water Science and Technology,* 31(12), pp. 267-273.

Chaudhuri, N., Tyagi, P. C., Niyogi, N., Thergaonkar, V. P. and Khanna, P. (1992) 'BOD test for tropical countries', *Journal of Environmental Engineering of the Amiercan Society of Civil Engineers,* 118(298-303).

Chen, P., Zhou, Q., Paing, J., Le, H. and Picot, B. (2003) 'Nutrient removal by the integrated use of high rate algal ponds and macrophyte systems in China', *Water Science and Technology,* 48(2), pp. 251-257.

Cheng, L., Zhang, L., Chen, H. and Gao, C. (2006) 'Carbon dioxide removal from air by microalgae cultured in a membrane-photobioreactor', *Separation and Purification Technology,* 50(3), pp. 324-329.

Chisti, Y. (2007) 'Biodiesel from microalgae', *Biotechnology Advances,* 25(3), pp. 295-306.

Chisti, Y. (2008) 'Biodiesel from microalgae beats ethanol', *Trends in Biotechnology,* 26(3), pp. 126-131.

Chisti, Y. and Yan, J. (2011) 'Energy from algae: current status and future trends', *Applied Energy,* 88(10), pp. 3277-3279.

Chisty, Y. (2007) 'Biodiesel from microalgae', *Biotechnology Advances,* 25(3), pp. 294-306.

Clayton, R. K. (1963) 'Photosynthesis: primary physical and chemical processes', *Annual Review of Plant Biology,* 14pp. 159-180.

Collings, A. F. and Critchley, C. (2005a), *Artificial Photosynthesis,* Wiley-VCH, Weinheim, Germany.

Culture Collection of Algae and Protozoa (2010) *Bold's Basal Medium for freshwater algae* [Online]. Available at: http://www.ccap.ac.uk/media/documents/BB_000.pdf (Accessed: 30-06-2010).

Curtis, T. P., Mara, D. D. and Silva, S. A. (1992) 'Influence of pH, oxygen, and humic substances on ability of sunlight to damage fecal coliforms in waste stabilisation pond water', *Applied and Environmental Microbiology,* 58(4), pp. 1335-1342.

de-Morais, M. G. and Costa, J. A. V. (2007a) 'Biofixation of carbon dioxide by Spirulina sp. and Scenedesmus obliquus cultivated in a three-stage serial tubular photobioreactor', *Journal of Biotechnology,* 129(9), pp. 439-445.

de-Morais, M. G. and Costa, J. A. V. (2007b) 'Carbon dioxide fixation by Chlorella kessleri, C vulgaris, Scenedesmus obliquus and Spirulina sp. cultivated in flasks and vertical tubular photobioreactors', *Biotechnology Letters,* 29(9), pp. 1349-1352.

de-Oliveira, R., Silva, S. A., Araujo, A. L. C., Soares, J., Mara, D. D. and Pearson, H. W. (1996) 'The performance of a pilot-scale series of ten ponds treating municipal sewage in Nertheast Brazil', *Water Science and Technology,* 33(7), pp. 57-61.

Del Nery, V., Damianovic, M. H. Z., Pozzi, E., de Nardi, I. R., Caldas, V. E. A. and Pires, E. C. (2013) 'Long-term performance and operational strategies of a poultry slaughterhouse waste stabilization pond system in a tropical climate', *Resources, Conservation and Recycling,* 71(0), pp. 7-14.

Department of Energy and Climate Change (2009) *UK Low Carbon Transition Plan: National Strategy for Climate and Energy* [Online]. Available at: http://www.decc.gov.uk/en/content/cms/publications/lc_trans_plan/lc_trans_plan.aspx (Accessed on 02-02-2010) (Accessed: 02-02-2010).

Driessen, W. and Vereijken, T. (2003) 'Recent developments in biological treatment of brewery effluent' The Institute and Guild of Brewing Convention, Livingstone, Zambia, 2nd - 7th March.

Eland, L. E., Davenport, R. and Mota, C. R. (2012) 'Evaluation of DNA extraction methods for freshwater eukaryotic microalgae', *Water Research,* 46(16), pp. 5355-5364.

Ellis, R. J. (1979) 'The most abundant protein in the world', *Trends in Biochemical Sciences,* 4(11), pp. 241-244.

Emerson, R. and Green, L. (1938) 'Effect of hydrogen-ion concentration on *Chlorella* photosynthesis', *Plant Physiology,* 13(1), pp. 157-168.

Environment Agency (2009) *Limiting Climate Change - Water Industry Carbon Reduction* [Online]. Available at: http://www.environment-agency.gov.uk/static/documents/Research/(16)_Carbon_water_mitigation_FINAL.pdf (Accessed: 29-01-2010).

Finney, B. A. and Middlebrooks, E. J. (1980) 'Facultative waste stabilisation pond design', *Water Pollution Control Federation,* 52(1), pp. 134-147.

Fred, S. E. (2006), *Light-emitting diodes,* 2nd ed, Cambridge University Press, Leiden.

Gillessen, K. and Schairer, W. (1987), *Light-emitting diodes,* Prentice-Hall, United Kingdom.

Giovannoni, S. J., Turner, S., Olsen, G. J., Barns, S., Lane, D. J. and Pace, N. R. (1988) 'Evolutionary relationships among cyanobacteria and green chloroplasts', *Journal of Bacteriology,* 170(8), pp. 3584-3592.

Golab, Z. and Smith, R. W. (1992) 'Accumulation of lead in two freshwater algae', *Minerals Engineering,* 5(9), pp. 1003-1010.

Goldman, J. C. (1979) 'Outdoor algal mass culture-II. photosynthetic yield limitations', *Water Research,* 13(1), pp. 1-9.

Gonzalez-Fernandez, C., Molinuevo-Salces, B. and Garcia-Gonzalez, M. C. (2011) 'Evaluation of anaerobic digestion of microalgal biomass and swine manure via response surface methodology', *Applied Energy,* 88(10), pp. 3448-3453.

Gregory, R. P. F. (1989a) 'Biochemistry of photosynthesis', in Third ed, John Wiley & Sons, pp. 60-80.

Gregory, R. P. F. (1989b), *Photosynthesis,* Chapman and Hall, United States of America.

Grobbelaar, J. (2010) 'Microalgal biomass production: challenges and realities', *Photosynthesis Research,* 106(1-2), pp. 135-144.

Grobbelaar, J. U. (2004) 'Algal nutrition', in Richmond, A.(ed), *Handbook of microalgal culture: biotechnology and applied phycology.* Blackwell Science, Oxford, pp. 97-115.

Grobbelaar, J. U. (2009) 'Upper limits of photosynthetic productivity and problems of scaling', *Journal of Applied Phycology,* 21(5), pp. 519-522.

Hall, D. O. and Rao, K. K. (1981), *Photosynthesis - Studies in Biology no. 37,* Third ed, Edward Arnold, Southampton, United Kingdom.

Hall, D. O. and Rao, K. K. (1994), *Photosynthesis,* Fifth ed, Cambridge University Press, Cambridge.

Hall, D. O. and Rao, K. K. (1999), *Photosynthesis,* 6th ed, Cambridge University Press, Cambridge.

Hammouda, O., Gaber, A. and Abdel-Raouf, N. (1995) 'Microalgae and wastewater treatment', *Ecotoxicology and Environmental Safety,* 31(3), pp. 205-210.

Hanagata, N., Takeuchi, T., Fukuju, Y., Barnes, D. J. and Karube, I. (1992) 'Tolerance of microalgae to high CO_2 and high temperature', *Phytochemistry,* 31(10), pp. 3345-3348.

Hart, B. A. and Scaife, B. D. (1977) 'Toxicity and bioaccumulation of Cadmium in *Chlorella pyrenoidosa*', *Environmental Research,* 14(3), pp. 401-413.

Harun, R., Singh, M., Forde, G. M. and Danquah, M. K. (2010) 'Bioprocess engineering of microalgae to produce a variety of consumer products', *Renewable and Sustainable Energy Reviews* 14(3), pp. 1037-1047.

Hodgson, B. and Paspaliaris, P. (1996) 'Melbourn Water's wastewater treatment lagoons: design modifications to reduce odours and enhance nutrient removal', *Water Science and Technology,* 33(7), pp. 157-164.

Hsueh, H. T., Li, W. J., Chen, H. H. and Chu, H. (2009) 'Carbon bio-fixation by photosynthesis of *Thermosynechoccus sp.* CL-1 and *Nannochloropsis oculata*', *Journal of Photochemistry and Photobiology B: Biology,* 95(1), pp. 33-39.

Humenik, F. J. and Hanna-Jr, G. P. (1971) 'Algal-bacterial symbiosis for removal and conservation of wastewater nutrients', *Water Pollution Control Federation,* 43(4), pp. 580-594.

Huse, S. M., Dethlefsen, L., Huber, J. A., Welch, D. M., Relman, D. A. and Sogin, M. L. (2008) 'Exploring Microbial Diversity and Taxonomy Using SSU rRNA Hypervariable Tag Sequencing', *PLoS Genet,* 4(11), pp. e1000255.

Jacob-Lopes, E., Revah, S., Hernández, S., Shirai, K. and Franco, T. T. (2009) 'Development of operational strategies to remove carbon dioxide in photobioreactors', *Chemical Engineering Journal,* 153(1–3), pp. 120-126.

Jeong, H., Lee, J. and Cha, M. (2013) 'Energy efficient growth control of microalgae using photobiological methods', *Renewable Energy,* 54pp. 161-165.

Jianlong, W. and Ning, Y. (2004) 'Partial nitrification under limited dissolved oxygen conditions', *Process Biochemistry,* 39(10), pp. 1223-1229.

Keffer, J. E. and Kleinheinz, G. T. (2002) 'Use of *Chlorella vulgaris* for CO_2 mitigation in a photobioreactor', *Journal of Industrial Microbiology and Biotechnology,* 29(5), pp. 275-280.

Kiely, G. (1997), *Environmental Engineering,* McGraw-Hill, United Kingdom.

Kirk, J. T. O. (1994), *Light and photosynthesis in aquatic ecosystems,* Second ed, Cambridge University Press, Cambridge.

Kleiner, D. (1985) 'Bacterial ammonium transport', *FEMS Microbiology Letters,* 32(2), pp. 87-100.

Klingenstein, W. (2004) 'Semiconductor fundamentals and historical overview', in AG, I. T.(ed), *Semiconductors.* 2nd ed, Erlangen: Publicis Corporate Publishing, pp. 14-44.

Knapp, C. W. and Graham, D. W. (2004) 'Development of alternate ssu-rRNA probing strategies for characterizing aquatic microbial communities', *Journal of Microbiological Methods,* 56(3), pp. 323-330.

Konig, A., Pearson, H. W. and Silva, S. A. (1987) 'Ammonia toxicity to algal growth in waste stabilisation ponds', *Water Science and Technology,* 19(12), pp. 115-122.

Kumar, R. and Goyal, D. (2010) 'Wastewater treatment and metal removal (Pb^{2+}, Zn^{2+}) by microalgal based stabilisation pond system', *Indian Journal of Microbiology,* 50(Suppl 1), pp. S34-S40.

Lai, P. C. C. and Lam, P. K. S. (1997) 'Major pathways of nitrogen removal in waste water stabilisation ponds', *Water, Air, and Soil Pollution,* 94(1), pp. 125-136.

Lee, K. and Lee, C.-G. (2001a) 'Effect of light/dark cycles on wastewater treatments by microalgae', *Biotechnology and Bioresource Engineering,* 6(3), pp. 194-199.

Lee, K. and Lee, C.-G. (2001b) 'Effect of light/dark cycles on wastewater treatments by microalgae', *Biotechnology and Bioprocess Engineering,* 6(3), pp. 194-199.

Lee, R. E. (1999), *Phycology,* 3rd ed, Cambridge University Press, Cambridge.

Long, S. P., Humphries, S. and Falkowski, P. G. (1994) 'Photoinhibition of photosynthesis in nature', *Annual Review of Plant Physiology and Plant Molecular Biology,* 45(1), pp. 633-662.

Ludwig, H. F., Oswald, W. J., Gotaas, H. B. and Lynch, V. (1951) 'Algae symbiosis in oxidation ponds I: growth characteristics of *Euglena gracilis* cultured in sewage', *Sewage and industrial wastes,* 23(11), pp. 1337-1355.

Mara, D. (2003a) 'Low-cost treatment systems', in Horan, D. M. a. N.(ed), *The handbook of water and wastewater microbiology.* London: Elsevier, pp. 441-448.

Mara, D. D. (1987) 'Waste stabilisation ponds: problems and controversies', *Water Quality International,* 1pp. 20-22.

Mara, D. D. (1996) 'Waste stabilisation ponds: effluent quality requirements and implications for process design', *Water Science and Technology,* 33(7), pp. 23-31.

Mara, D. D. (2003b), *Domestic wastewater treatment in developing countries,* Earthscan Publications, London.

Mara, D. D. (ed.) (2006) *Natural wastewater treatment.* CIWEM, England.

Mara, D. D. (2008) 'Waste stabilisation ponds: a highly appropriate wastewater treatment technology for mediterranean countries ', in Baz, I. A., Otterpohl, I. and Wendland, C.(eds) *Efficient management of wastewater: its treatment and reuse in water scarse countries.* Heidelberg: Springer, pp. 113-123.

Mara, D. D., Cogman, C. A., Simkins, P. and Schembri, M. C. A. (1998) 'Performance of the Burwarton Estate waste stabilisation ponds', *Water and Environment Journal of the Chatered Institution of Water and Environmental Management,* 12(4), pp. 260-264.

Mara, D. D. and Horan, N. J. (1993) 'BOD test for tropical countries: discussion', *Journal of Environmental Engineering of the Amiercan Society of Civil Engineers,* 119(4), pp. 764-766.

Mara, D. D. and Johnson, M. L. (2007) 'Waste stabilisation ponds and rock filters: solutions for small communities', *Water Science & Technology,* 55(7), pp. 103-107.

Marais, G. v. R. (1974) 'Fecal bacterial kinetics in stabilisation ponds', *Journal of Environmental Engineering of the Amiercan Society of Civil Engineers,* 100(1), pp. 119-139.

Martinez, M. E., Jimenez, J. M. and Yousfi, F. E. (1999) 'Influence of phosphorus concentration and temperature on growth and phosphorus uptake by the microalga *Snedesmus obliquus*', *Bioresource Technology,* 67(3), pp. 233-240.

Martinez, M. E., Sanchez, S., Jimenez, J. M., Yousfi, F. E. and Munoz, L. (2000) 'Nitrogen and phosphorus removal from urban wastewater by the microalgae *Scendesmus obliquus*', *Bioresource Technology,* 73(3), pp. 263-272.

Matthews, D. H., Matthews, H. S., Jaramillo, P. and Weber, C. L. (2009) 'Energy consumption in the production of high-brightness light-emitting diodes' *IEEE International Symposium on Sustainable Systems and Technology.* Tempe, AZ, USA:IEEE.

Mayo, A. W. (1996) 'BOD_5 removal in facultative ponds: experience in Tanzania', *Water Science and Technology,* 34(11), pp. 107-117.

Mbwele, L. A. (2006) *Microbial phosphorus removal in waste stabilisation ponds.* Licentiate thesis. Royal Institute of Technology, Stockholm, Sweden.

Medina, M. and Neis, U. (2007) 'Symbiotic algal bacterial wastewater treatment: effect of food to microorganism ratio and hydraulic retention time on the process performance', *Water Science and Technology,* 55(11), pp. 165-171.

Mehta, R., Deshpande, D., Kulkarni, K., Sharma, S. and Divan, D. (2008) 'LEDs - A competitive solution for general lighting applications*', IEEE Energy 2030 Conference.* Atlanta, Georgia, IEEE, pp.

Mendes, B. S., do-Nascimento, M. J., Pereira, M. I., Bailey, G., Lapa, N., Morais, J. and Oliveira, J. S. (1995) 'Efficiency of removal in stabilisation ponds I: influence of climate', *Water Science and Technology,* 31(12), pp. 219-229.

Meng, X., Yang, J., Xu, X., Zhang, L., Nie, Q. and Xian, M. (2009) 'Biodiesel production from oleaginous microorganisms', *Renewable Energy,* 34(1), pp. 1-5.

Metcalf and Eddy. (2003), *Wastewater engineering, treatment and reuse,* 4th ed, McGraw-Hill, New York.

Miskelly, A. and Scragg, A. H. (1996) 'Removal of heavy metals by microalgae', *International Biodeterioration & Biodegradation,* 37(3-4), pp. 243.

Miyachi, S., Kanai, R., Mihara, S., Miyachi, S. and Aoki, H. (1964) 'Metabolic roles of inorganic polyphosphates in chlorella cells', *Biochimica et Biophysica Acta,* 93(3), pp. 625-634.

Mohammed, K., Ahammad, S. Z., Sallis, P. J. and Mota, C. R. (2013a) 'Energy-efficient photobioreactors for simultaneous carbon capture and municipal wastewater treatment' *10th IWA International Conference on Ponds Technology: Advances and Innovations in Wastewater Pond Technology.* Cartagena, Colombia, 19th - 23rd August, 2013.

Mohammed, K., Ahammad, S. Z., Sallis, P. J. and Mota, C. R. (2013b) 'Optimisation of red light-emitting diodes irradiance for illuminating mixed microalgal culture to treat municipal wastewater' *7th International Conference on Sustainable Water Resources Management.* New Forest, UK, 21-23 May 2013.

Negoro, M., Hamasaki, A., Ikuta, Y., Makita, T., Hirayama, K. and Suzuki, S. (1993) 'Carbon dioxide fixation by microalgae photosynthesis using actual flue gas discharged from a boiler', *Applied Biochemistry and Biotechnology,* 39/40(1), pp. 643-653.

Nelson, N. and Yocum, C. F. (2006) 'Structure and function of photosystems I and II', *Annual Review of Plant Biology,* 57pp. 521-565.

Nesbitt, J. B. (1969) 'Phosphorus removal - the state of the art', *Water Pollution Control Federation,* 41(5), pp. 701-713.

Ng, K. K. (1995), *Complete Guide to Semiconductor Devices* McGraw-Hill, United States of Ameria.

Nijhof, M. and Klapwijk, A. (1995) 'Diffusional transport mechanisms and biofilm nitrification characteristics influencing nitrite levels in nitrifying trickling filter effluents', *Water Research,* 29(10), pp. 2287-2292.

Nurdogan, Y. and Oswald, W. J. (1995) 'Enhanced nutrient removal in high-rate ponds', *Water Science and Technology,* 31(12), pp. 33-43.

Oehmen, A., Lemos, P. C., Carvalho, G., Yuan, Z., Keller, J., Blackall, L. L. and Reis, M. A. M. (2007) 'Advances in enhanced biological phosphorus removal: From micro to macro scale', *Water Research,* 41(11), pp. 2271-2300.

Ogbonna, J. C., Soejima, T. and Tanaka, H. (1999) 'An integrated solar and artificial light system for internal illumination of photobioreactors', *Journal of Biotechnology,* 70(1-3), pp. 289-297.

Ogbonna, J. C., Soejima, T., Ugwu, C. U. and Tanaka, H. (2001) 'An integrated system of solar light, artificial light and organic carbon supply for cyclic photoautotrophic-heterotrophic cultivation of photosynthetic cells under day-night cycles', *Biotechnology Letters,* 23(17), pp. 1401-1406.

Oliveira, R. d., Silva, S. A., Araujo, A. L. C., Soares, J., Mara, D. D. and Pearson, H. W. (1996) 'The performance of a pilot-scale series of ten ponds treating municipal sewage in Northeast Brazil', *Water Science & Technology,* 33(7), pp. 57-61.

Ong, S.-C., Kao, C.-Y., Chiu, S.-Y., Tsai, M.-T. and Lin, C.-S. (2010) 'Characterisation of the thermal-tolerant mutants of *Chlorella* sp with high growth rate and application in outdoor photobioreactor cultivation', *Bioresource Technology,* 101(8), pp. 2880-2883.

Oswald, W. J. (1990) 'Advanced integrated wastewater pond systems' *Supplying Water and Saving the Environment for Six Billion People.* San Francisco, November 5-8, 1990.American Society of Civil Engineers.

Oswald, W. J. (1995) 'Ponds in the 21st Century', *Water Science and Technology,* 31(12), pp. 1-8.

Oswald, W. J., Gotaas, H. B., Golueke, C. G. and Kellen, W. R. (1957) 'Algae in waste treatment', *Sewage and industrial wastes,* 29(4), pp. 437-457.

Oswald, W. J., Gotaas, H. B., Ludwig, H. L. and Lynch, V. (1953) 'Algae symbiosis in oxidation ponds II: growth characteristics of Chlorella pyrenoidosa cultured in sewage', *Sewage and industrial wastes,* 25(1), pp. 26-37.

Packer, M. (2009) 'Algal capture of carbon dioxide; biomass generation as a tool for greenhouse gas mitigation with reference to New Zealand energy strategy and policy', *Energy Policy,* 37(9), pp. 3428-3437.

Pano, A. and Middlebrooks, E. J. (1982a) 'Ammonia and total Kjeldahl nitrogen removal in aerated lagoons', *Water Science and Technology,* 14(1-2), pp. 381-391.

Pano, A. and Middlebrooks, E. J. (1982b) 'Ammonia nitrogen removal in facultative wastewater stabilisation ponds', *Water Pollution Control Federation,* 54(4), pp. 344-351.

Park, J. B. K. and Craggs, R. J. (2010) 'Wastewater treatment and algal production in high rate algal ponds with carbon dioxide addition', *Water Science and Technology,* 61(3), pp. 633-639.

Park, J. B. K. and Craggs, R. J. (2011) 'Nutrient removal in wastewater treatment high rate algal ponds with carbon dioxide addition', *Water Science and Technology,* 63(8), pp. 1758-1764.

Park, J. B. K., Craggs, R. J. and Shilton, A. N. (2011) 'Wastewater treatment high rate algal ponds for biofuel production', *Bioresource Technology,* 102(1), pp. 35-42.

Paterson, C. and Curtis, T. (2005) 'Physical and chemical environments', in Shilton, A.(ed), *Pond Treatment Technology.* London: IWA Publishing, pp. 49-65.

Pearson, H. (2005) 'Microbiology of waste stabilisation ponds', in Shilton, A.(ed), *Pond Treatment Technology.* London: IWA Publishing, pp. 15-48.

Pearson, H. W., Athayde-Jr., S. T. S. and Silva, S. A. (2005) 'Implications for physical design: the effect of depth on the performance of waste stabilisation ponds', *Water Science and Technology,* 51(12), pp. 69-74.

Pearson, H. W., Mara, D. D. and Arridge, H. A. (1995) 'The influence of pond geometry and configuration on facultative maturation waste stabilisation pond performance and effcicency', *Water Science and Technology,* 31(12), pp. 129-139.

Pearson, H. W., Mara, D. D. and Bartone, C. R. (1987) 'Guidelines for the minimum evaluation of the performance of full-scale waste stabilisation ponds systems', *Water Research,* 21(9), pp. 1067-1075.

Pena-Castro, J. M., Martinez-Jeronimo, F., Esparza-Garcia, F. and Canizares-Villanueva, R. O. (2004) 'Heavy metals removal by the microalga *Scenedesmus incrassatulus* in continuous cultutres', *Bioresource Technology,* 94(2), pp. 219-222.

Perez-Garcia, O., Bashan, Y. and Puente, M. E. (2011a) 'Organic carbon supplementation of sterilized municipal wastewater is essential for heterotrophic growth and removing ammonium by the microalga *Chlorella vulgaris*', *Journal of Phycology,* 47(1), pp. 190-199.

Perez-Garcia, O., Escalante, F. M. E., de-Bashan, L. E. and Bashan, Y. (2011b) 'Heterotrophic cultures of microalgae: metabolism and potential products', *Water Research,* 45(1), pp. 11-36.

Philips, S., Laanbroek, H. J. and Verstraete, W. (2002) 'Origin, causes, and effects of increased nitrite concentrations in aquatic environments', *Re/Views in Environmental Science & Bio/Technology,* 1(2), pp. 115-141.

Powell, N. (2009) *Biological phosphorus removal by microalgae in waste stabilisation ponds.* PhD thesis. Massey University, New Zealand.

Powell, N., Shilton, A., Chisti, Y. and Pratt, S. (2009) 'Towards a luxury uptake process via microalgae - Defining the polyphosphate dynamics', *Water Research,* 43(17), pp. 4207-4213.

Powell, N., Shilton, A., Pratt, S. and Chisti, Y. (2011) 'Luxury uptake of phosphorus by microalgae in full-scale waste stabilisation ponds', *Water Science and Technology,* 63(4), pp. 704-709.

Powles, S. B. (1984) 'Photoinhibition of photosynthesis induced by visible-light', *Annual Review of Plant Physiology and Plant Molecular Biology,* 35pp. 15-44.

Prance, L. (2006) *Algae-based cosmetic ingredient set to impact anti-aging market* [Online]. Available at: http://www.cosmeticsdesign.com/Formulation-Science/Algae-based-cosmetic-ingredient-set-to-impact-anti-aging-market (Accessed: 15-01-2012).

Racault, Y., Boutin, C. and Seguin, A. (1995) 'Waste stabilisation ponds in France: a report on fifteen years experience', *Water Science and Technology,* 31(12), pp. 91-101.

Raja, R. and Hemaiswarya, S. (2010) 'Microalgae and immune potential', in Watson, R. R., Zibadi, S. and Preedy, V. R.(eds) *Dietary components and immune function.* 1st ed, New York: Springer, pp. 515-527.

Reed, S. C. (1985) 'Nitrogen removal in wastewater stabilisation ponds', *Water Pollution Control Federation,* 57(1), pp. 39-45.

Renger, G. and Renger, T. (2008) 'Photosytem II: The machinery of photosynthetic water splitting', *Photosynthesis Research,* 98(1-3), pp. 53-80.

Rockne, K. J. and Brezonik, P. L. (2006) 'Nutrient removal in a cold-region wastewater stabilisation pond: importance of ammonia volatilisation', *ASCE Journal of Environmental Engineering,* 132(4), pp. 451-459.

Roy, H. and Cannon, S. (1988) 'Ribulose bisphophate carboxylase assembly: what is the role of the large subunit binding protein?', *Trends in Biochemical Sciences,* 13(5), pp. 163-165.

Ruffier, P. J., Boyle, W. C. and Kleinschmidt, J. (1981) 'Short-Term Acute Bioassays to Evaluate Ammonia Toxicity and Effluent Standards', *Journal (Water Pollution Control Federation),* 53(3), pp. 367-377.

Rutherford, A. W. and Faller, P. (2001) 'The heart of photosynthesis in glorious 3D', *Trends in Biochemical Sciences,* 26(6), pp. 341-344.

Saito, T., Brdjanovic, D. and Loosdrecht, M. C. M. v. (2004) 'Effect of nitrite on phosphate uptake by phosphate accumulating organisms', *Water Research,* 38(17), pp. 3760-3768.

Schetrite, S. and Racault, Y. (1995) 'Purification by a natural waste stabilisation pond: influence of weather and ageing on treatment quality and sediment thichness', *Water Science and Technology,* 31(12), pp. 191-200.

Sheehan, J., Dunahay, T., Benemann, J. and Roessler, P. (1998) *A look back at the US Department of Energy's Aquatic Species Program - Biodiesel from Algae.* National Renewable Energy Laboratory, Golden, Colarado.

Shelef, G. (1982) 'High-rate algae ponds for wastewater treatment and protein production', *Water Science and Technology,* 14(1-2), pp. 439-452.

Shelp, B. J. and Canvin, D. T. (1980) 'Photorespiration and oxygen inhibition of photosynthesis in *Chlorella pyrenoidosa*', *Plant Physiology,* 65(5), pp. 780-784.

Shilton, A. and Harrison, J. (2003), *Guidelines for the hydraulic design of waste stabilisation ponds,* New Zealand, Massey University, Palmerston North.

Silva-Benavides, A. and Torzillo, G. (2012) 'Nitrogen and phosphorus removal through laboratory batch cultures of microalga Chlorella vulgaris and cyanobacterium Planktothrix isothrix grown as monoalgal and as co-cultures', *Journal of Applied Phycology,* 24(2), pp. 267-276.

Sinha, B. and Annachhatre, A. P. (2007) 'Partial nitrification - operational parameters and microorganisms involved', *Reviews in Environmental Science & Biotechnology,* 6pp. 285-313.

Soler, A., Torrella, F., Saez, J., Martinez, I., Nicolas, J., MLlorens and Torres, J. (1995) 'Performance of two municipal sewage stabilisation pond systems with high and low loading in south-east Spain', *Water Science and Technology,* 31(12), pp. 81-90.

Sperling, M. v. and Chernicharo, C. A. d. L. (2005), *Biological wastewater treatment in warm climate regions,* International Water Association, London.

Spolaore, P., Joannis-Cassan, C., Duran, E. and Isambert, A. (2006) 'Commercial applications of microalgae', *Journal of Bioscience and Bioengineering,* 101(2), pp. 87-96.

Stanley, J. G. and Jones, J. B. (1976) 'Feeding algae to fish', *Aquaculture,* 7(3), pp. 219-223.

Stolz, P. and Obermayer, B. (2005) 'Manufacturing microalgae for skin care', Cosmetics & Toiletries, 120, 3, p.99-106.

Sung, K.-D., Lee, J.-S., Shin, C.-S., Park, S.-C. and Choi, M.-J. (1999) 'CO_2 fixation by *Chlorella* sp. KR-1 and its cultural characteristics', *Bioresource Technology,* 68(3), pp. 269-273.

Surampalli, R. Y., Banerji, S. K., Pycha, C. J. and Lopez, E. R. (1995) 'Phosphorus removal in ponds', *Water Science and Technology,* 31(12), pp. 331-339.

Sydney, E. B., Sturm, W., de-Carvalho, J. C., Thomas-Soccol, V., Larroche, C., Pandey, A. and Soccol, C. R. (2010) 'Potential carbon dioxide fixation by industrially important microalgae', *Bioresource Technology,* 101(15), pp. 5892-5896.

Takeuchi, T., Utsunomiya, K., Kaboyashi, K., Owada, M. and Karube, I. (1992) 'Carbon dioxide fixation by a unicellular green alga *Oocystis* sp.', *Journal of Biotechnology,* 25(3), pp. 261-267.

Tandukar, M., Ohashi, A. and Harada, H. (2007) 'Performance comparison of a pilot-scale UASB and DHS system and activated sludge process for the treatment of municipal wastewater', *Water Research,* 41(12), pp. 2697-2705.

Termini, I. D., Prassone, A., Catteno, C. and Rovatti, M. (2011) 'On the nitrogen and phosphorus removal in algal photobioreactors', *Ecological Engineering,* 37(6), pp. 976-980.

Terry, K. L. and Raymond, L. P. (1985) 'System design for the autotrophic production of microalgae', *Enzyme Microbial Technology,* 7(10), pp. 474-487.

Tredici, M. R. (2004) 'Mass production of microalgae: photobioreactors', in Richmond, A.(ed), *Handbook of microalgal culture: biotechnology and applied phycology.* Blackwell Science, Oxford, pp. 178-214.

Tuchman, N. C. (1996) '10 - The Role of Heterotrophy in Algae', in Stevenson, R. J., Max, L. B., Rex L. LoweA2 - R. Jan Stevenson, M. L. B. and Rex, L. L.(eds) *Algal Ecology.* San Diego: Academic Press, pp. 299-319.

Ugwu, C. U., Aoyagi, H. and Uchiyama, H. (2008) 'Photobioreactors for mass cultivation of algae', *Bioresource Technology,* 99(10), pp. 4021-4028.

van-der-Linde, E. R. C., Mara, D. D. and Newton, R. J. (2009) 'Nitrogen removal during summer and winter in a primary facultative pond: preliminary findings from ^{15}N-labelled ammonium tracking techniques*', 88th IWA Specialist Group Conference on Waste Stabilisation Ponds.* Belo Horizonte, Brazil, White Rose, pp. 1-9.

Van Den Hende, S., Vervaeren, H. and Boon, N. (2010) 'Industrial symbiosis: C, N and P scavenging from sewage and flue gas with algal bacterial flocs', *Journal of Biotechnology,* 150(Supplement), pp. 278.

Vishay Intertechnology Inc (2004) *Classification of components* [Online]. Available at: http://www.vishay.com/docs/80093/classifi.pdf (Accessed: 15-02-2011).

von-Sperling, M. and Chernicharo, C. A. d. L. (2005), *Biological wastewater treatment in warm climate regions,* International Water Association, London.

von-Sperling, M. and Mascarenhas, L. C. A. M. (2005) 'Performance of very shallow ponds treating effluents from UASB reactors', *Water Science and Technology,* 51(12), pp. 83-90.

Vonshak, A. (ed.) (1986) *Laboratory techniques for the cultivation of microalgae.* Boca Rotan: CRC Press.

Wang, B., Li, Y., Wu, N. and Lan, C. Q. (2008) 'CO_2 bio-mitigation using microalgae ', *Applied Microbiology and Biotechnology,* 79(5), pp. 707-718.

Wang, C.-Y., Fu, C.-C. and Liu, Y.-C. (2007) 'Effects of using light-emitting diodes on the cultivation of *Spirulina platensis* ', *Biochemical Engineering Journal,* 37(1), pp. 21-25.

Weatherell, C. A., Elliott, D. J., Fallowfield, H. J. and Curtis, T. P. (2003) 'Variable photosynthetic characteristics in waste stabilisation ponds', *Water Science and Technology,* 48(2), pp. 219-226.

Wilde, E. W. and Benemann, J. R. (1993) 'Bioremoval of heavy metals by the use of microalgae', *Biotechnology Advances,* 11(4), pp. 781-812.

Yamada, H., Ohkuni, N., Kajiwara, S. and Ohtaguchi, K. (1997) 'CO_2-removal characteristics of Anacystis nidulans R2 in airlift bioreactors', *Energy,* 22(2/3), pp. 349-352.

Yamada, K., Tamano, K., Mori, T., Mizutani, T. and Sugiyama, M. (2003) 'Organic light-emitting diodes using semi-transparent anode for flexible display' *Proceedings of the 7th International Conference on Properties and Applications of Dielectric Materials.* Nagoya:IEEE.

Yamaguchi, K. (1997) 'Recent advances in microalgal bioscience in Japan, with special reference to utilization of biomass and metabolites: A review', *Journal of Applied Phycology,* 8(6), pp. 487-502.

Yan, C., Zhang, L., Luo, X. and Zheng, Z. (2013) 'Effects of various LED light wavelengths and intensities on the performance of purifying synthetic domestic sewage by microalgae at different influent C/N ratios', *Ecological Engineering,* 51pp. 24-32.

Yokota, A. and Shigeoka, S. (2008) 'Engineering Photosynthetic Pathways', in Bohnert, H. J., Nguyen, H. and Lewis, N. G.(eds) *Bioengineering and Molecular Biology of Plant Pathways*. Vol. 1 pp 81-105.

Yoshida, Y., Takahashi, K., Saito, T. and Tanaka, K. (2006) 'The effect of nitrite on aerobic phosphate uptake and denitrifying activity of phosphate-accumulating organisms', *Water Science & Technology,* 53(6), pp. 21-27.

Yu, Y., Lee, C., Kim, J. and Hwang, S. (2005) 'Group-specific primer and probe sets to detect methanogenic communities using quantitative real-time polymerase chain reaction', *Biotechnology and Bioengineering,* 89(6), pp. 670-679.

Yun, Y.-S., Lee, S. B., Park, J. M., Lee, C.-I. and Yang, J.-W. (1997) 'Carbon dioxide fixation by algal cultivation using wastewater nutrients', *Chemical Technology and Biotechnology,* 69(4), pp. 451-455.

Yun, Y.-S., Park, J. M. and Yang, J.-W. (1996) 'Enhancement of CO_2 tolerance of *Chlorella vulgaris* by gradual increase of CO_2 concentration', *Biotechnology Techniques,* 10(9), pp. 713-716.

Zamalloa, C., Boon, N. and Verstraete, W. (2012) 'Anaerobic digestibilty of *Scenedesmus obliquus* and *Phaeodactylum tricornutum* under mesophilic and thermophilic conditions', *Applied Energy,* 92pp. 733-738.

Zeiler, K. G., Heacox, D. A., Toon, S. T., Kadam, K. L. and Brown, L. M. (1995) 'The use of microalgae for assimilation and utilisation of carbon dioxide from fossil fuel-fired power plant flue gas', *Energy Conversion and Management,* 36(6-9), pp. 707-712.

Zhu, F., Massana, R., Not, F., Marie, D. and Vaulot, D. (2005) 'Mapping of picoeucaryotes in marine ecosystems with quantitative PCR of the 18S rRNA gene', *FEMS Microbiology Ecology,* 52(1), pp. 79-92.

Zimmo, O. R., Steen, N. P. v. d. and Gijzen, H. J. (2004) 'Nitrogen mass balance across pilot-scale algae and duckweed-based wastewater stabilisation ponds', *Water Research,* 38(4), pp. 913-920.

Appendix

Phase I experiments data

Table A3.1 Red LED light measurement data

PBR	Clamping height (cm)	Irradiance (µmol s^{-1} m^{-2})			Average	SD	SE
Without aluminium foil (in air)							
R2/R8	30.6	20.06	20.26	19.99	20.10	0.14	0.08
R3/R9	28.0	48.12	48.39	48.30	48.27	0.14	0.08
R4/R10	23.0	82.29	82.61	82.73	82.54	0.23	0.13
R5/R11	15.5	118.30	119.10	118.74	118.71	0.40	0.23
R6/R12	16.0	149.94	149.69	150.98	150.20	0.68	0.39
Distilled water							
R2/R8	30.6	13.84	13.98	13.79	13.87	0.10	0.06
R3/R9	28.0	33.20	33.39	33.33	33.31	0.10	0.06
R4/R10	23.0	56.78	57.00	57.08	56.95	0.16	0.09
R5/R11	15.5	81.63	82.18	81.93	81.91	0.28	0.16
R6/R12	16.0	103.46	103.29	104.18	103.64	0.47	0.27
Algal culture							
R2/R8	30.6	2.21	2.23	2.20	2.21	0.02	0.01
R3/R9	28.0	5.29	5.32	5.31	5.31	0.02	0.01
R4/R10	23.0	9.05	9.09	9.10	9.08	0.03	0.02
R5/R11	15.5	13.01	13.10	13.06	13.06	0.05	0.03
R6/R12	16.0	16.49	16.47	16.61	16.52	0.08	0.04
With foil aluminium (in air)							
R2/R8	30.6	25.27	25.31	25.29	25.29	0.02	0.01
R3/R9	28.0	64.55	64.47	64.39	64.47	0.08	0.05
R4/R10	23.0	112.00	115.05	114.57	113.87	1.64	0.95
R5/R11	15.5	181.57	181.33	180.68	181.19	0.46	0.27
R6/R12	16.0	235.00	234.10	233.80	234.30	0.62	0.36
Distilled water							
R2/R8	30.6	17.44	17.46	17.45	17.45	0.01	0.01
R3/R9	28.0	44.54	44.48	44.43	44.48	0.06	0.03
R4/R10	23.0	77.28	79.38	79.05	78.57	1.13	0.65
R5/R11	15.5	125.28	125.12	124.67	125.02	0.32	0.18
R6/R12	16.0	162.15	161.53	161.32	161.67	0.43	0.25
Algal culture							
R2/R8	30.6	2.78	2.77	2.79	2.78	0.01	0.01
R3/R9	28.0	7.10	7.09	7.08	7.09	0.01	0.01
R4/R10	23.0	12.32	12.66	12.60	12.53	0.18	0.10
R5/R11	15.5	19.97	19.95	19.87	19.93	0.05	0.03
R6/R12	16.0	25.85	25.75	25.72	25.77	0.07	0.04

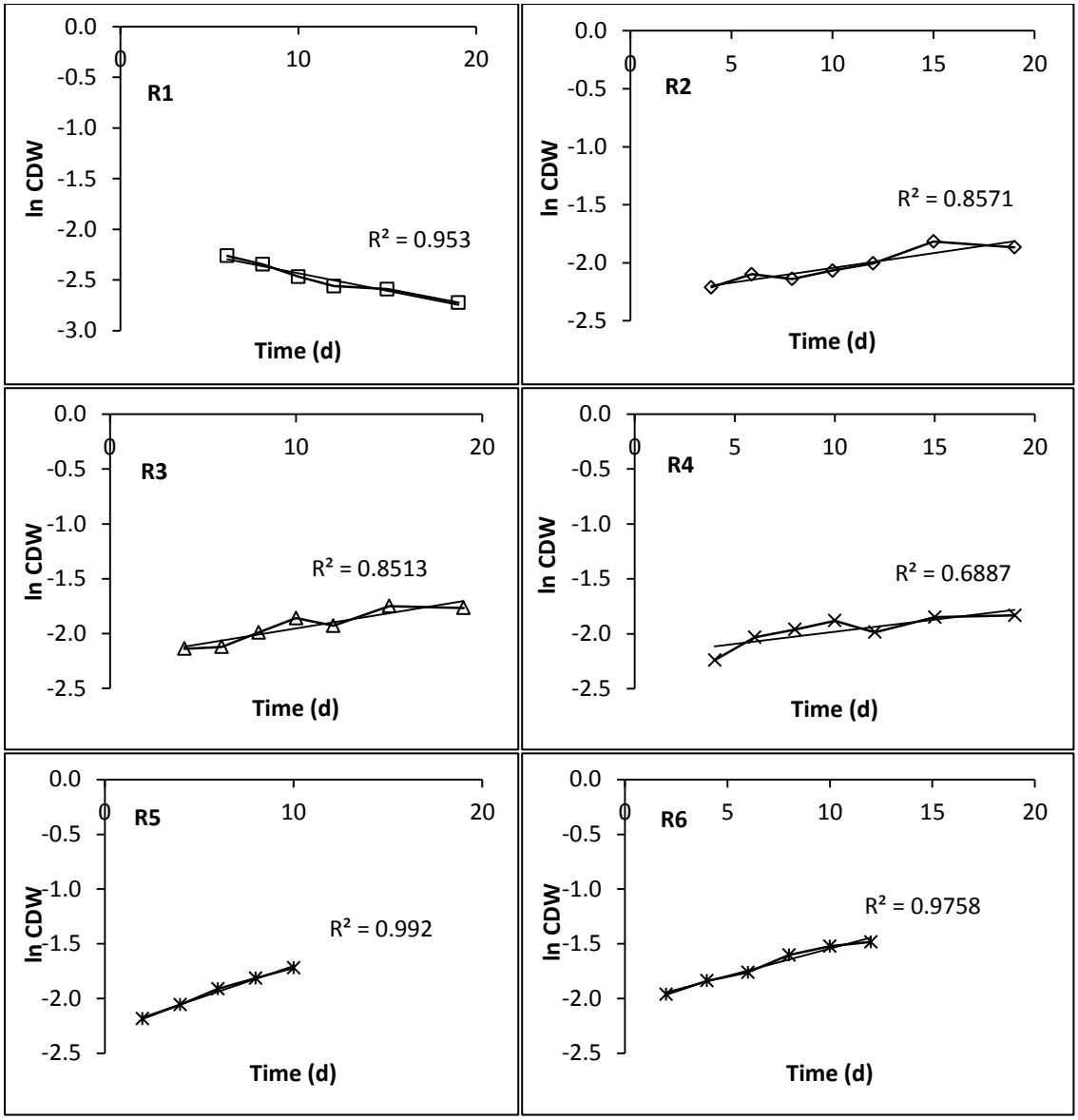

Figure A3.1 Maximum specific growth rates plots for bench-scale PBR with CO_2 addition in Phase I experiments

Table A3.2 Microalgal CDW and natural logarithm values used to calculate maximum specific growth rates in the 1 L PBR

Time (d)	CDW ($g.L^{-1}$)						ln CDW					
	R1	R2	R3	R4	R5	R6	R1	R2	R3	R4	R5	R6
0	0.09	0.09	0.09	0.09	0.09	0.09	-2.39	-2.39	-2.39	-2.39	-2.39	-2.39
2	0.10	0.12	0.13	0.12	0.11	0.14	-2.28	-2.16	-2.06	-2.09	-2.18	-1.96
4	0.10	0.11	0.12	0.11	0.13	0.16	-2.26	-2.21	-2.14	-2.24	-2.06	-1.84
6	0.10	0.12	0.12	0.13	0.15	0.17	-2.26	-2.10	-2.12	-2.03	-1.91	-1.76
8	0.10	0.12	0.14	0.14	0.16	0.20	-2.34	-2.14	-1.99	-1.96	-1.81	-1.60
10	0.09	0.13	0.16	0.15	0.18	0.22	-2.47	-2.07	-1.86	-1.88	-1.72	-1.52
12	0.08	0.14	0.15	0.14	0.17	0.23	-2.56	-2.01	-1.93	-1.99	-1.75	-1.48
15	0.08	0.16	0.17	0.16	0.19	0.27	-2.59	-1.82	-1.75	-1.85	-1.64	-1.33
19	0.07	0.16	0.17	0.16	0.21	0.27	-2.72	-1.87	-1.77	-1.83	-1.59	-1.31

Phase II experiments data

Red LED light measurement data in STPBR wrapped with aluminium foil

Table A4.1 Transmitted irradiance in batch-operated STPBR measured in air

Air						
SR 1						
Horizontal distance (cm)	Irradiance (µmol.s^{-1}.m^{-2})			Average	SD	SE
0	429.8	430.8	429.2	429.9	0.81	0.5
2	261.2	261.0	260.8	261.0	0.20	0.1
4	162.6	163.2	162.1	162.6	0.55	0.3
6	119.8	120.4	119.8	120.0	0.35	0.2
8	88.9	89.2	88.9	89.0	0.17	0.1
10	75.4	74.8	76.2	75.5	0.70	0.4
12	60.3	60.6	60.1	60.3	0.25	0.1
14	49.1	49.2	48.1	48.8	0.61	0.4
SR 2						
0	581.4	580.4	586.3	582.7	3.16	1.8
2	339.0	338.4	338.2	338.5	0.42	0.2
4	249.5	249.3	249.0	249.3	0.25	0.1
6	165.0	165.0	164.7	164.9	0.17	0.1
8	135.0	134.8	134.7	134.8	0.15	0.1
10	118.6	118.7	118.6	118.6	0.06	0.0
12	90.1	90.0	89.5	89.9	0.32	0.2
14	73.8	73.4	73.3	73.5	0.26	0.2
SR 3						
0	730.5	729.4	732.4	730.8	1.52	0.9
2	392.3	392.0	391.6	392.0	0.35	0.2
4	263.9	262.1	260.6	262.2	1.65	1.0
6	194.2	193.7	193.0	193.6	0.60	0.3
8	171.2	170.7	170.5	170.8	0.36	0.2
10	149.4	149.2	148.8	149.1	0.31	0.2
12	143.8	143.2	142.6	143.2	0.60	0.3
14	117.6	117.0	117.6	117.4	0.35	0.2

Table A4.2 Transmitted irradiance in batch-operated STPBR measured in distilled water

Distilled water						
SR 1						
Horizontal distance (cm)	Irradiance (µmol.s^{-1}.m^{-2})			Average	SD	SE
0	410.5	410.0	410.9	410.5	0.5	0.3
2	210.1	211.3	210.4	210.6	0.6	0.4
4	147.1	147.9	147.6	147.5	0.4	0.2
6	107.6	108.4	106.9	107.6	0.8	0.4
8	84.5	85.9	85.0	85.1	0.7	0.4
10	63.2	62.8	63.0	63.0	0.2	0.1
12	48.2	48.6	48.8	48.5	0.3	0.2
14	44.1	43.3	43.6	43.7	0.4	0.2
SR 2						
0	506.1	506.6	506.2	506.3	0.3	0.2
2	299.0	302.0	298.6	299.9	1.9	1.1
4	190.3	189.1	188.3	189.2	1.0	0.6
6	132.1	131.5	131.2	131.6	0.5	0.3
8	109.7	109.5	108.4	109.2	0.7	0.4
10	85.3	86.8	87.6	86.6	1.2	0.7
12	71.9	71.0	70.8	71.2	0.6	0.3
14	50.4	49.8	48.5	49.6	1.0	0.6
SR 3						
0	605.0	606.2	605.2	605.5	0.6	0.4
2	321.9	320.7	323.0	321.9	1.2	0.7
4	196.7	198.2	199.8	198.2	1.6	0.9
6	148.5	148.3	147.8	148.2	0.4	0.2
8	126.1	125.0	125.9	125.7	0.6	0.3
10	107.1	109.7	111.0	109.3	2.0	1.1
12	93.3	93.6	93.7	93.5	0.2	0.1
14	82.9	82.4	82.2	82.5	0.4	0.2

Table A4.3 Transmitted irradiance in batch-operated STPBR measured in algal culture

Mixed microalgal culture (CDW = 0.082 g.L^{-1})						
SR 1						
Horizontal distance (cm)	Irradiance (µmol.s^{-1}.m^{-2})			Average	SD	SE
0	369.90	370.30	369.60	369.93	0.35	0.20
2	159.10	160.90	159.70	159.90	0.92	0.53
4	64.30	64.80	64.70	64.60	0.26	0.15
6	39.30	39.50	39.60	39.47	0.15	0.09
8	18.20	17.90	18.10	18.07	0.15	0.09
10	12.40	12.00	12.40	12.27	0.23	0.13
12	7.02	7.07	7.04	7.04	0.03	0.01
14	4.17	4.37	4.23	4.26	0.10	0.06
SR 2						
0	437.20	437.00	437.30	437.17	0.15	0.09
2	194.70	193.60	194.40	194.23	0.57	0.33
4	84.30	84.20	84.60	84.37	0.21	0.12
6	44.20	44.80	44.30	44.43	0.32	0.19
8	22.20	22.00	22.30	22.17	0.15	0.09
10	14.30	14.20	14.30	14.27	0.06	0.03
12	8.21	8.16	8.40	8.26	0.13	0.07
14	6.55	6.53	6.56	6.55	0.02	0.01
SR 3						
0	465.60	469.60	468.90	468.03	2.14	1.23
2	214.20	214.60	213.90	214.23	0.35	0.20
4	96.30	95.80	96.60	96.23	0.40	0.23
6	51.40	51.90	51.30	51.53	0.32	0.19
8	29.80	29.50	29.80	29.70	0.17	0.10
10	18.80	18.90	18.70	18.80	0.10	0.06
12	12.90	12.60	13.20	12.90	0.30	0.17
14	9.93	9.82	9.90	9.88	0.06	0.03

Ammonium and SCOD removal data

Table A4.4 Maximum ammonium removal (%) data in batch-operated STPBR

Before CO_2 addition						
Reactor no.	NH_4-N rem (%)		Ave	SD	SE	Irradiance (µmol.s^{-1}.m^{-2})
SR 0	54.3	56.0	55.2	1.182	0.836	0
SR 1	38.2	42.0	40.1	2.681	1.896	429.9
SR 2	48.1	51.1	49.6	2.180	1.542	582.7
SR 3	44.5	46.6	45.5	1.481	1.047	730.8
After CO_2 addition						
Reactor no.	NH_4-N rem (%)		Ave	SD	SE	Irradiance (µmol.s^{-1}.m^{-2})
SR 0	92.5	93.1	92.8	0.428	0.303	0
SR 1	69.6	70.0	69.8	0.317	0.224	429.9
SR 2	71.0	73.1	72.1	1.484	1.049	582.7
SR 3	69.3	69.4	69.3	0.124	0.087	730.8

Table A4.5 Maximum SCOD removal data in batch-operated STPBR

Maximum SCOD removal (%)						
Before CO_2 addition						
Reactor no.	SCOD rem (%)		Ave	SD	SE	Irradiance (µmol.s^{-1}.m^{-2})
SR 0	77.9	78.5	78.2	0.430	0	0
SR 1	77.1	78.8	77.9	1.152	429.9	429.9
SR 2	80.7	81.3	81.0	0.375	582.7	582.7
SR 3	81.7	81.5	81.6	0.175	730.8	730.8
After CO_2 addition						
Reactor no.	SCOD rem (%)		Ave	SD	SE	Irradiance (µmol.s^{-1}.m^{-2})
SR 0	64.0	62.0	63.0	1.421	0	0
SR 1	64.0	64.0	64.0	0.007	429.9	429.9
SR 2	67.1	68.0	67.5	0.640	582.7	582.7
SR 3	73.3	73.0	73.1	0.187	730.8	730.8

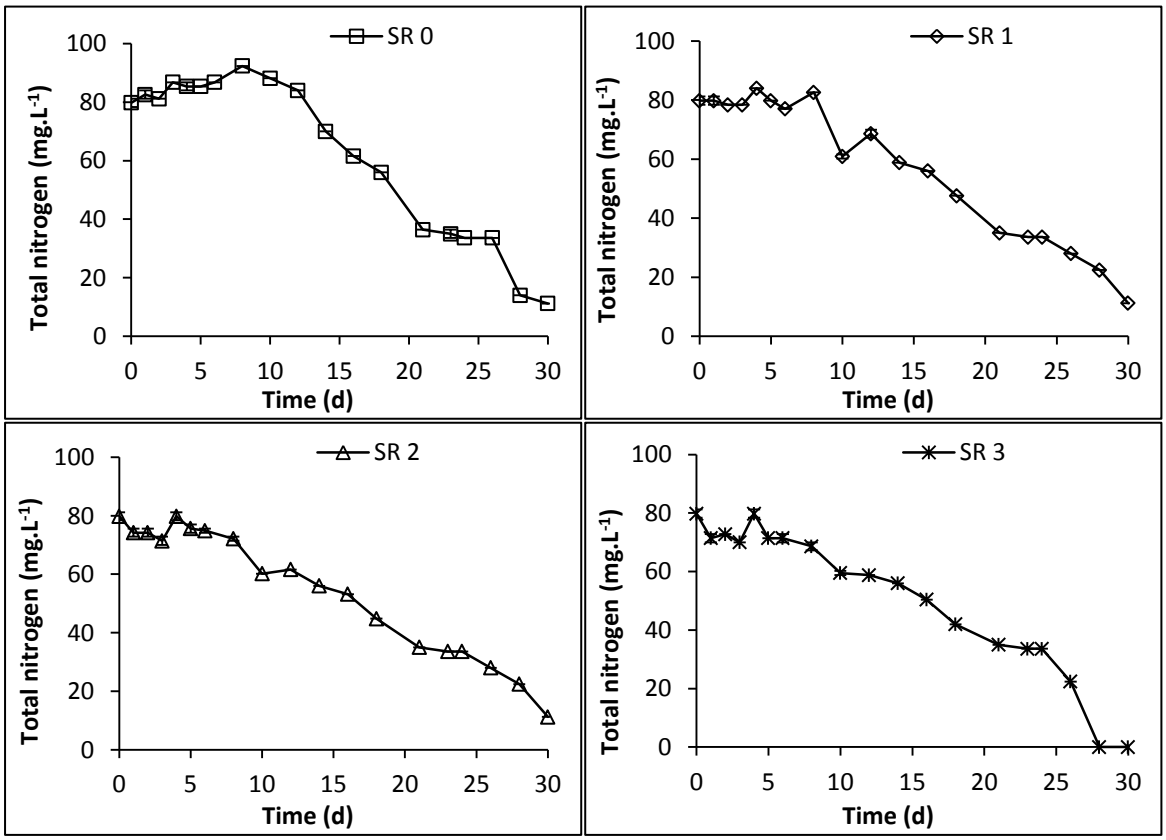

Figure A4. 1 Total nitrogen (TKN) concentrations in batch-operated STPBR

Table A4.6 Effluent ammonium concentration in batch-operated STPBR

Time (d)	Effluent NH_4-N concentration ($mg.L^{-1}$)							
	SR 0		SR 1		SR 2		SR 3	
0	52.1	54.4	52.1	54.4	52.1	54.4	52.1	54.4
1	66.9	65.3	64.6	64.6	63.8	63.0	63.0	63.8
2	73.1	74.7	60.7	61.4	59.1	60.7	56.8	56.0
3	72.3	69.2	63.0	61.4	58.3	60.7	56.8	56.0
4	73.9	76.2	63.0	63.0	62.2	62.2	58.3	58.3
5	73.1	73.1	63.0	63.0	59.9	58.3	56.8	55.2
6	76.2	77.8	63.0	63.8	60.7	56.8	54.4	53.7
8	84.0	81.7	63.0	63.8	55.2	55.2	52.9	53.7
10	85.6	85.6	56.0	56.0	56.0	56.0	56.0	55.2
12	77.0	76.2	56.8	56.8	51.3	52.9	51.3	51.3
14	65.3	65.3	57.6	56.8	52.9	53.7	49.8	50.6
16	53.7	52.9	49.8	49.8	48.2	48.2	49.8	49.0
18	49.8	49.8	47.4	47.4	44.3	44.3	46.7	45.1
21	31.9	31.9	38.1	38.1	32.7	32.7	35.8	35.8
23	23.8	24.0	32.2	31.6	27.1	26.6	28.9	29.1
24	22.9	22.2	31.6	31.4	26.8	27.1	28.9	28.8
26	23.2	23.0	30.2	30.2	25.7	25.7	16.0	16.6
28	21.8	22.1	28.2	27.1	21.2	21.0	0.0	0.0
30	14.5	14.2	15.9	16.3	15.1	14.6	0.0	0.0

Table A4.7 Effluent SCOD concentration in batch-operated STPBR

Time (d)	Effluent COD concentration ($mg.L^{-1}$)							
	SR 0		SR 1		SR 2		SR 3	
0	389	400	389	400	389	400	389	400
1	298	307	253	264	224	222	217	214
2	235	231	120	119	121	114	119	118
3	99	93	89	85	75	75	71	74
4	86	86	90	90	110	106	90	90
5	111	114	115	109	117	111	119	114
6	108	102	112	108	114	111	118	113
8	107	107	91	91	86	90	101	98
10	81	83	98	100	85	87	94	99
12	87	90	92	93	88	86	83	83
14	133	141	133	137	118	123	119	116
16	118	125	105	108	90	95	88	92
18	117	120	117	120	92	96	83	82
21	143	136	109	109	101	102	90	91
23	160	164	134	128	124	128	128	120
24	200	200	168	172	166	162	154	154
26	140	152	140	144	128	128	104	108
28	200	202	174	174	176	170	188	188
30	214	220	200	196	190	180	202	200

Specific growth rate and biomass productivity data

Table A4.8 Maximum specific growth rate in batch-operated STPBR

Specific growth rate (μ_{ave})				
Before CO_2 addition				Irradiance ($\mu mol.s^{-1}.m^{-2}$)
STPBR no.	μ_{ave} (d^{-1})	SD	SE	Average
SR 0	-0.409	0.129	0.091	0
SR 1	0.060	0.002	0.001	429.9
SR 2	0.095	0.035	0.025	582.7
SR 3	0.069	0.011	0.008	730.8
After CO_2 addition				
STPBR no.	μ_{ave} (d^{-1})	SD	SE	Irradiance ($\mu mol.s^{-1}.m^{-2}$)
SR 0	-0.367	0.047	0.033	0
SR 1	0.043	0.000	0.000	429.9
SR 2	0.109	0.033	0.024	582.7
SR 3	0.065	0.024	0.017	730.8

Table A4.9 Average biomass productivity (P_{ave}) in batch-operated STPBR

Before CO_2 addition				
STPBR no.	P_{ave} ($g.L^{-1}.d^{-1}$)	SD	SE	Irradiance ($\mu mol.s^{-1}.m^{-2}$)
SR 0	-0.006	0.0048	0.0018	0
SR 1	0.009	0.0044	0.0016	429.9
SR 2	0.018	0.0081	0.0029	582.7
SR 3	0.016	0.0069	0.0025	730.8
After CO_2 addition				
STPBR no.	P_{ave} ($g.L^{-1}.d^{-1}$)	SD	SE	Irradiance ($\mu mol.s^{-1}.m^{-2}$)
SR 0	-0.008	0.0035	0.0025	0
SR 1	0.014	0.0083	0.0041	429.9
SR 2	0.034	0.0139	0.0070	582.7
SR 3	0.026	0.0052	0.0026	730.8

Phase III experiments data

MLVSS control data

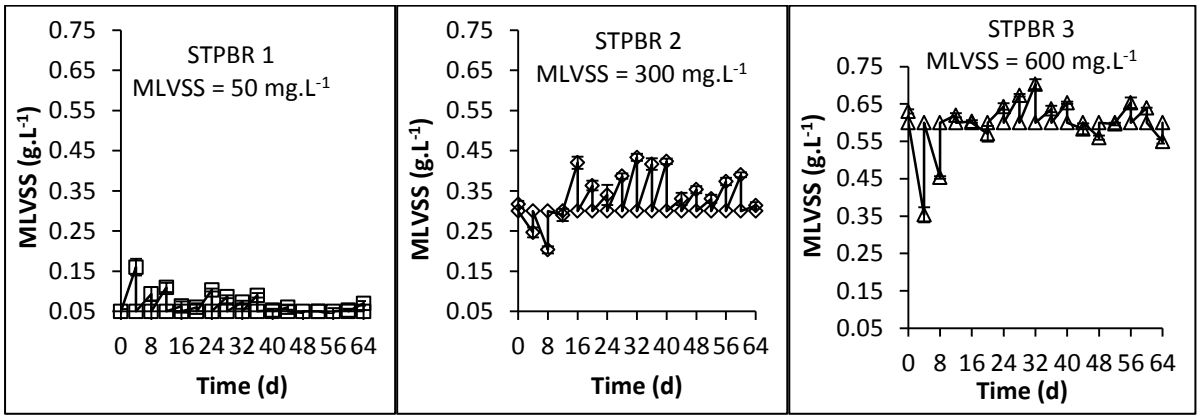

Figure A5.1 MLVSS control data showing returned biomass after every HRT cycle

Table A5. 1 Effluent SCOD concentrations for the continuously operated STPBR

	SCOD concentration (mg.L^{-1})											
Day		**R1**		**Average**		**R2**		**Average**		**R3**		**Average**
0	258	261	254	258	251	248	238	246	248	250	246	248
4	180	176	178	178	172	178	186	179	180	172	168	173
8	170	170	170	170	182	182	186	183	164	166	165	165
12	156	160	156	157	162	166	166	165	134	136	130	133
16	142	148	144	145	104	112	110	109	104	104	110	106
20	186	186	186	186	134	140	134	136	134	142	138	138
24	140	140	144	141	102	104	112	106	100	102	100	101
28	154	150	154	153	114	120	116	117	116	114	120	117
32	182	188	182	184	136	136	144	139	140	132	136	136
36	124	130	124	126	108	112	108	109	110	112	122	115
40	146	142	144	144	142	144	136	141	126	136	136	133
44	106	106	112	108	108	108	110	109	104	106	104	105
48	144	142	144	143	138	136	138	137	130	132	130	131
52	94	100	94	96	94	92	92	93	102	106	108	105
56	72	72	70	71	68	68	66	67	70	64	66	67
60	154	142	154	150	152	148	150	150	152	142	146	147
64	50	48	46	48	44	38	40	41	40	40	36	39

Some flow cytometry images

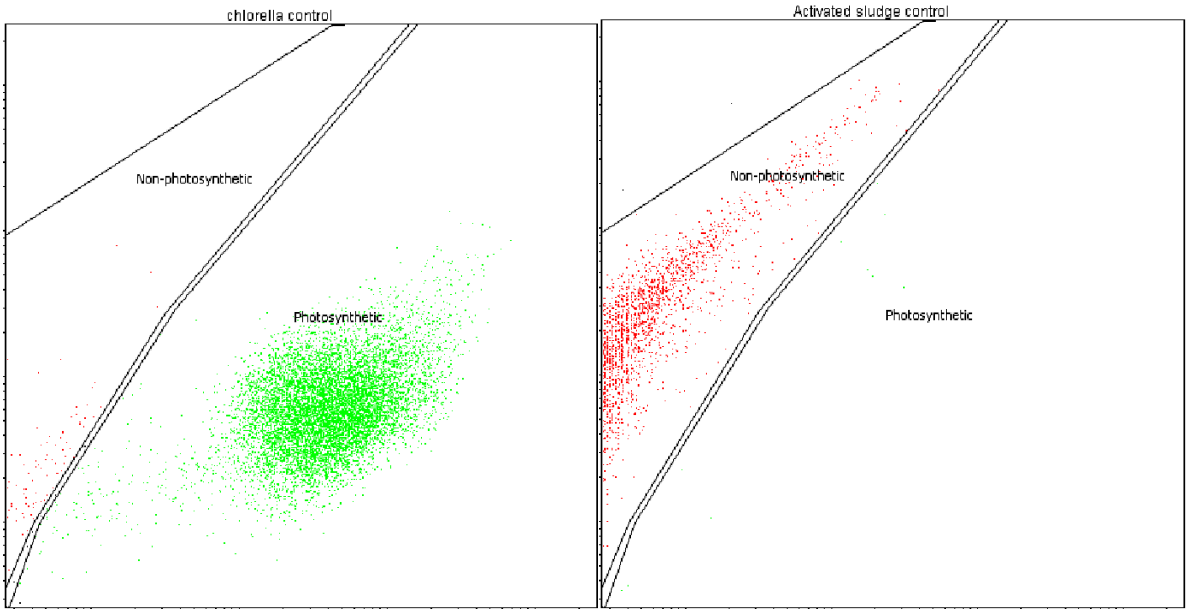

Figure A5.2 FCM images showing *Chlorella* positive control (left) and activated sludge negative control (right), with each green dot and red dot representing a photosynthetic and non-photosynthetic cell)

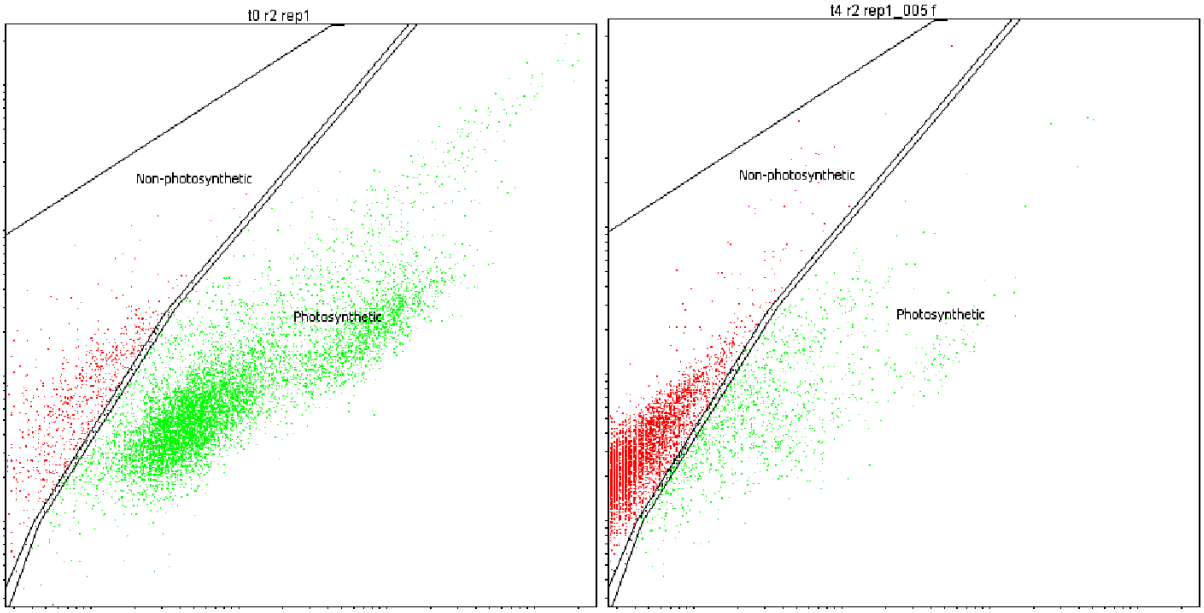

Figure A5.3 FCM images showing samples in STPBR 2, (left: t0 r2 rep1), initial M:B ≈ 90:10 on day 0; and (right: t4 r2 rep1), M:B ≈ 10:90 on day 28

Table A5.2 HMAS microbial proportions data (flow cytometry)

Time (d)	Bacteria (%)			Average	SD	SE	Microalgae (%)			Average	SD	SE
STPBRR 1												
0	11.4	11.6	11.1	11.3	0.275	0.159	87.7	87.4	88.1	87.7	0.377	0.218
4	79.3	79.6	80.0	79.6	0.351	0.203	19.2	19.0	18.6	18.9	0.306	0.176
12	25.0	22.8	23.8	23.9	1.102	0.636	73.4	75.6	74.7	74.6	1.106	0.639
20	14.7	15.1	16.2	15.3	0.777	0.448	81.7	81.4	80.0	81.0	0.907	0.524
28	5.6	5.0	4.7	5.1	0.458	0.265	93.0	93.6	94.1	93.6	0.551	0.318
36	6.5	4.6	5.4	5.5	0.954	0.551	91.1	93.8	92.6	92.5	1.353	0.781
48	28.7	29.0	29.3	29.0	0.300	0.173	66.1	65.9	65.5	65.8	0.306	0.176
56	91.6	91.4	91.6	91.5	0.115	0.067	7.8	7.8	7.4	7.7	0.231	0.133
64	52.6	53.0	52.7	52.8	0.208	0.120	42.8	42.3	42.4	42.5	0.265	0.153
STPBRR 2												
0	11.4	11.6	11.1	11.3	0.275	0.159	87.7	87.4	88.1	87.7	0.377	0.218
4	65.1	64.9	65.5	65.2	0.306	0.176	34.2	34.5	33.8	34.2	0.351	0.203
12	30.4	31.3	31.0	30.9	0.458	0.265	67.2	66.4	66.8	66.8	0.400	0.231
20	84.2	85.6	86.5	85.4	1.159	0.669	14.4	13.1	12.2	13.2	1.106	0.639
28	85.4	85.7	85.4	85.5	0.173	0.100	13.3	13.0	13.4	13.2	0.208	0.120
36	52.1	52.3	52.6	52.3	0.252	0.145	43.9	44.0	43.4	43.8	0.321	0.186
48	71.1	72.4	71.8	71.8	0.651	0.376	26.8	25.6	26.1	26.2	0.603	0.348
56	54.9	54.5	53.2	54.2	0.889	0.513	41.9	42.0	43.4	42.4	0.839	0.484
64	42.6	42.1	42.4	42.4	0.252	0.145	53.3	53.6	53.7	53.5	0.208	0.120
STPBRR 3												
0	11.4	11.6	11.1	11.3	0.275	0.159	87.7	87.4	88.1	87.7	0.377	0.218
4	59.6	60.2	61.1	60.3	0.755	0.436	39.5	38.7	38.0	38.7	0.751	0.433
12	11.5	11.0	11.0	11.2	0.289	0.167	87.4	88.0	88.0	87.8	0.346	0.200
20	64.9	64.4	64.2	64.5	0.361	0.208	32.4	33.1	33.1	32.9	0.404	0.233
28	57.3	57.2	56.9	57.1	0.208	0.120	39.6	39.9	39.9	39.8	0.173	0.100
36	23.2	22.5	22.7	22.8	0.361	0.208	73.3	74.0	73.9	73.7	0.379	0.219
48	50.9	49.6	51.5	50.7	0.971	0.561	46.2	47.3	46.2	46.6	0.635	0.367
56	55.9	55.2	56.1	55.7	0.473	0.273	41.3	42.2	41.2	41.6	0.551	0.318
64	39.9	41.0	40.0	40.3	0.608	0.351	56.4	55.8	56.5	56.2	0.379	0.219

Table A5.3 Triplicate microbial gene copy numbers (SD = standard deviation; qPCR data)

Time (d)	Microalga				Bacteria			
	Gene copy numbers			SD	Gene copy numbers			SD
				STPBR 1				
0	1.02E+12	1E+12	1.03E+12	1.09E+10	5.92E+11	6.65E+11	5.75E+11	4.76E+10
4	1.96E+12	1.94E+12	1.93E+12	1.49E+10	2.80E+12	2.95E+12	2.79E+12	8.75E+10
12	1.96E+12	1.92E+12	1.98E+12	3.49E+10	5.57E+12	6.05E+12	5.52E+12	2.89E+11
20	3.37E+12	3.57E+12	3.41E+12	1.05E+11	1.56E+12	1.55E+12	1.60E+12	2.75E+10
28	1.51E+12	1.61E+12	1.63E+12	6.70E+10	1.88E+12	2.22E+12	2.05E+12	1.74E+11
36	6.30E+12	6.69E+12	6.32E+12	2.16E+11	8.13E+11	8.41E+11	7.64E+11	3.88E+10
48	3.76E+12	3.69E+12	3.71E+12	3.45E+10	3.47E+12	3.07E+12	3.51E+12	2.46E+11
56	2.99E+12	2.97E+12	3.09E+12	6.74E+10	2.73E+12	2.58E+12	2.66E+12	7.60E+10
64	4.65E+12	4.48E+12	4.76E+12	1.37E+11	1.56E+12	1.56E+12	1.64E+12	4.53E+10
				STPBR 2				
4	1.43E+12	1.48E+12	1.58E+12	7.63E+10	1.47E+12	1.54E+12	1.55E+12	4.43E+10
12	1.33E+12	1.26E+12	1.39E+12	6.41E+10	3.88E+12	4.52E+12	4.01E+12	3.35E+11
20	2.68E+12	2.82E+12	2.49E+12	1.64E+11	5.73E+12	6.05E+12	5.22E+12	4.16E+11
28	2.87E+12	2.77E+12	2.70E+12	8.86E+10	7.15E+12	7.03E+12	6.38E+12	4.14E+11
36	2.44E+12	2.38E+12	2.60E+12	1.10E+11	4.29E+12	4.42E+12	4.46E+12	8.66E+10
48	2.25E+12	2.22E+12	2.20E+12	2.24E+10	4.85E+12	4.50E+12	4.57E+12	1.88E+11
56	2.04E+12	2.21E+12	2.21E+12	9.70E+10	5.16E+12	5.12E+12	4.97E+12	1.02E+11
64	1.91E+12	2.02E+12	1.84E+12	9.17E+10	2.49E+12	2.28E+12	2.37E+12	1.05E+11
				STPBR 3				
4	2.24E+12	2.41E+12	2.15E+12	1.32E+11	2.37E+12	2.45E+12	2.38E+12	4.35E+10
12	1.79E+12	1.79E+12	1.78E+12	8.05E+09	3.02E+12	3.07E+12	2.79E+12	1.47E+11
20	1.56E+12	1.71E+12	1.51E+12	1.02E+11	3.33E+12	3.06E+12	2.98E+12	1.83E+11
28	2.48E+12	2.55E+12	2.40E+12	7.44E+10	3.51E+12	3.76E+12	3.82E+12	1.67E+11
36	1.94E+12	2.12E+12	1.98E+12	9.29E+10	4.16E+12	4.60E+12	4.45E+12	2.26E+11
48	1.64E+12	1.70E+12	1.65E+12	3.09E+10	2.90E+12	3.04E+12	3.42E+12	2.68E+11
56	1.54E+12	1.66E+12	1.64E+12	6.72E+10	2.95E+12	3.17E+12	3.09E+12	1.13E+11
64	1.38E+12	1.32E+12	1.39E+12	3.78E+10	2.99E+12	2.76E+12	3.02E+12	1.45E+11

Table A5.4 SCOD removed through algal activity in continuously operated STPBR

HRT (d)	= 4
CO_2 flow rate ($mL.min^{-1}$)	**=** 25
CO_2 flow rate ($L.h^{-1}$)	= (25 x 60 min)/1000 = 1.5
Concentration of CO_2 (i.e. 25% v/v)	= 0.25
Volume **of CO_2 (L)**	= 25 x 0.25 x 24 h = 36
Molar volume of **CO_2 @STP (L/mol)**	= 22.4
Mole of assimilated **CO_2**	= 36 x 22.4 = 1.61
CO_2 conversion to glucose (80%)	= 0.8
CO_2 assimilated (mol)	= 1.61 x 0.8 = 1.29
In photosynthetic carbon capture, 6 moles of CO_2 are used to produce 1 mole of glucose	
Moles of CO_2 used in photosynthesis	= 6
Glucose from algal photosynthesis (mol)	= 1.29/**6** = 0.214
Molar mass of glucose (g.**mol^{-1}**)	= 180
Mass of glucose from photosynthesis (g)	= 0.214 x 180 = 38.6
But, 1 g of glucose produces 1.67 g COD (in bacterial degradation of organic matter)	
COD conversion factor	= 1.67
COD converted from glucose by algae (g)	= 1.67 x 38.6 = **64.414**

Table A5.5 SCOD removed through bacterial activity in continuously operated STPBR

Bioreactor	SCOD removed (kg)
STPBR 1	0.251 g x 0.72 x 14.92 L = **0.00270**
STPBR 2	0.251 g x 0.73 x 14.92 L = **0.00273**
STPBR 3	0.251 g x 0.73 x 15.44 L = **0.00283**

Table A6.1 Initial sample volumes used for DNA extraction

qPCR no.	Sample no.	Initial volume used in DNA extraction (mL)*	Experiment
58	SR 0-3, t0	3.445	Phase II
59	SR 0, t3	25.64	
60	SR 1, t3	11.365	
61	SR 2, t3	8.695	
62	SR 3, t3	9.615	
63	SR 0, t5	50	
64	SR 1, t5	9.434	
65	SR 2, t5	7.52	
66	SR 3, t5	7.935	
67	STPBR 1, t0	50	Phase III
68	STPBR 2, t0	8.3	
69	STPBR 3, t0	4.15	
70	STPBR 1, t1	50	
71	STPBR 2, t1	8.3	
72	STPBR 3, t1	4.15	
73	STPBR 1, t2	50	
74	STPBR 2, t2	8.3	
75	STPBR 3, t2	4.15	
76	STPBR 1, t3	50	
77	STPBR 2, t3	8.3	
78	STPBR 3, t3	4.15	
79	STPBR 1, t4	50	
80	STPBR 2, t4	8.3	
81	STPBR 3, t4	4.15	
82	STPBR 1, t5	50	
83	STPBR 2, t5	8.3	
84	STPBR 3, t5	4.15	
85	STPBR 1, t6	50	
86	STPBR 2, t6	8.3	
87	STPBR 3, t6	4.15	
88	STPBR 1, t7	50	
89	STPBR 2, t7	8.3	
90	STPBR 3, t7	4.15	
91	STPBR 1, t8	50	
92	STPBR 2, t8	8.3	
93	STPBR 3, t8	4.15	

* Variable to account for cell dry weight differences between samples